ORNL-2647
Instruments
TID-4500 (14th ed.)

INSTRUMENTATION AND CONTROLS DIVISION

ANNUAL PROGRESS REPORT

FOR PERIOD ENDING JULY 1, 1958

[redacted]

OAK RIDGE NATIONAL LABORATORY

operated by

UNION CARBIDE CORPORATION

for the

U.S. ATOMIC ENERGY COMMISSION

Printed in USA. Price $2.75. Available from the
Office of Technical Services
Department of Commerce
Washington 25, D.C.

ORNL-2647
Instruments
TID-4500 (14th ed.)

Contract No. W-7405-eng-26

INSTRUMENTATION AND CONTROLS DIVISION

ANNUAL PROGRESS REPORT

For Period Ending July 1, 1958

C. J. Borkowski, Director
C. S. Harrill, Associate Director

DATE ISSUED

JUN 16 1959

OAK RIDGE NATIONAL LABORATORY
Oak Ridge, Tennessee
operated by
UNION CARBIDE CORPORATION
for the
U.S. ATOMIC ENERGY COMMISSION

CONTENTS

DECIMAL PRINTOUT FOR 256-CHANNEL PULSE-HEIGHT ANALYZER

N. W. Hill

In magnetic-core multichannel analyzers employing binary logic for the address or channel number generation, "locked-in" printout in the decimal form for each address requires binary-to-decimal conversion. Since this conversion necessitates a large number of components and further manipulation to make it compatible with present printout machines, either decimal printout of the channel number has been avoided entirely or an auxiliary decimal scaler has been employed to count serially each pulse used to advance the address scaler during the printout operation. In this scheme it is relatively easy for one scaler to get out of step with the other. Such a system is usually referred to as a "non-locked-in" address readout and requires complete reliability in both scalers for the readout address number to be meaningful.

One printout method now in use on a 256-channel pulse-height analyzer at the Bulk Shielding Facility which does have a semi-locked-in feature is a binary-to-octal conversion of the six least significant binary stages of the address scaler. This readout system requires a minimum of components and has proved reliable, but its octal code is not readily interpreted by the inexperienced. Further, since the address scaler is not completely decoded, there is still some doubt as to the actual address of the channel being read out.

Another method that does have a completely "locked-in" feature has been in use at the Bulk Shielding Facility for six months. This system achieves binary-to-decimal conversion by use of a ferrite core plane with 22 special sense windings, sense amplifiers, and three modified Hewlett-Packard AC-4A decade scaling units. The address current drive lines to this plane in the analyzer memory are identical with the drive lines of a normal memory plane; each time a particular core in a normal plane is selected by the full switching current, the core occupying this same position in the special plane is also selected. As its selection is uniquely determined by one of the 256 possible combinations of the eight binary stages of the address scaler, a decimal number from 0 to 255 can be assigned to the core. Since there is no inhibit winding in this plane, a selected core during a memory cycle goes through two reversals of magnetic state, inducing two current pulses on any sense winding threading this core. As is indicated in Table 1, these pulses suitably amplified are used to set the proper decimal numbers into the three decade scalers.

The AC-4A decade scaling units used generate an analog stairstep voltage designed for use with the Hewlett-Packard model 560A digital recorder. With suitable programing of the pulse-height analyzer and digital recorder, this method furnishes a completely synchronized printout regardless of the sequence in which the channel readout occurs. For instance, at low counting rates (limited by printer speed of 4 lines/sec) it is possible to record the channel number while the information is being accumulated in the memory, in contrast with the older system in which the printer cannot be used simultaneously with the acquisition of data in the memory.

Table 1. Decimal Numbers of Cores Threaded by Printout Sense Windings for 16 × 16 Matrix Plane

Sense Winding No.	Decimal Numbers of Cores Threaded	Decimal Number Set into Scalers	
		Digit	Decade
1	1, 11, 21, ..., 101, 111, ..., 251	1	Units
2	2, 12, 22, ..., 102, 112, ..., 252	2	Units
...	...	...	...
9	9, 19, 29, ..., 109, 119, ..., 249	9	Units
10	10, 11, 12, 13, ..., 110, 111, ..., 219	1	Tens
11	20, 21, 22, ..., 120, 121, ..., 229	2	Tens
...	...	...	...
21	100, 101, 102, ..., 199	1	Hundreds
22	200, 201, 202, ..., 255	2	Hundreds

NEW COUNT-RATE METERS FOR AREA MONITORING (Q-1951 AND Q-1957)

F. M. Glass

Two new count-rate meters for area monitoring have been designed and are now in the production stage. These instruments feature built-in amplifiers, regulated high-voltage supplies for detectors, and long-time stability. The circuitry is simple and the packaging compact. The basic circuits for the count-rate meters and the high-voltage supplies are identical in the two instruments.

Voltage doublers employing silicon rectifiers supply 1900 v without the necessity of a separate high-voltage transformer. This 1900 v is then regulated by corona regulators to the desired voltage. It is believed that the reliability of these high-voltage supplies depends almost entirely on the life of the corona regulators. No trouble is anticipated with any of the other components.

The count-rate meter consists of a biased-off, sharp-cutoff pentode having a meter and an appropriate integrating storage capacitor in its plate circuit. This tube is driven by a trigger pair which produces a constant-height, adjustable-width pulse. The pulse width (which depends on the R-C product of the cross-coupling elements of the trigger pair) determines the full-scale sensitivity of the rate meter. Full-scale deflection on the meter represents a 0.3% duty cycle. Since no diode clamps are used in the grid circuits of the trigger pair, the counting loss is fixed for all ranges at approximately 0.5% at full scale. Although this type of circuit does not have the dynamic range of the conventional pump circuit and vacuum-tube voltmeter, it has certain advantages for monitoring-type instruments, the most important of which is the complete absence of zero drift — a weakness inherent in the conventional count-rate meter. Another important advantage is its simplicity, which cuts both the cost of production and maintenance.

The Q-1951 area monitor count-rate meter meets the following specifications:

Input sensitivity	200 mv
Ranges	300, 1000, 3000, 10,000 and 30,000 counts/min
Integrating time constants	1, 11, and 21 sec
Outputs in addition to panel meter	10-mv recorder; 1-ma recorder and alarm or control signal
Accuracy	3%
Linearity	2%
Zero drift	None
Maximum counting loss	1/2%

This instrument is intended to be used with G-M tubes but may be used with any detector requiring positive high voltage, having a current drain less than 50 μa, and producing negative pulses with amplitudes between 0.2 and 50 v.

The Q-1957 alpha count-rate meter is intended for use with those alpha-scintillation probes designed for positive high-voltage supplies and low divider current (less than 50 μa). This instrument has a loudspeaker that gives an audible click for each alpha disintegration counted. A volume control provides adjustment from zero level to 10-w audio peaks. Other specifications are as follows:

Input sensitivity	25 mv
Range	300 and 1000 counts/min
Integrating time constants	1, 11, and 21 sec
Accuracy	3%
Linearity	2%
Zero drift	None
Maximum counting loss	1/2%
Outputs in addition to panel meter	10-mv recorder

HAND AND FOOT RADIATION MONITOR

H. N. Wilson G. A. Holt

A hand and foot beta-gamma radiation monitor was developed and is designated ORNL Q-1939. The important features of the instrument include the following:

1. Simplified circuitry using glow transfer scaler tubes and electrical reset registers.

2. High-reliability circuits utilizing silicon rectifiers, halogen-quenched stainless-wall G-M tubes, and type 85A2 voltage-regulated high-voltage power supply.

3. Automatic count-stop-reset feature providing adjustable counting time. Total duration of cycle is 1 min.

4. Four identical modular counting assemblies for left hand, right hand, feet, and survey probe. These assemblies are quickly replaceable.

5. Four separate variable high-voltage outputs adjustable by means of recessed, panel-mounted screw-driver adjustments.

6. Survey probe so positioned that, when not in use as a survey probe, it will monitor the mid-section of the person using the instrument. As a survey probe it may be removed from the hanger to localize contamination (see Fig. 1).

7. Simplified procedure for removing the protective liners in the hand counters, changing the paper cover over the foot counters, and replacing the foot counter cover-paper roll (see Fig. 2).

A circuit diagram of the instrument is shown in Fig. 3.

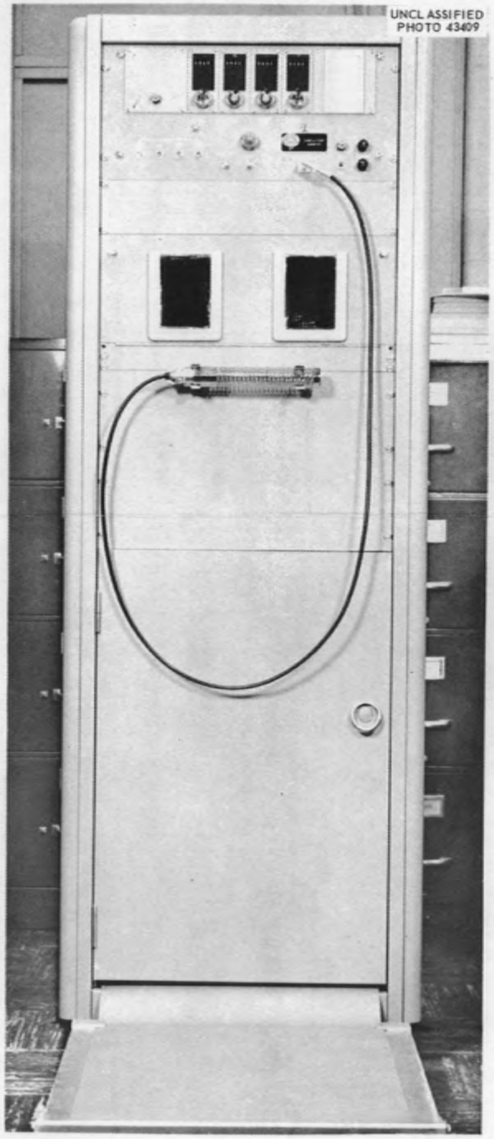

Fig. 1. Hand and Foot Beta-Gamma Radiation Monitor, ORNL Q-1939. Front view.

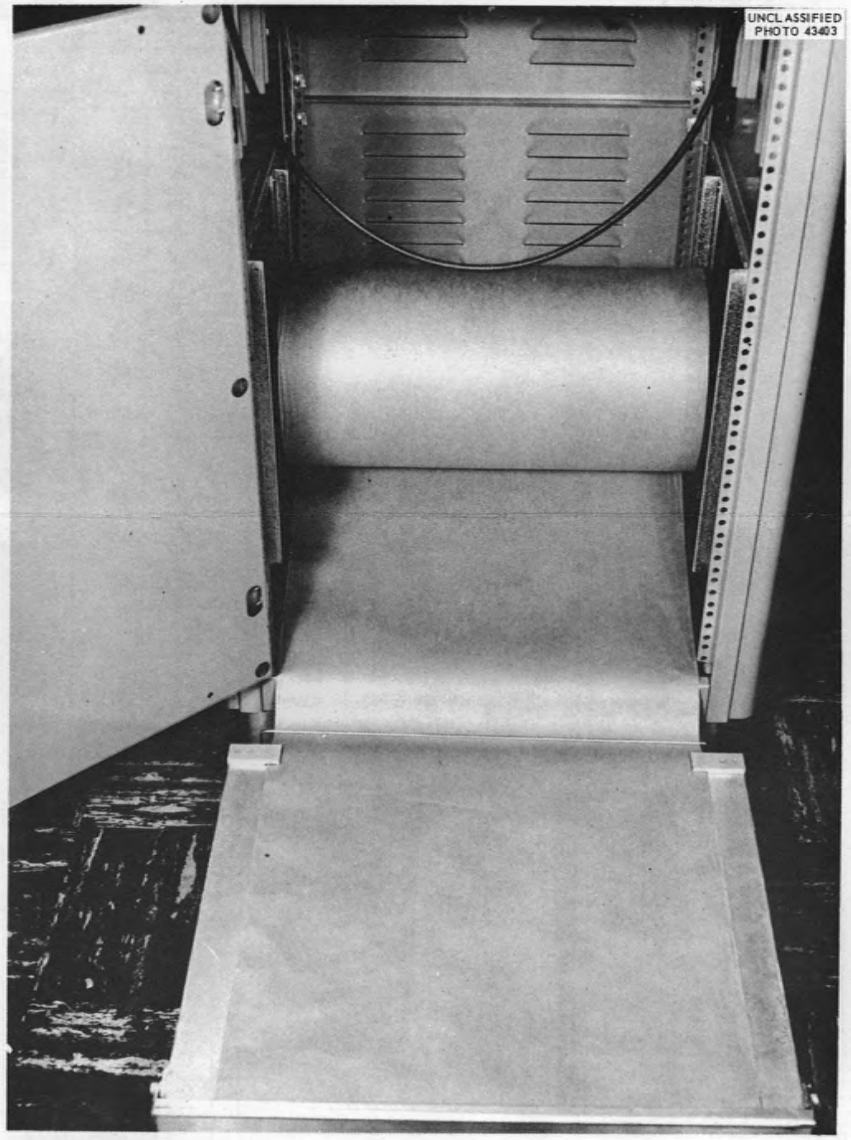

Fig. 2. Hand and Foot Beta-Gamma Radiation Monitor, ORNL Q-1939. Cover-paper roll.

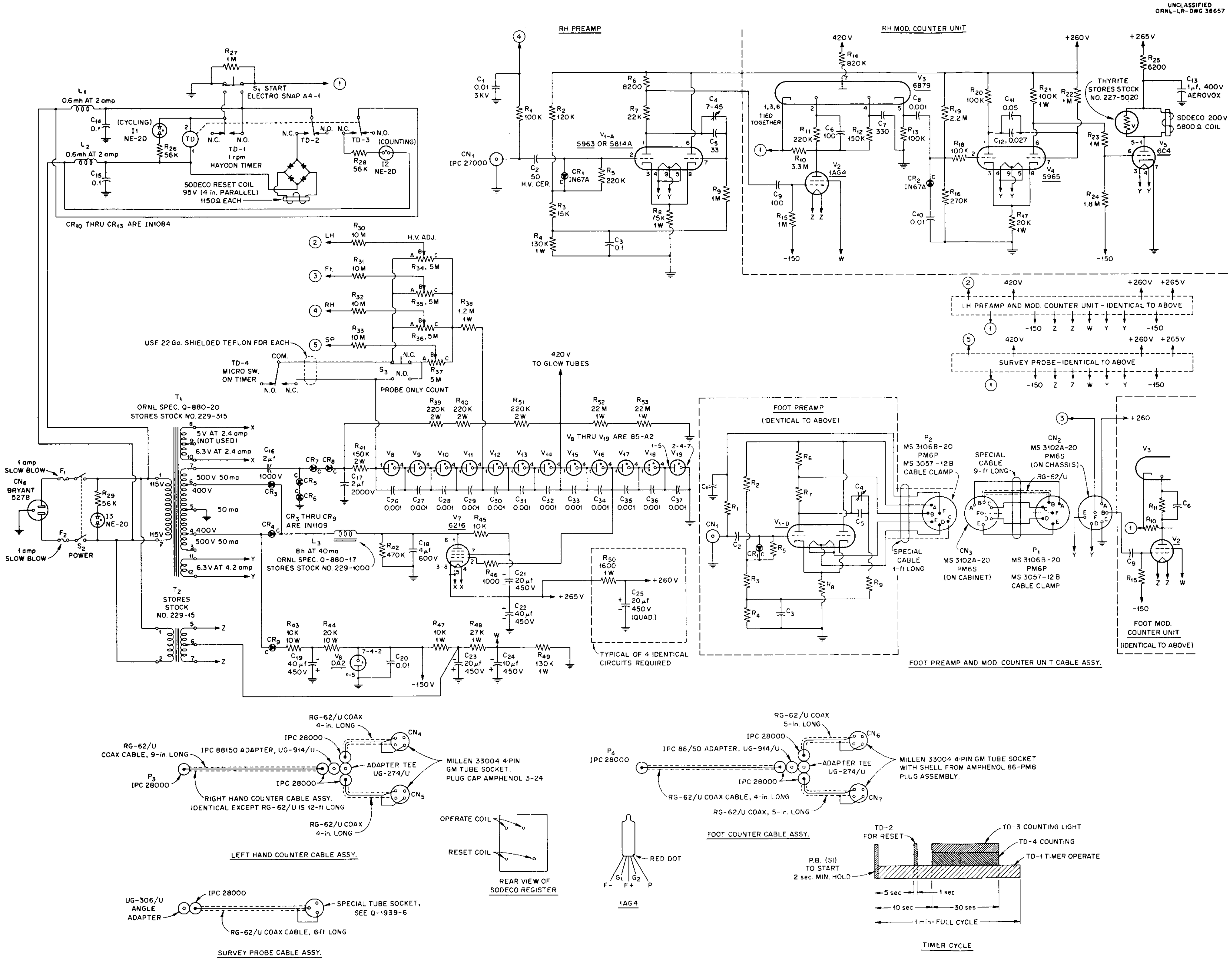

Fig. 3. Hand and Foot Beta-Gamma Radiation Monitor, ORNL Q-1939. Circuit diagram.

COMPUTER ENGINEERING GROUP PROJECTS

J. W. Woody, Jr.

Data acquisition and interpretation at the Laboratory have become problems of large proportions in the past few years. The time and effort required to adequately peruse and digest miles of strip-chart recordings are rapidly becoming prohibitive. In order to help alleviate this problem, the Computer Engineering Group designed and built three instruments which record data in a form compatible with Oracle input. These devices are binary in nature and make use of analog-to-digital converters where the data is not already in digital form. They produce punched paper tape automatically, using modified Teletype BRPE paper-tape punches. Data thus acquired can be used in a multitude of high-speed calculations on the Oracle, making the processing of data many times more accurate and efficient than was previously possible.

The first of these units (Fig. 4), designed by J. W. Reynolds, is for use with RCL 256-channel analyzers. It is a self-contained unit and may be transferred from one to another of these analyzers; slight modification of the analyzers is necessary. Information is taken in binary form from the memory via the add-1 scaler in the analyzer. When the start button is pressed, the unit begins punching out in sequence the contents of the memory addresses until overflow is obtained from the analyzer address register. Overflow automatically stops the punch. This punched tape may now be read directly into the Oracle.

The second of these units, designed by C. H. Schalbe, is a custom installation included as an integral part of the 2048 neutron time-of-flight spectrometer. The control chassis is shown in Fig. 5. Its function is essentially the same as that of the first unit in that it takes data in binary form from the memory of the spectrometer and prepares it in Oracle format on punched tape. However, it differs from the first unit in one respect – it punches a code word at the beginning of the tape which indicates to the Oracle the manner in which the data were obtained.

The third unit (Fig. 6), designed by J. W. Woody, Jr., is essentially the same as the first two with the exception that it is completely transistorized and is intended for use with the Cary spectrophotometer. It is composed of commercially available transistor plug-in packages and transistor regulated power supplies. Binary information is obtained from a Datex shaft angle encoder mounted on a strip-chart recorder. As before, information is punched in Oracle format.

Another instrument which was recently completed is a gas sampling timer (Fig. 7) designed by J. W. Woody, Jr. Its function is to successively fire explosive-actuated valves at certain fixed times between 10 msec and 11 sec. This is accomplished by means of a 1-kc multivibrator, a 5-decade scaler, gating circuits out of the scaler, and thyratrons for the actual firing of the valves. For example, a gas sample may be obtained by firing a normally closed valve, allowing the gas to flow into a storage tank. After a preset time interval of 10 msec, a normally open valve in the line is fired, shutting off the gas flow and trapping the 10-msec sample in the storage tank.

UNCLASSIFIED
PHOTO 44367

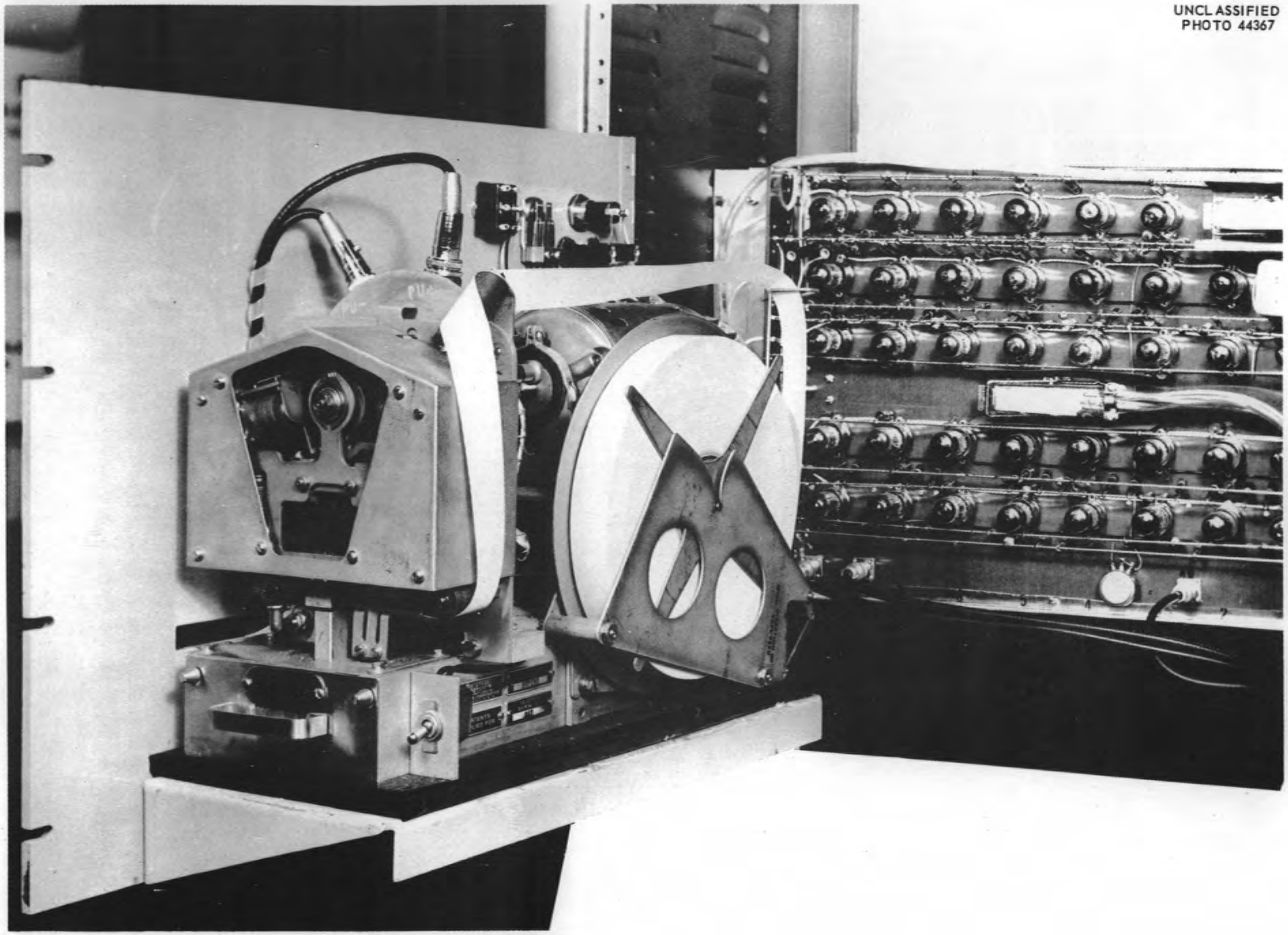

Fig. 4. Tape Punch for Use with 256-Channel Analyzer.

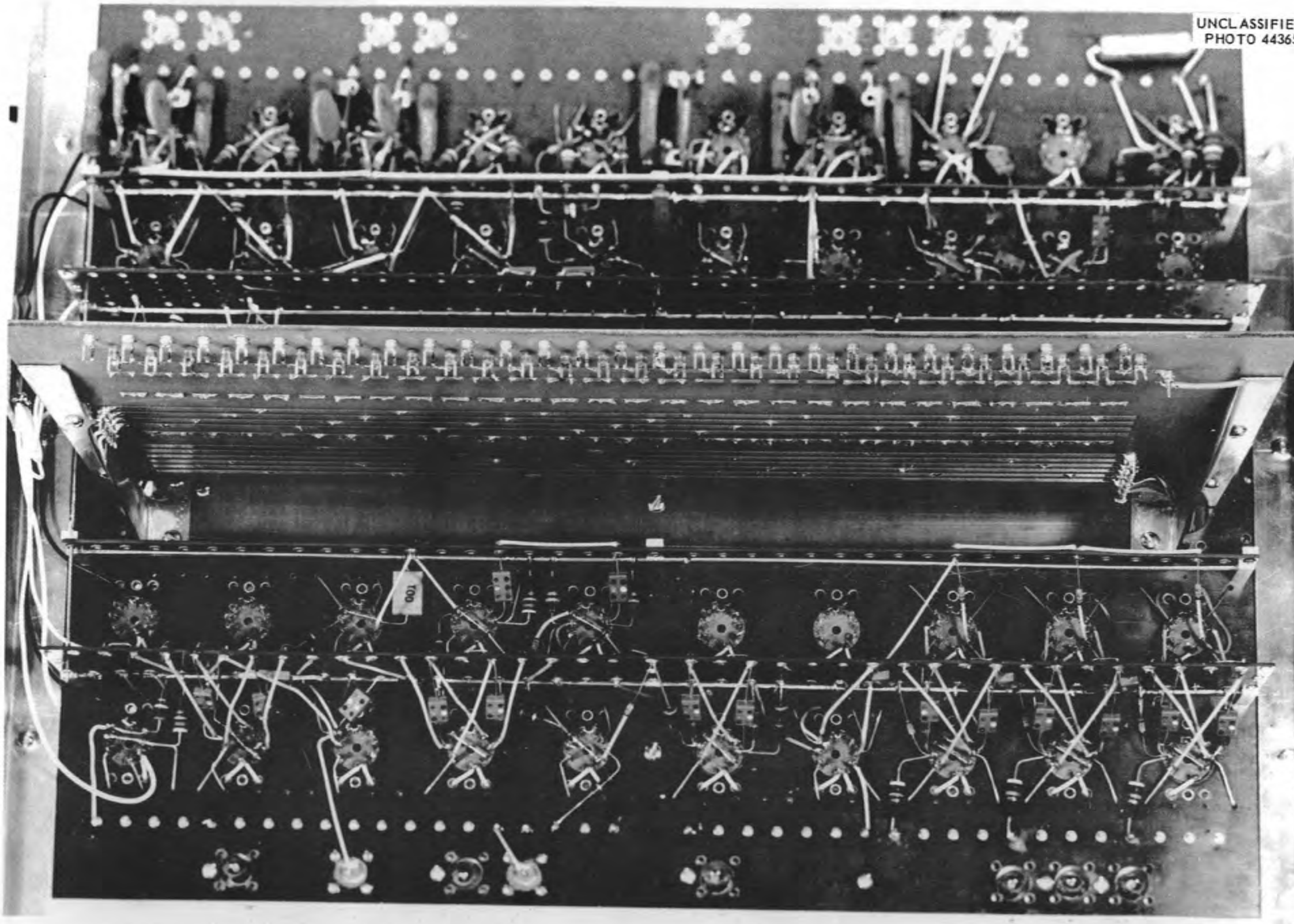

Fig. 5. Punch Control Chassis for the 2048 Neutron Time-of-Flight Spectrometer.

UNCLASSIFIED
PHOTO 44355

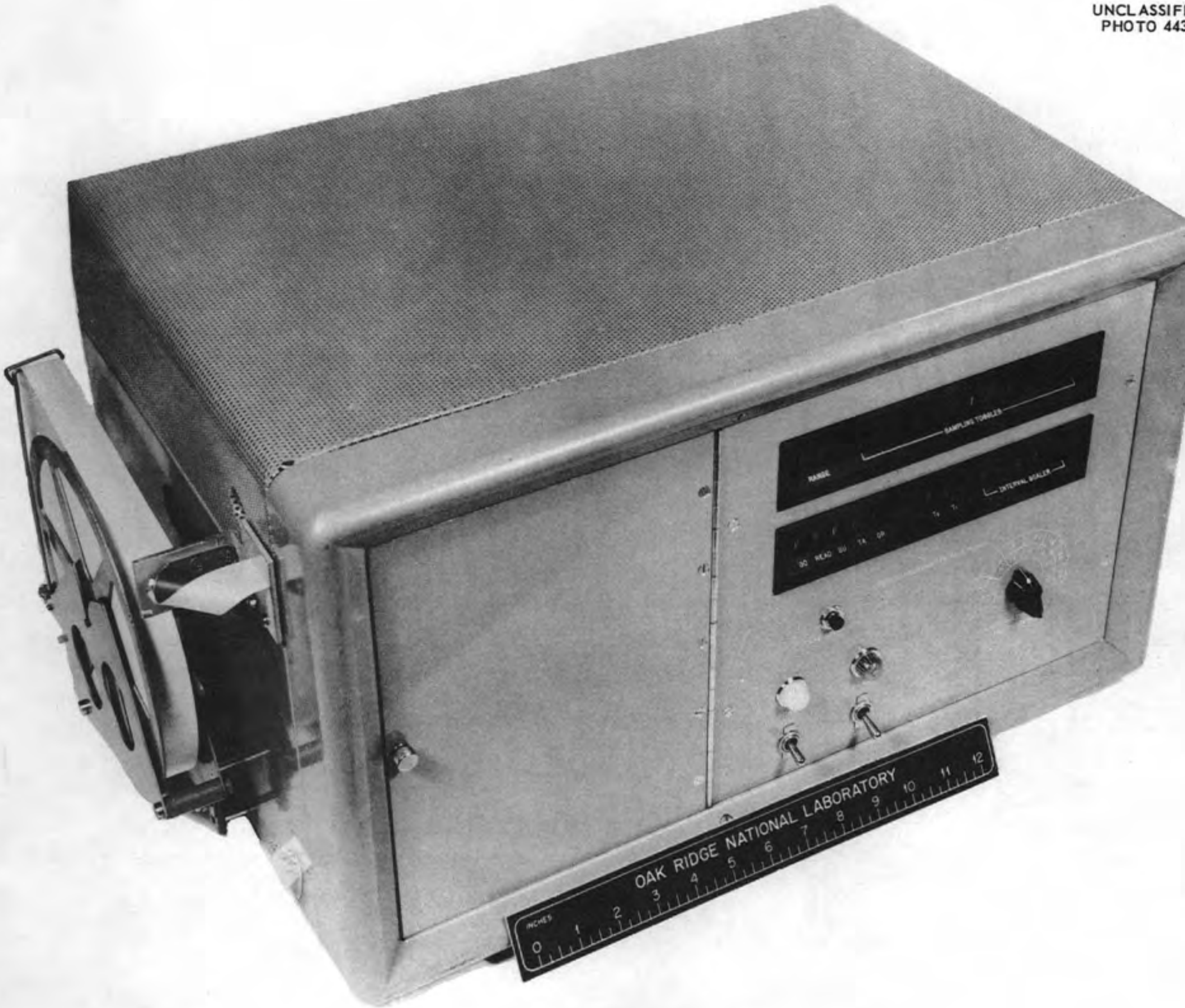

Fig. 6. Tape Punch for Use with the Cary Spectrophotometer.

UNCLASSIFIED
PHOTO 44873

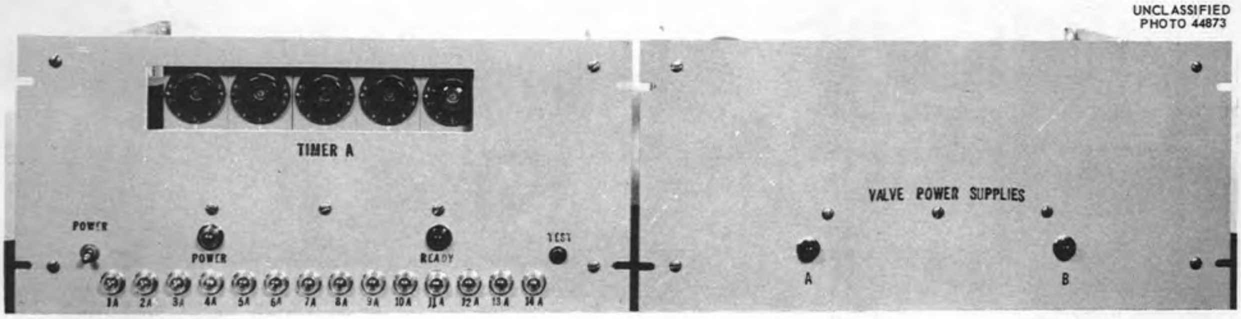

Fig. 7. Gas Sampling Timer.

THE DUO-PLASMATRON ION SOURCE

C. D. Moak[1] J. W. Johnson
R. F. King H. E. Banta

The duo-plasmatron ion source (Fig. 8) is an East German development and has been known in this country for a relatively short time. It is both a high-current and a high-intensity source. Total ion currents of the order of amperes and current densities of the order of 100 amp/cm^2 may be realized. The source has been described in the Physics Division publications and meetings.[2] A few specialized problems connected with the source will be discussed here.

Since several hundred watts of heat are developed in the source, forced cooling must be provided. Neither power for pumps nor space for heat exchangers is easily provided in the terminal of a Van de Graaff generator, so the coolant must also be a good dielectric. Freon 113 was used; a column of it in Tygon tubing has withstood 2.5 Mv in the Van de Graaff column.

Filaments to give electron currents of approximately an ampere have been constructed. It is desirable that filament life be several hundred hours, and the service is very severe. The first filament to meet this criterion was a 1/16-in. tantalum hairpin. This filament dissipated 220 w. Its life test was terminated at 430 hr with appreciable filament life remaining. Experience with oxide-coated filaments had indicated that they deteriorated rapidly under the ion bombardment. It was suggested[3] that a specialized platinum screen filament coated with emission mixture might withstand the bombardment. Such a filament was life-tested; its best life was more than 1400 hr and the minimum heating power was 70 w.

---

[1]Physics Division.

[2]C. D. Moak *et al.*, *Phys. Semiann. Prog. Rep. March 15, 1958*, ORNL-2501, p 75; D. Maeder, *Phys. Semiann. Prog. Rep. Sept. 20, 1958*, ORNL-2610, p 47.

[3]Private communication from T. Lauritsen, J. L. McKibben, and A. S. Langsdorf, Jr.

UNCLASSIFIED
ORNL-LR-DWG 34273R

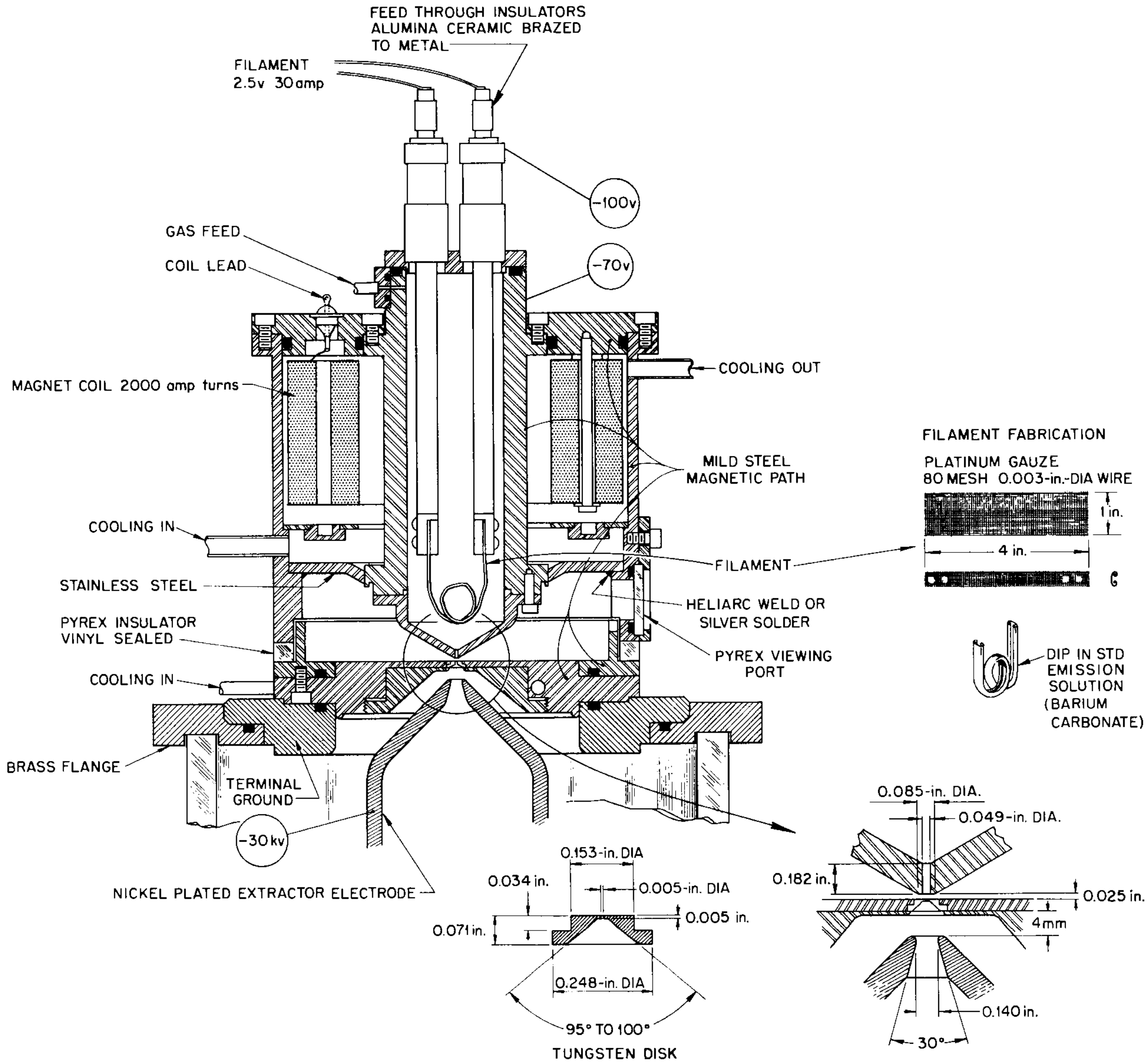

Fig. 8. Duo-Plasmatron Ion Source.

BULK SHIELDING FACILITY PARTICLE ACCELERATOR

F. R. Duncan F. M. Glass

Engineering and construction of a 300-kv electrostatic ion accelerator was completed recently at the Bulk Shielding Facility laboratory. This accelerator will be used as a source of gamma rays of known energy for the calibration of gamma-ray spectrometers. It will also be used as a neutron source for a variety of experiments, the first of which is the determination of neutron diffusion coefficients for certain materials.

This accelerator is a scaled-down close copy of an existing 600-kv machine located originally in Building 5500. However, because of the conditions of use of the bulk shielding equipment several differences of detail exist, and it is really a description of these differences which is the subject of this report.

Figure 9 is a photograph of the accelerator. This photograph was made in the early stages of construction and does not show all the final features of the installation. It will, however, serve to define the component systems of an accelerator of this type and to describe their general physical shapes and locations with respect to each other.

The heart of the device is the accelerator tube, which appears here as a stack of insulators, metallic electrodes, and series resistors in the center of the picture. At the high-potential end of this stack is an enclosure to contain all ion generation equipment, beam focusing and control equipment, and the necessary electronics to supply this equipment. At the ground-potential end are vacuum pumps to exhaust the air from the accelerator tube. Not shown in this figure but necessary to the installation are a high-voltage supply and a control center for adjusting and monitoring the operational variables.

The accelerator tube in this machine is mounted with its axis horizontal; the parent accelerator has its axis vertical. The horizontal mount was preferred in this case since it offers greater flexibility for the planned experiments. It also eliminates a beam-bending magnet but sacrifices the sorting of the accelerated particles according to energy and mass which is offered by such a magnet. The accelerator proper and as much of the associated equipment as is practical are mounted as a unit on a wheeled base so that the unit may be rolled about and aimed in various directions. Most often, however, it will be pointed either toward the swimming pool for gamma-ray calibration or rotated 180° and pointed at an area suitable for research activities. It will be possible to quickly dissociate the accelerator from long-term research apparatus for calibration activities without dismantling the research setup.

Figure 10 shows the ground-potential end of the accelerator together with a console containing all the accelerator controls. Also visible on the right side of the picture is one edge of the refrigeration unit used with the cold trap in the vacuum system.

The console is compact and is movable on casters within a radius of approximately 30 ft from the accelerator. It can thus be located as required during an experiment to permit accelerator operation concurrent with close observation of the progress of the experiment. It contains all controls and meters essential to the operation and monitoring of the vacuum system, the ion generating apparatus, the beam focusing devices, and the high-voltage supply itself. Particular attention is called to the meter which measures the beam ion current incident upon a target. The circuitry associated with this meter is such that the meter zero is constant regardless of which of the ten available meter ranges from 5 to 2000 μa is being used.

Since a pulsed source of radiation is required in some experiments, equipment to produce a pulsed ion beam is an integral part of the accelerator electronics. Basically this equipment consists of a power supply which delivers a step function voltage of 750 v to a set of deflector plates built into one of the electrostatic focusing lenses. The pulse power supply is located in the high-potential enclosure of the accelerator and is controlled as to on-off period by a radio transmitter located at ground and a receiver at high potential. This arrangement makes it very convenient to synchronize beam pulsing with associated counting and time-base-analyzer instruments. Figure 11 is a photograph of the interior of the high-potential enclosure and shows a portion of the electronics.

The power supply was purchased from Beta Electric Company and was manufactured in France by the Sames Company. Figure 12 shows this supply in place in Building 3010. The cabinet on the right is the high-voltage generator proper, while the tank on the left is an oil-filled isolation transformer to furnish 115-v a-c power for operation of the electronics in the high-voltage enclosure. The interconnecting cables between the high-voltage power section and the accelerator are in the upper left-hand section of the picture. The small size of the high-voltage generator is possible since the voltage is produced electrostatically by spraying charge onto the surface of a rotating insulated cylinder in a pressurized vessel after the manner of a Van de Graaff. The cylindrical protrusion at the top rear of the high-voltage unit is one end of this pressurized vessel.

Figure 13 shows the termination of the high-voltage cables at the accelerator end and offers a general view of the high-voltage enclosure. The small cabinet in the background is the radio transmitter for operation of the beam pulser. The small cylinder at the lower left of the high-voltage enclosure is the antenna for reception of the transmitted signals. The interconnecting tubing between the cable termination and high-voltage housing telescopes and/or rotates perpendicular to the cable terminal to provide the flexibility necessary for moving the accelerator.

Performance of the accelerator to date has been quite gratifying. The high-voltage generator is rated by the manufacturer at 300 kv and was tested by him at 350 kv. At present, operation at 300 kv is considered to be routine. Well-focused ion beams of up to 180 μa have been obtained. While neither of these values appears to be a limit of performance, they are more than adequate for presently scheduled activities. It is expected that at some time in the future operations up to 350 kv will be attempted for short intervals.

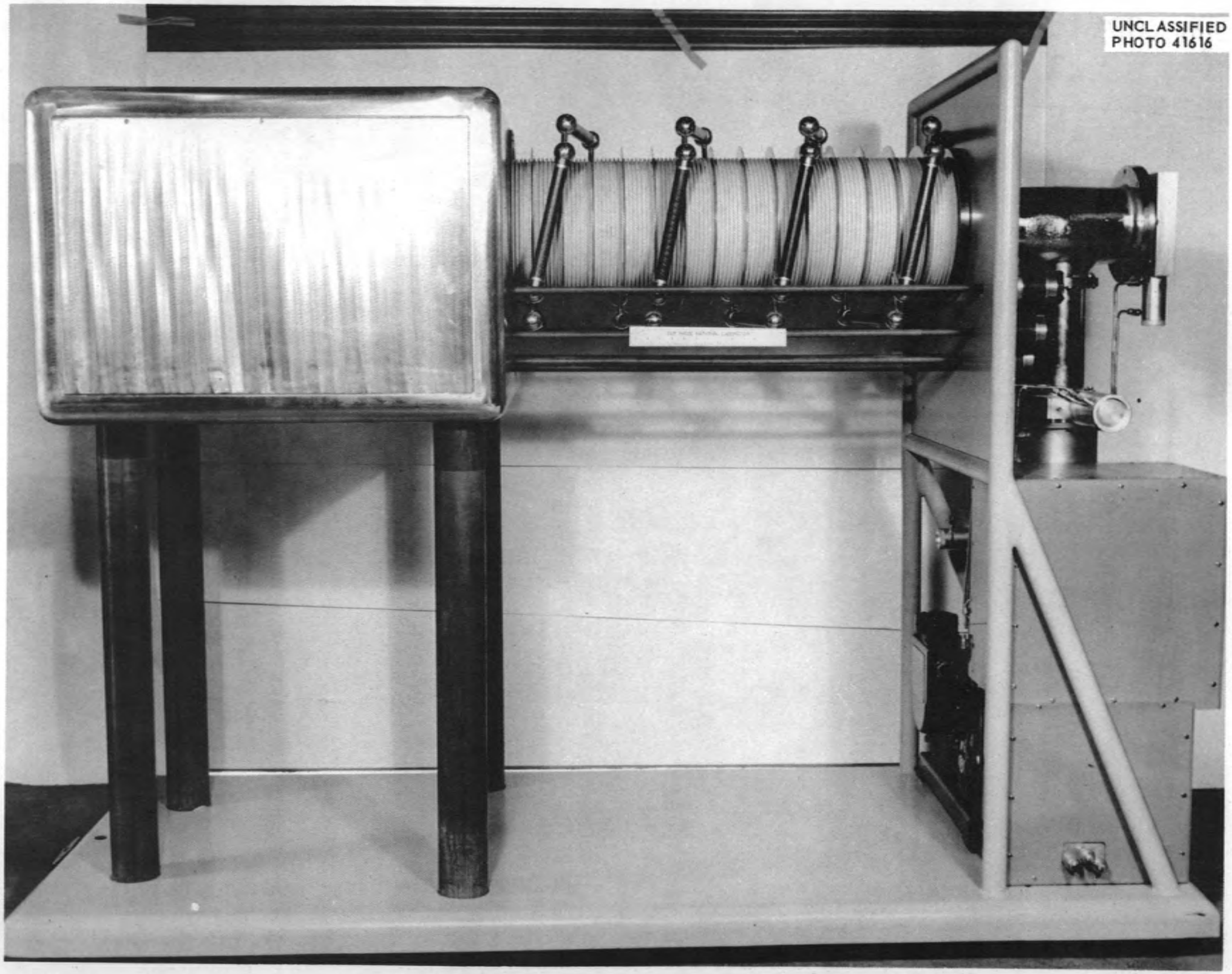

Fig. 9. General View of Accelerator During Construction.

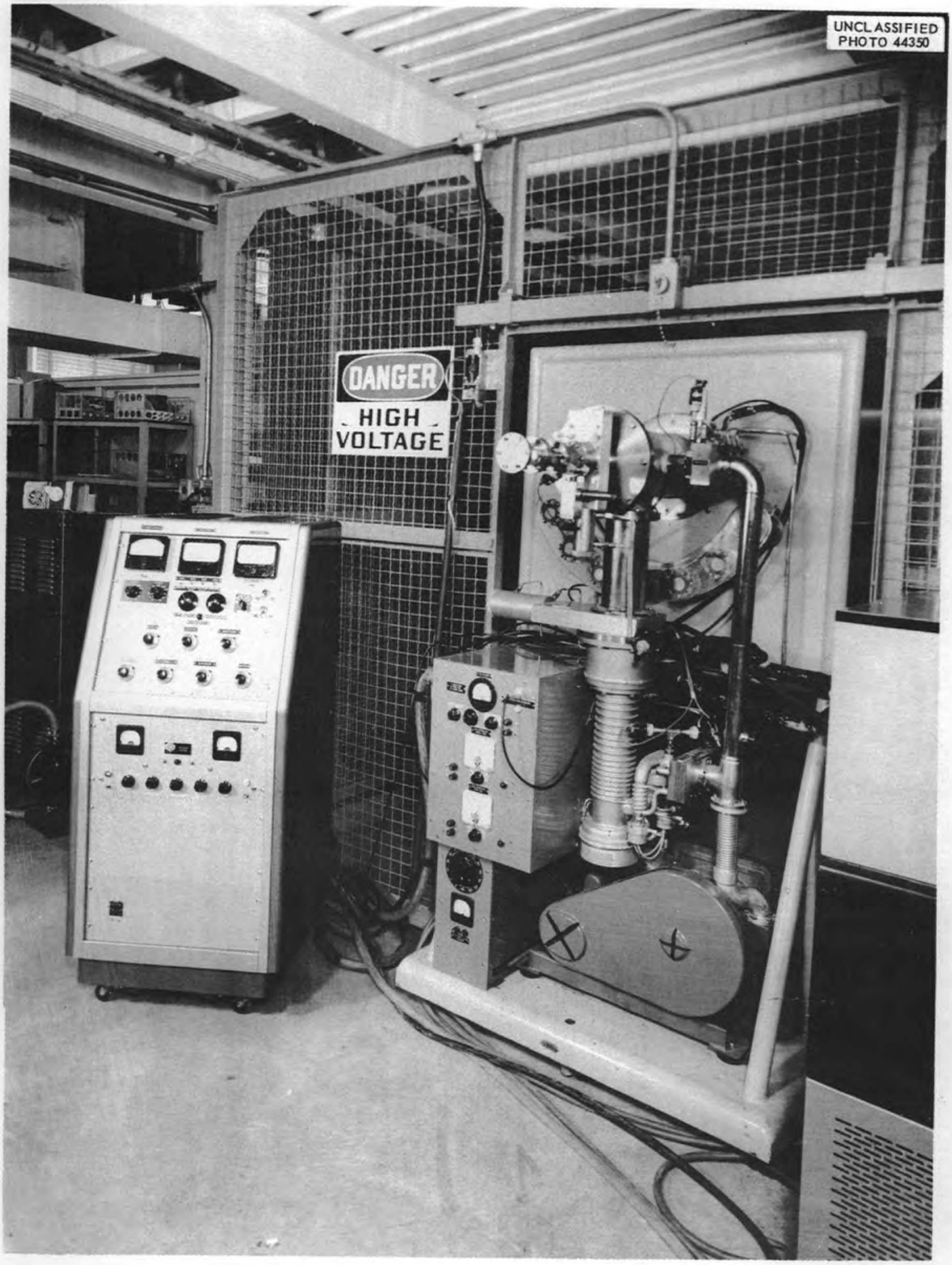

Fig. 10. Ground-Potential End of Installed Accelerator. Control console at left; cold trap refrigerator at right.

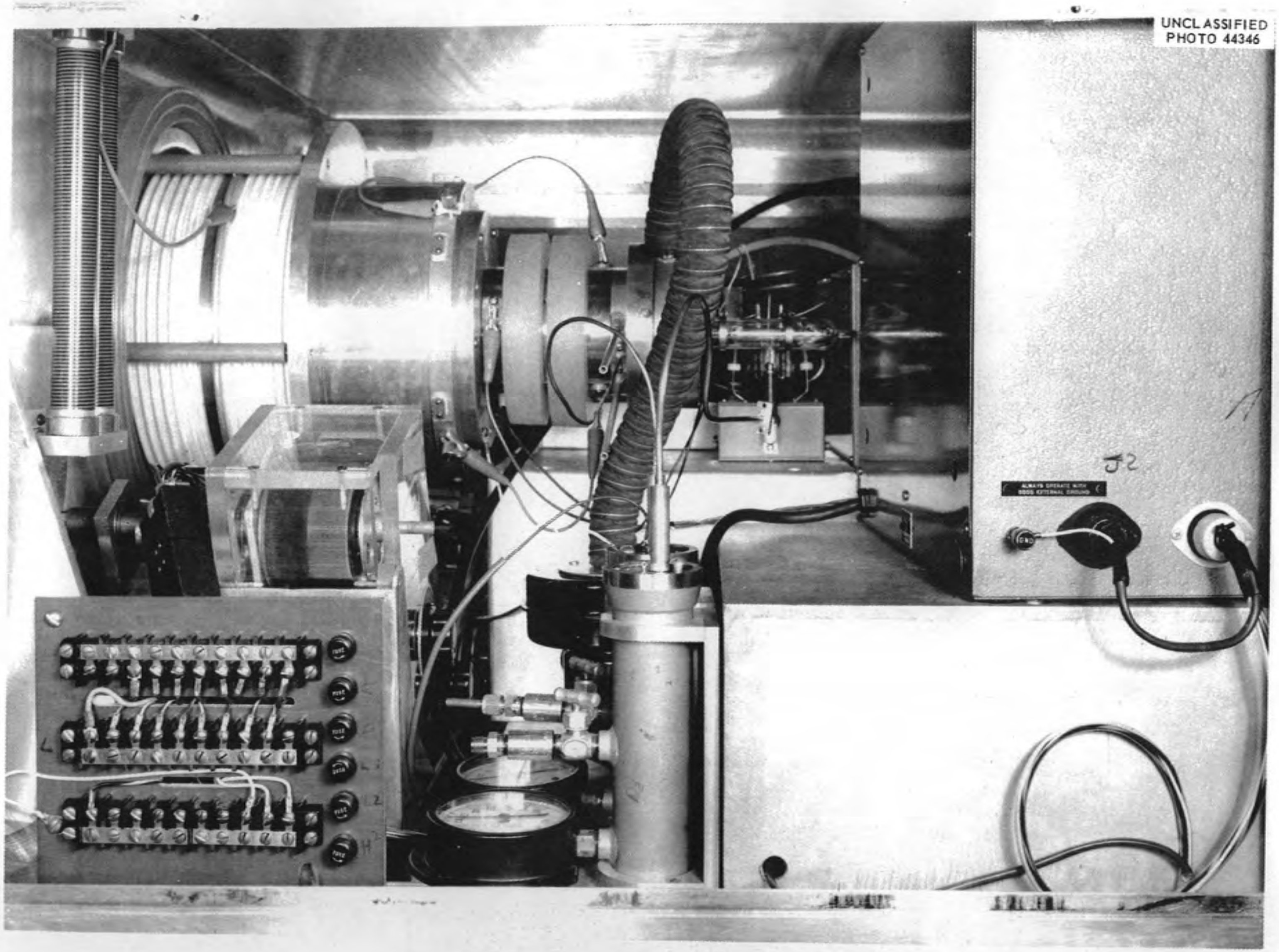

Fig. 11. Interior of High-Voltage Enclosure.

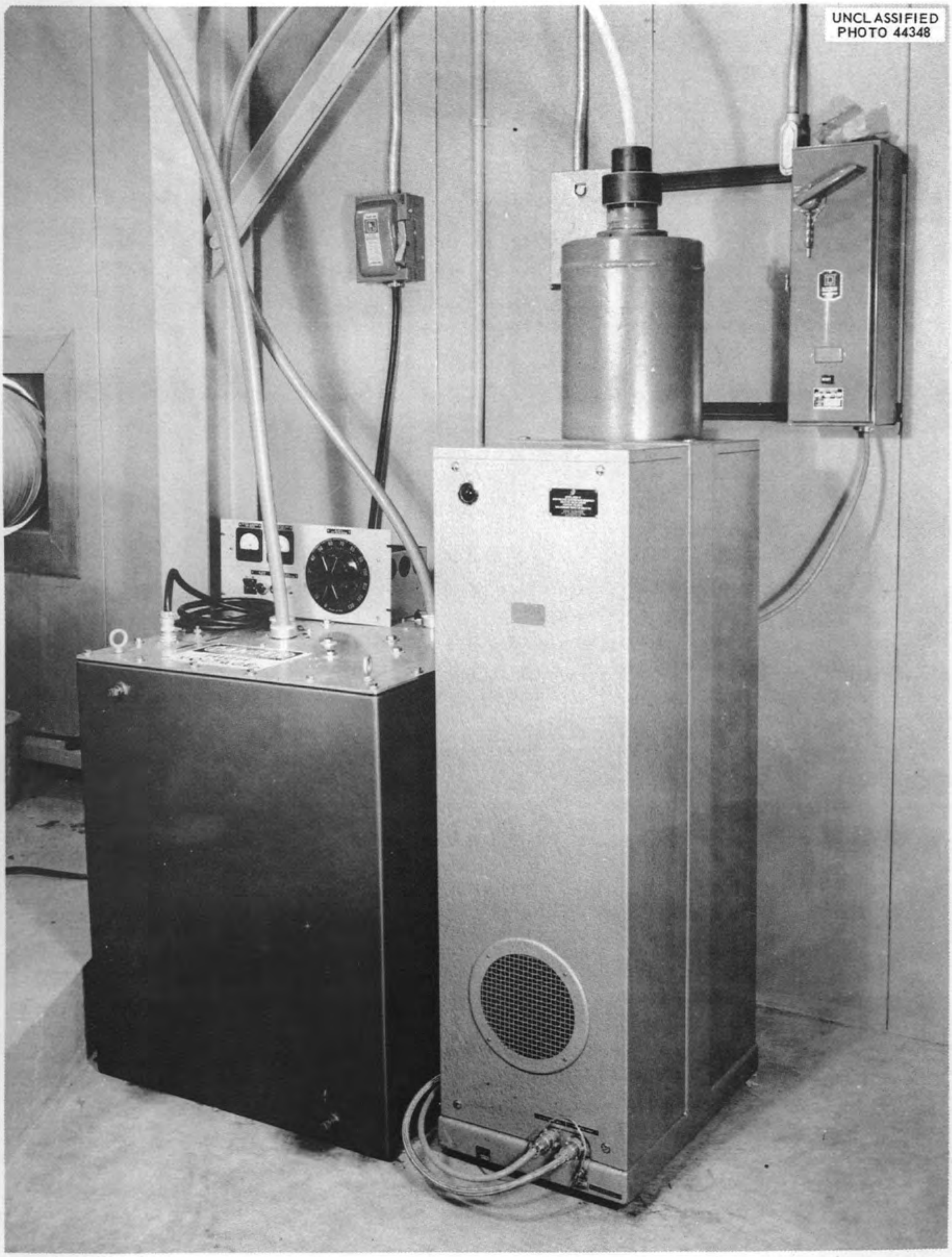

Fig. 12. Beta Electric Co. Model 6300-1 P(a) High-Voltage Supply. Isolation transformer at left; high-voltage generator at right.

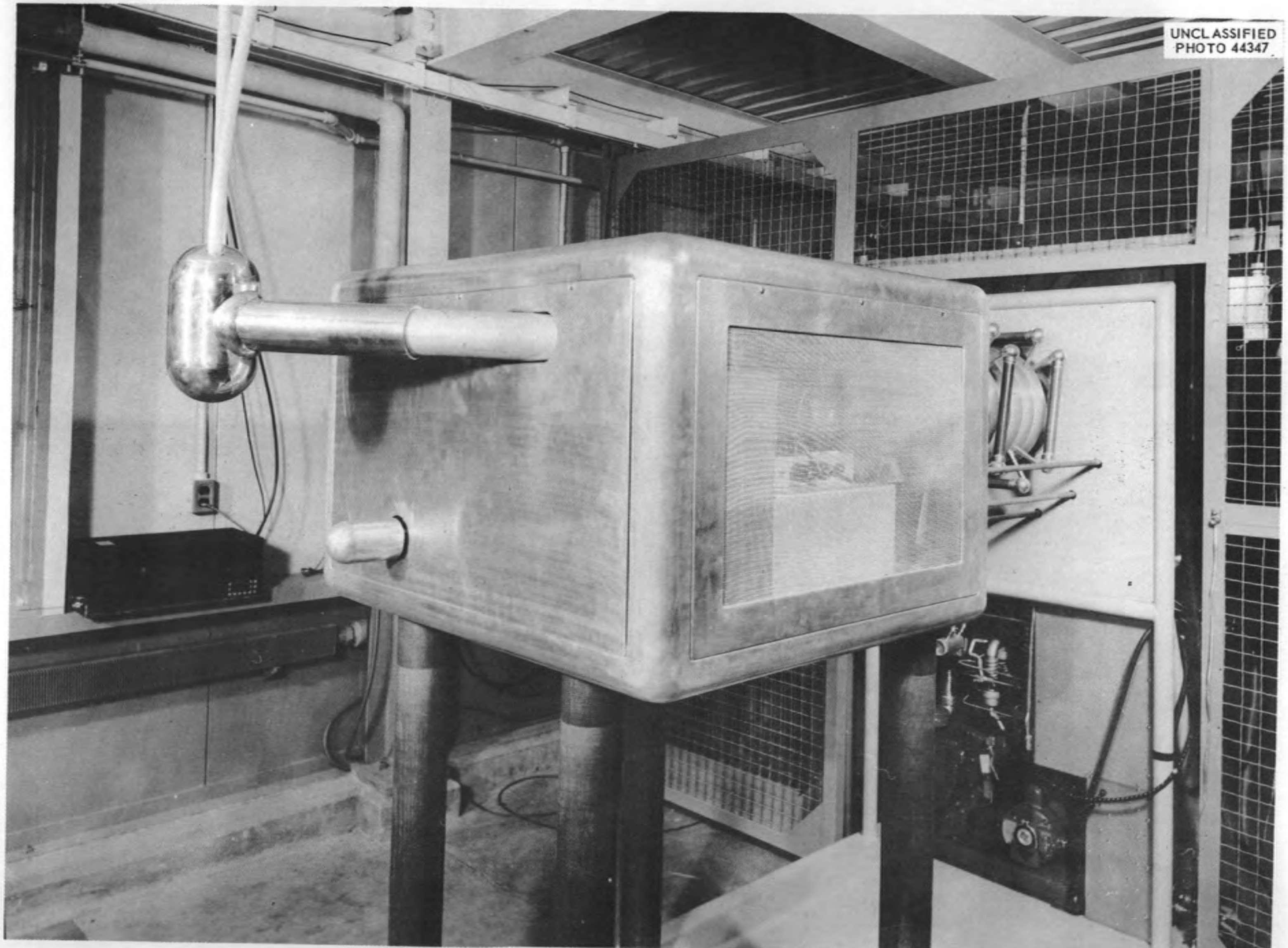

Fig. 13. General View of High-Voltage Enclosure, Showing High-Voltage Terminal, Cable Terminations, and Pulse Signal Transmitter.

CONTINUOUS WATER MONITOR FOR RADIOACTIVE WASTES[1]

F. E. Gillespie   R. E. Zedler

Introduction. – As the production and use of radioactive materials increase, the problem of control and processing of radioactive wastes becomes more important. A continuous water monitor for control of low-level, large-volume process water from ORNL has been in operation since April 1958. Before this date samples were taken from the waste water, and if the radioactivity was above the recommended level, the waste water would be manually diverted for processing. The waste water is now automatically controlled by the counting rate from the detector. Because the hazard of Sr^{90} is much greater than that of other radioisotopes, the major requirement for this monitor was the sensitivity for detection of Sr^{90}. The decay scheme of Sr^{90} and its daughter product Y^{90} is shown in Fig. 14.

Description and Operation of Water Monitor. – The components of the detector and sample container are shown in Fig. 15. There are five halogen-filled thin-walled (30 mg/cm^2 wall thickness) Geiger tubes, each protected from water and radioactive contamination by a celluloid centrifuge tube.

Some radioactivity will deposit on parts 1, 3, 4, and 5 of Fig. 15. Parts 1, 3, and 5 are disposable or can be decontaminated if desired. The stainless tubing, part 4, will need decontaminating occasionally, but not so often as the other parts since the Geiger counters are shielded from the deposited contamination on the tubing by a greater amount of water than the other part.

The detector and container are placed inside a lead shield as shown in Fig. 16. The lead shield, pump, high-voltage supply, and cable driver are mounted on a concrete pad. Below the concrete pad is the pipe carrying the waste water to be measured.

A sample rate of 1 gal/min is used at this time. A greater sample rate would give a larger lifting effect on solid particles and help to prevent the solid particles from settling to the bottom of the container.

In a building approximately 300 ft from the concrete pad are located the count-rate meter, control panel, and single-point recorder. The signal to divert the waste water for processing is obtained from switches on the recorder. The valve controlling the waste water is operated by a single-phase motor with limit switches. A block diagram of the system is shown in Fig. 17. The instruments on the left-hand side of Fig. 17 are mounted on the concrete pad at the diversion site, and the instruments on the right-hand side of Fig. 17 are located in the building referred to above. The Q numbers refer to available ORNL drawing numbers.

The control of the valve by the counting rate is illustrated in Fig. 18. The waste water is diverted when the activity reaches the high-level mark, line 1 in Fig. 18. The valve is held in the divert position until the activity goes down below the high-level release, line 2 of Fig. 18.

---

[1]This paper (No. PNW-6-58) was given at the 13th Annual ISA Instruments-Automation Conference, Philadelphia, Sept. 13–19, 1958.

The high-level release is used to prevent the continuous opening and closing of the valve if the activity should be just on the high-level line. Line 3 of Fig. 18 is the low-level divert line, which diverts the waste water if the counting rate should go below some set level. Thus, if the Geiger counters should fail, the water would be diverted for processing as a safety feature.

The control panel contains lights to indicate the position of the motor-controlled valve. Also, three lights are used to indicate the signal (high-level divert, normal operation, or low-level divert) taken from the recorder and sent to the motor-controlled valve. A manual control switch is provided to override the recorder information. A switch is provided to check the operation of the Geiger counters; the cathodes of all Geiger counters except the one to be checked are raised to 200 v, putting them out of operation.

Calibration. — The water monitor was calibrated by counting a solution having 1000 disintegrations of Sr^{90} (in equilibrium with Y^{90}) per minute from each milliliter. The observed counting rate of the five Geiger counters for this solution was 5600 counts/min with an original background of 120 counts/min. The solution was drained and the container washed with fresh water. The background then read approximately 300 counts/min.

Where this monitor is used at low activity levels, the statistical fluctuations in counting set a limit to the sensitivity. The sensitivity limit is approximately 6.8×10^{-6} μc of Sr^{90} per milliliter. The maximum permissible concentration in water for Sr^{90} in equilibrium with Y^{90} is 8.0×10^{-7} μc/ml. In order to bring the threshold of detection for this monitor down to drinking water tolerance, the sensitivity would have to be increased by a factor of 9. In its present use there is sufficient dilution by other water sources so that this extra sensitivity is not required.

Conclusions. — This paper has illustrated a design of a water monitor with low-cost disposable parts. In this way operating personnel are able to keep the contamination of the container to an acceptable level. The cost of the electronic equipment needed for this system is approximately $2250. This amount includes recorder and control panel. The cost of valves, piping, and construction will vary with the size of the installation.

This method allows monitoring at a remote location without requiring the cost of a building to house the monitor. Also, a check on the operation of the detector can be obtained without visiting the remote site.

Future work is planned for calibrating the monitor with Sr^{90} solutions that are not in equilibrium with Y^{90}.

Acknowledgment. — The electronic design for this project was done by F. M. Glass. The design of the lead shield and piping was under the direction of W. R. Sanford. The authors would like to acknowledge the help of many other members of the Laboratory without whose service and guidance this project could not have been completed.

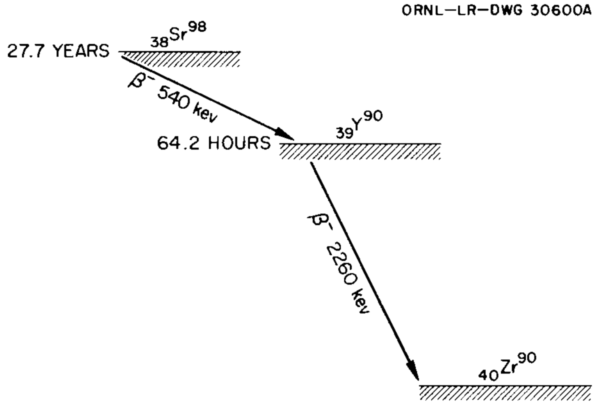

Fig. 14. Decay Scheme of Sr^{90} and Y^{90}.

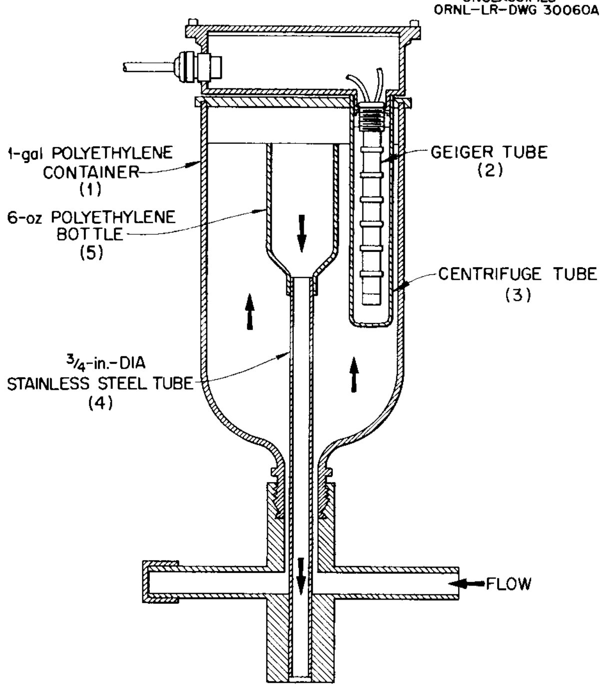

Fig. 15. Detector and Container for Water Monitor.

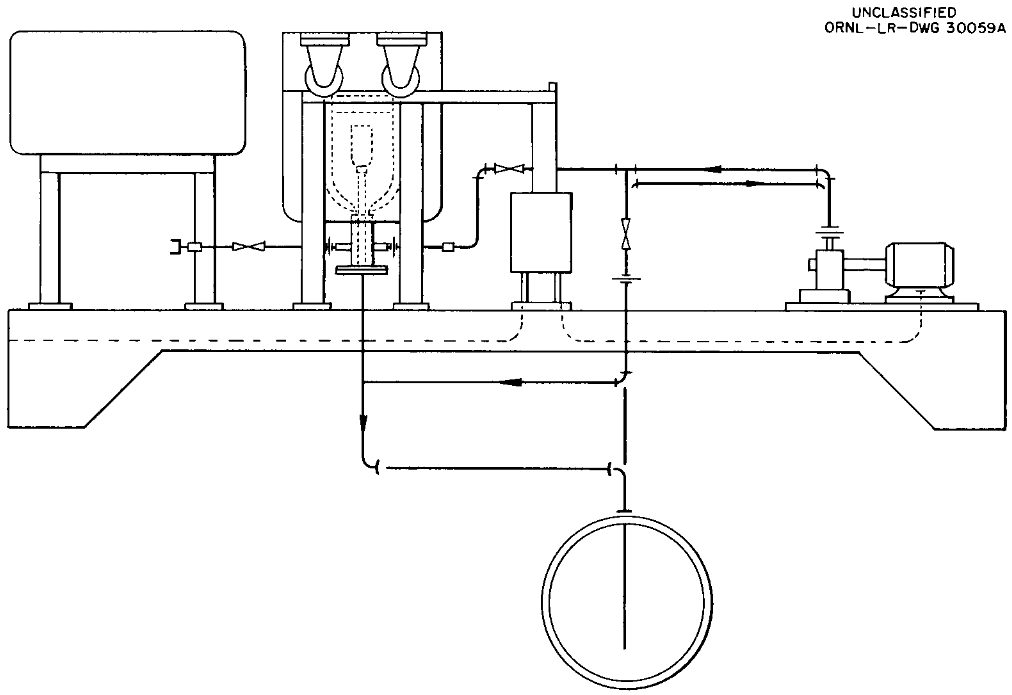

Fig. 16. Piping Diagram for Water Monitor. Located on the concrete pod from left to right are: high-voltage supply and cable driver, lead shield with contoiner and Geiger counters, starter for pump motor, and water pump. Below the concrete pad is the pipe carrying the waste water to be measured for beta and gamma radioactivity.

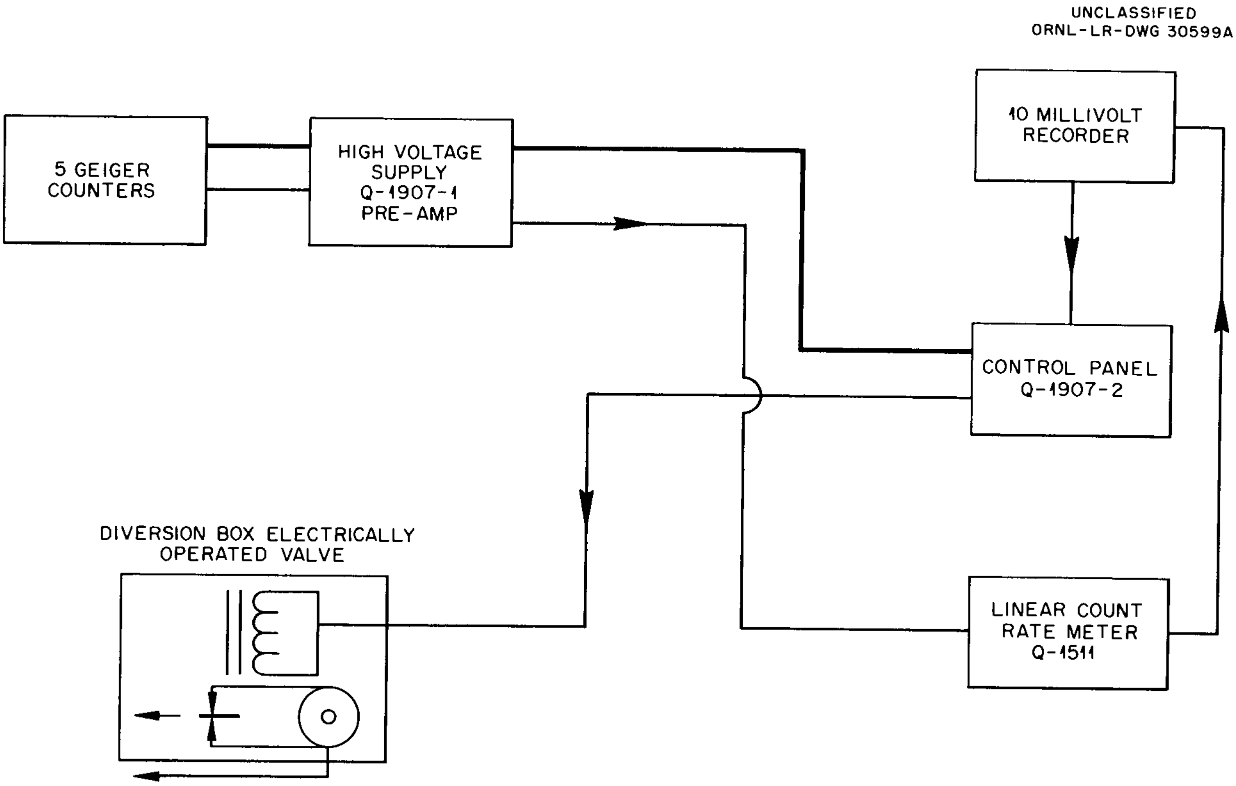

Fig. 17. Block Diagram of the Water Monitoring System.

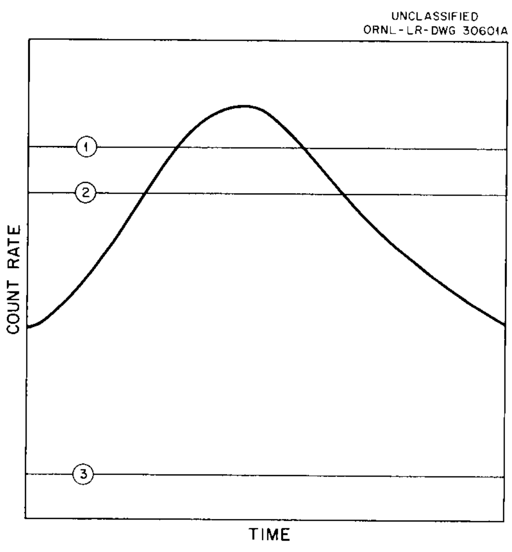

Fig. 18. Response of Monitoring System to Active Waste. Line 1 is the high-level divert line, line 2 is the high-level release, and line 3 is the low-level divert line.

X-RAY SCINTILLATION CRYSTALS

V. A. McKay

Two sodium iodide x-ray crystals have been prepared by the Radiation Detection Section. These two crystals have been in use since early in May 1958. The crystals are potted in vacuo and have low-absorption beryllium windows for photon entrance.

The crystals were examined as regards their low-energy sensitivity by irradiation with Fe^{55}. This isotope decays by electron capture, with the subsequent emission of Mn^{55} K x rays ranging in energy from approximately 5.8 to 6.5 kev. The detectors were capable of resolving the x rays well enough from the noise to get a definite photopeak, but the valley between the peak and noise was too close to the half height to permit a percentage resolution to be defined accurately. These tests were performed in the presence of much gamma background and without optimum noise levels in the electronics. High-gain phototubes were used in the above tests.

One crystal, in use by the Chemistry Division, is 3/4 in. in diameter by slightly less than 0.008 in. in thickness. It is used to measure the intensity of Mo Kα x rays scattered at the Bragg angle by single crystals of various compositions. The other crystal is 1 in. in diameter and the same thickness as the first. It is being used by the Microstresses in Crystals Department of the Metallurgy Division. This department reports a counting efficiency of 98% for Cu Kα radiation, as compared with 62% efficiency obtained with a Geiger counter.

Preparation of NaI(Tl) Crystals. – The crystal blanks were string-sawed from larger crystals that had been lathe-cut to approximately the finish diameter. After vacuum-drying, the blanks were finished in a dry atmosphere. The face of each crystal was machine-polished, and the back was finished with 400-grit abrasive paper to obtain a diffuse reflector.

Figure 19 shows the crystal position relative to the electron multiplier phototube and glass disk light pipers. The crystal was bonded to the glass disk with 2 1/2-million-centistoke DC-200 series silicone damping fluid. A 0.67-μ (180-μg/cm^2) aluminum foil was optically coupled to the back of the crystal with a trace layer of Dow Corning high-vacuum grease. Silicone fluid was used to couple the light pipers and the phototube.

The window material is high-purity beryllium. The beryllium disk was bonded to the aluminum cap with Miracle epoxy No. 185. Other epoxies were used, but they broke when the window flexed as a consequence of withstanding atmospheric pressure during evacuation.

The capsule was assembled in a dry box and then sealed by compressing the neoprene gasket by means of the retaining screws. Subsequently the capsule was removed to a manipulator vacuum chamber; the chamber was then evacuated, and the capsule unsealed by the use of the manipulator. The chamber reached a pressure of 0.03 μ Hg, whereupon the capsule was resealed. The chamber was then returned to atmospheric pressure, leaving the capsule evacuated. As was mentioned previously, the capsule was coupled to the phototube and secured by the holder assembly. Black electrical tape was used to complete the light shield.

UNCLASSIFIED
ORNL-LR-DWG 36658

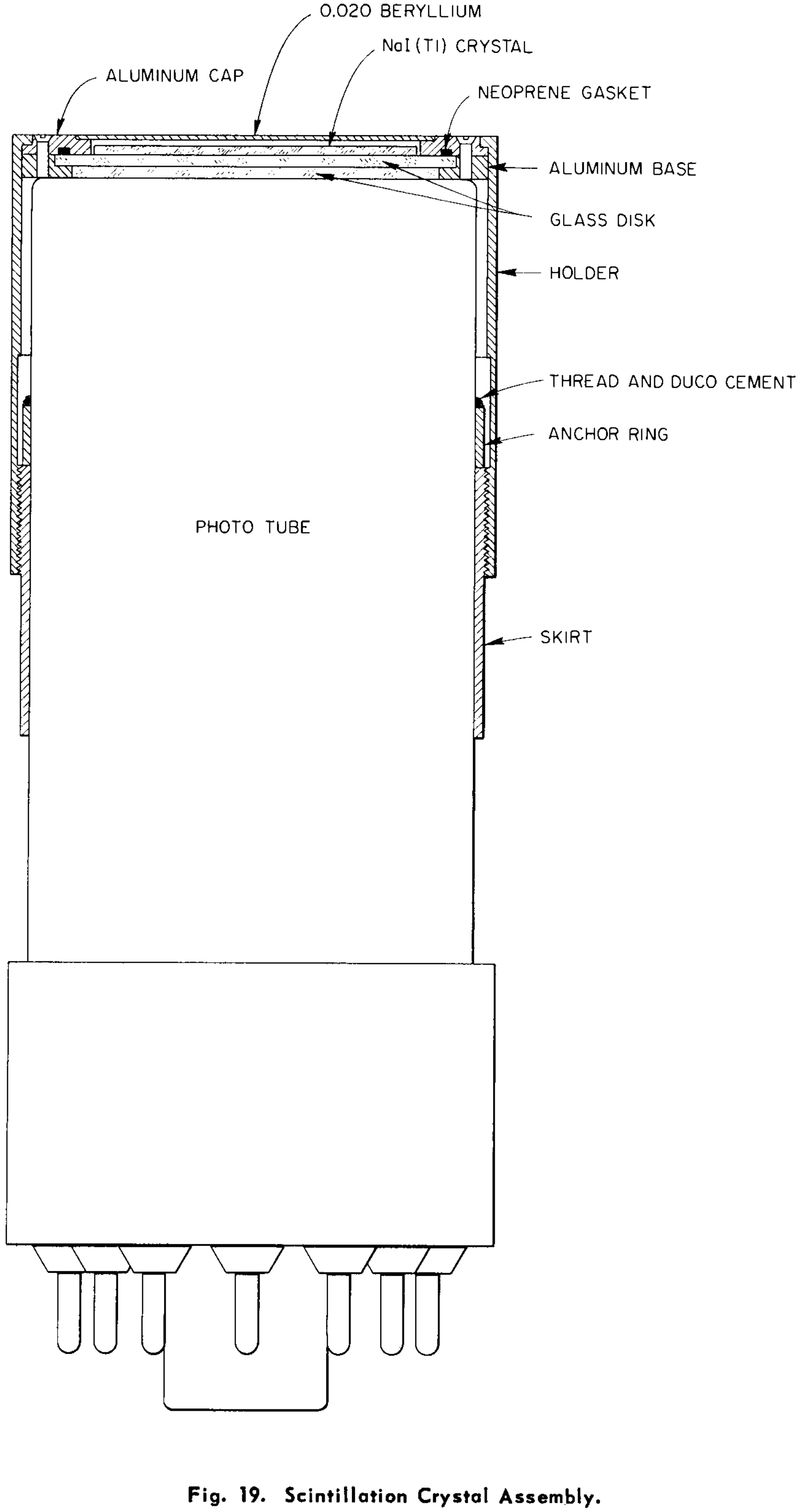

Fig. 19. Scintillation Crystal Assembly.

INSTRUMENTATION FOR SELF-SINTERING WASTE DISPOSAL

T. M. Gayle

The self-sintering waste project of the Health Physics Division is concerned with the concentration and disposal of highly radioactive waste. The waste products will initially be mixed with crushed limestone rock and boiled to drive off aqueous components. Further heating to as high as 900°C would presumably produce a sintered rock mass in which the fission products are fixed and not soluble or leachable in water. A primary aim of the study is to determine the feasibility of utilizing the inherent gamma activity as a source of heat for both boildown and sintering of the waste. It was desired in the initial study to provide an adiabatic shield for the sintering vessel and to use a smaller mass of waste than would normally be necessary to supply all the heat required. Figure 20 shows the sintering vessel with the upper mixing chambers and associated equipment.

Instrumentation consisted of temperature recording for some 36 points in the vicinity of the vessel and in the off-gas processing facility, differential temperature control for six zones between vessel and shield, power recording and totalizing for heaters, level and gravity measurement in the off-gas plant, and viscosity recording during the rock addition operation.

Differential temperature control of the six adiabatic zones was accomplished by a single multipoint controller positioning six 20-kva induction regulators in the heater circuits. The multipoint controller system was designed specifically for this application but is readily adaptable to other uses.

Due to the configuration and physical requirements of the vessel and shield, it was necessary to use 1/4-in.-OD swaged (metal-clad) Chromel-Alumel thermocouple material. At that time little was known about the effects of radiation on such material. For the differential temperature measurements, couples mounted inside the metal sheath but insulated from it were required. It was expected that gamma radiation levels for the couples would run as high as 5×10^6 r/hr for a period of two months. There were two points of concern:

1. What would be the effect of gamma radiation on the insulated couples? More specifically, would the insulated couples be raised in temperature relative to the sheath temperature due to the gamma flux or would they read the sheath temperature without correction?

2. What would be the permanent effect of the gamma flux on thermocouple calibration?

Tests were run on four samples of swaged couples in the Graphite Reactor canal with cobalt slugs as a gamma source. Average gamma radiation was 6×10^5 r/hr over a total exposure time of 230 hr. Temperature was controlled by an electrical heater and was varied from 20 to 500°C. Swaged material used was 1/4-in.-OD Inconel sheath with 16-gage Chromel-Alumel wire and magnesium oxide insulation.

UNCLASSIFIED
ORNL-LR-DWG 25073R

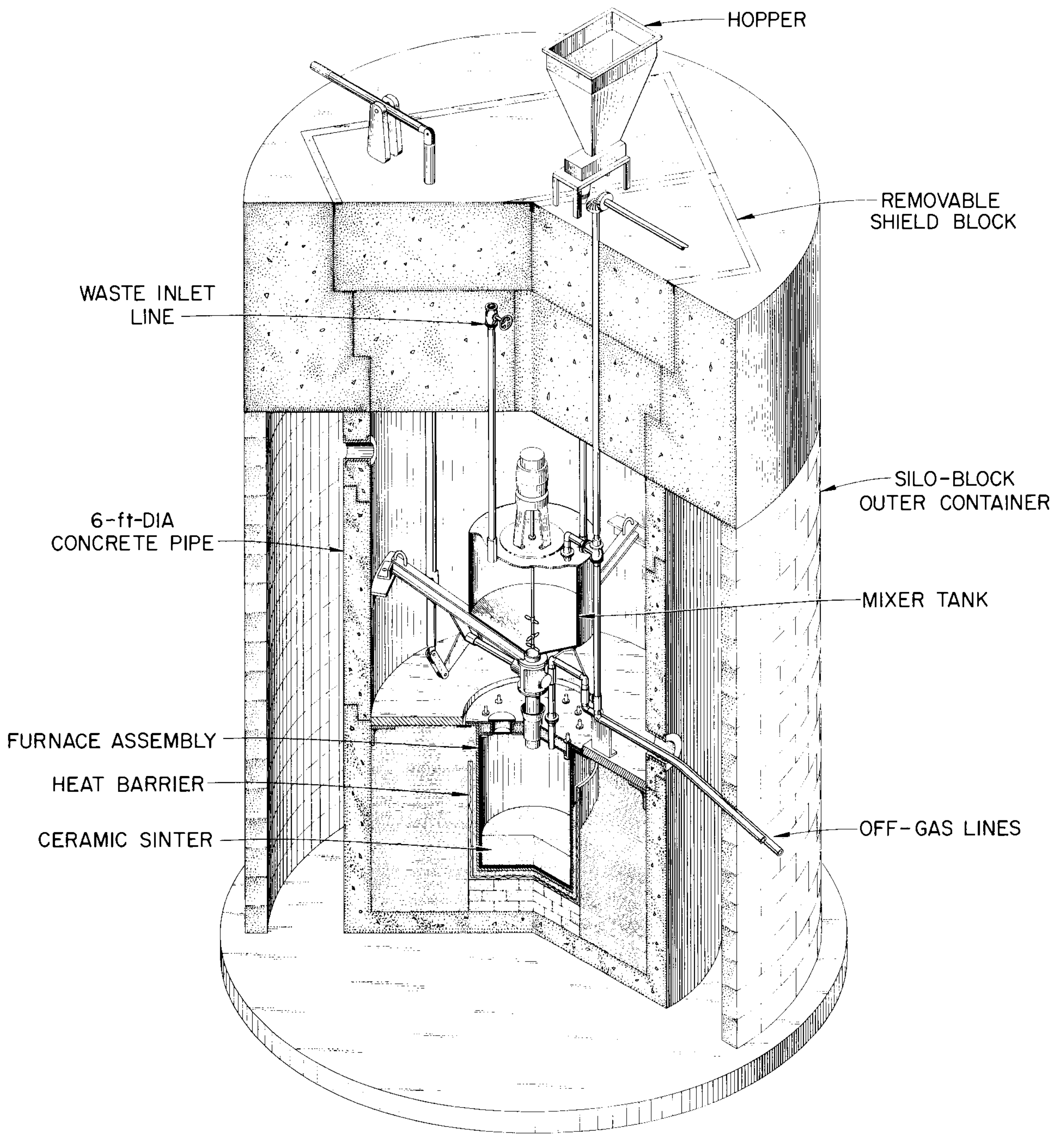

Fig. 20. Experimental Facility for High-Level Self-Sintering.

Results of the test were:

1. The insulated couple in the swaged material read the same as a couple grounded to the sheath. Addition of a 5×10^5 r/hr gamma field caused a rise in both couple temperatures from 23 to 36°C. Under the conditions of this test, it was not possible to separate the components of temperature rise due to gamma heating of the couple, the sheath, the containing vessel, and the surrounding water.

2. No permanent shift in calibration could be found in either type of couple due to the integrated gamma exposure of approximately 7.5×10^8 r. No damage to the magnesium oxide insulation was found, although only superficial checks of insulation resistance were made.

Viscosity measurement of the liquid in the mixing chamber was made with a Bendix ultrasonic viscosity transducer. Readout was made on the main control panel, and provision for recording the viscosity signal during the mixing cycle was provided. The Bendix unit functioned well in all simulated tests and cold runs, and it is apparent that the design of the particular probe used is completely adequate for the radiation levels expected. A second viscosity meter incorporating a motor-driven drag cylinder was developed but has not received extensive testing.

Although final completion and operation of the sintering project has been delayed, instrumentation is essentially complete.

INSTRUMENTATION FOR POWER REACTOR FUEL ELEMENT DISSOLUTION

P. D. Koster

The laboratory-scale hydrofluorination facility for power reactor fuel element dissolution was designed and built primarily to determine the feasibility of dissolving zirconium-jacketed fuel elements in a molten fluoride salt. Moderate successes were attained, with resulting dissolution rates in the milligrams per square centimeter per minute range.

The original physical setup of the process elements is shown in Fig. 21. The two hinged tube furnaces contain the salt preparation tank (in the center foreground) and the dissolver (on the left). Hydrogen fluoride gas was supplied to the system from a bottle (far right on Toledo scale) through a pressure regulator and a Monel Research Controls valve. In this process, when it is necessary to transfer the molten salt from tank to tank, valving is accomplished by thawing and freezing the salt in a trap formed by a loop in the line. The lines are thawed by autoresistance heating of the pipes and by furnaces located at the traps of the "freeze valves." The two freeze valves and their associated furnaces can be seen in the center of Fig. 21. On the left side of the cell are the product tank (sitting on scale) and (in white insulation) the condenser for excess HF from the dissolver.

Fig. 21. Laboratory-Scale Hydrofluorination Facility for Power Reactor Fuel Element Dissolution.

The problems in instrumenting the hydrofluorination facility fell into three major categories: temperature measurement and control, valving and flow control for the HF, and liquid level and density measurement.

The temperature controls for all the furnaces in the system are Wheelco model 401 Capacitrols (see Fig. 22) with the contactors and associated Variacs located on the outside of the cell (see Fig. 23). The temperature controls for the dissolver and salt preparation tanks have two controllers for each unit. This arrangement was installed so that either a possible exothermic reaction or overheating of the furnace element winding would cut off the power. The installation and operation of this system have been satisfactory. Two Minneapolis-Honeywell strip-chart recorders (see Fig. 22) were used for monitoring temperatures at various points in the system. In order to measure the temperature of the salt transfer lines it was necessary to weld thermocouples directly to the autoresistance-heated pipes (which carry 500 amp at 5 v ac). It was anticipated that a-c pickup might affect the accuracy of the thermocouple readout system, but operation proved to be satisfactory and the a-c pickup of no consequence.

The flow metering, measurement, and control for the HF in the system presented some problems because of the corrosive nature of the fluid. The flow metering was done by rotameters fabricated of fluorothene and Monel at the Oak Ridge Gaseous Diffusion Plant. Research Controls valves were used exclusively both for metering and shutoff. These valves are all-Monel with bellows seal. The on-off valves have Teflon seats. The Research Controls valves have given completely satisfactory service to date.

The measurement of level and density was accomplished by the conventional method of dip tubes purged with inert gas, and the resulting differential gas pressure was measured by a differential pressure transmitter. These systems gave trouble because the molten salt would freeze and plug the dip tubes during pressure surges. There is currently under test an autoresistance-heated dip tube which it is hoped will solve this plugging problem.

The instrument panel board, shown in Fig. 22, utilized standard industrial indicators and recorders wherever possible. There is, however, one instrument that might be of special interest. Above and slightly to the right of center are two black-faced selsyn indicators originally produced for use as radio compasses. These compasses have been adapted as receiving selsyns for position transmitters attached to the pointers of the Toledo scales. In this fashion, remote reading of the scales can be accomplished.

The process piping has undergone considerable change during the 18-month period of operation in order to accommodate design modifications. During this time enough experimental information has been obtained to warrant building a full-scale unit in the Volatility Pilot Plant.

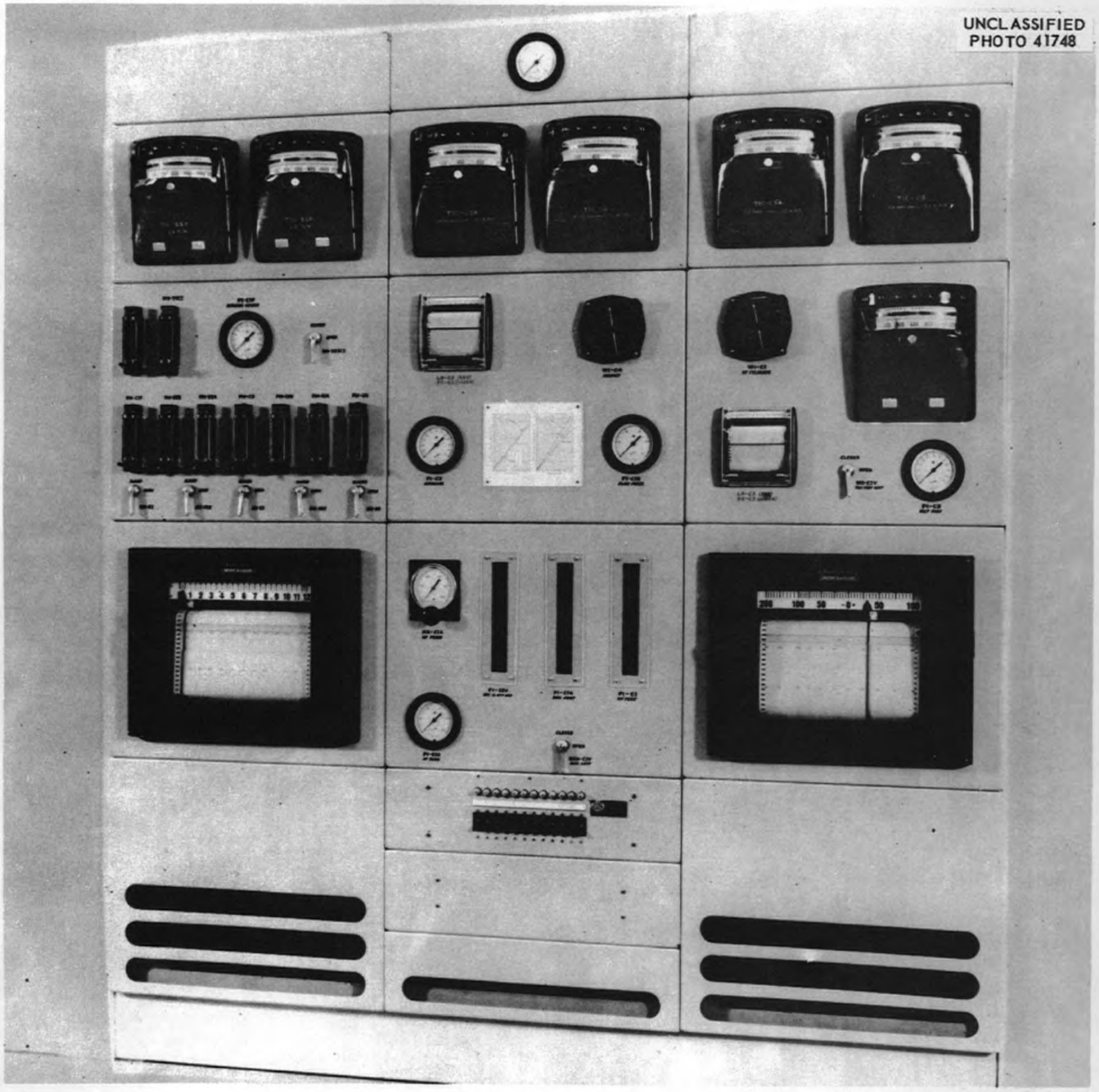

Fig. 22. Control Panel for Hydrofluorination Facility.

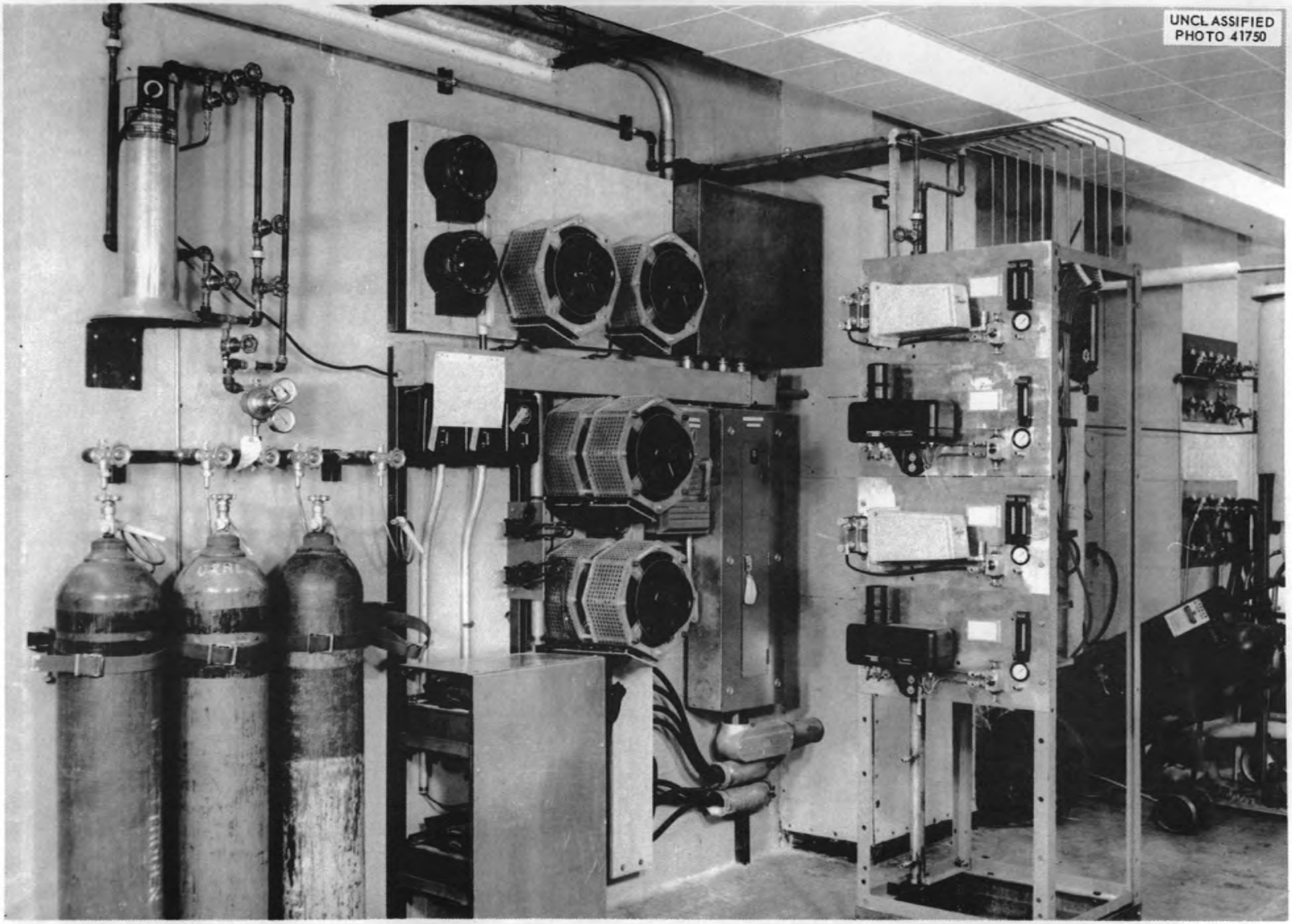

Fig. 23. Contactors and Associated Variacs for the Hydrofluorination Facility.

PARTICLE COUNTING AND INVENTORY TECHNIQUES
IN A JURY ION EXCHANGE COLUMN

M. J. Kelly T. M. Gayle

Continuous and semicontinuous moving-bed ion exchange columns were investigated by Higgins *et al*. at ORNL and by Jury at ORNL and the University of Tennessee.[1] A resin flowmeter for the Higgins packed column was developed and previously described.[2]

Dynamic chemical balances necessary for efficient operation of the Jury column could be more easily obtained if an accurate determination of resin flow rate were available. To this end, preliminary efforts have been made to determine mass resin rates in the return leg and to count individual particles.

Mass rate determinations were obtained by multiplying the carrier water flow rates by the resin concentrations. The flow rates were measured with a conventional orifice meter, and the resin concentrations were obtained with a photoelectric device. The general arrangement of this equipment is shown in the left-hand side of Fig. 24.

The system was calibrated by collecting the moving resin in a settled bed and measuring the volume under conditions similar to those encountered in normal operation of a Jury column. While the resultant calibration curve was somewhat nonlinear, it was reasonably reproducible, and this device proved successful for determining mass rates.

Two techniques were used in the experimental determination of particle rates: counting by means of a reflecting photoelectric transducer and counting by means of dynamic changes in electrolytic conductivity.

The photoelectric transducer employed was a model 442 unit manufactured by Berkeley Division of Beckman Instruments. This device consists of a light source, a photocell detector, an optical system, a high-gain a-c amplifier, and a cathode-follower output circuit. General arrangement of the accessory equipment is shown in Fig. 24. Light from the source in the unit is transmitted through a semireflecting mirror and focused by the lens system on an external reflecting surface. The reflecting surface used in the tests was a polished stainless steel tube mounted concentrically within a glass pipe. Reflected light from the stainless steel surface passed back through the lens system in the Berkeley unit to the mirror, which reflected the return light through an aperture to the phototube. Interruption of the light beam by a resin particle passing between the stainless tube and the glass wall in the critical focal region produced an output pulse of about 7 v. Interruption of as little as 10% of the light could produce a pulse. With normal flow rates, pulses of about 15 μsec rise time were noted.

---

[1]See T. A. Arehart *et al*., Chem. Eng. Prog. 52, 353 (1956).

[2]T. Gayle and P. D. Koster, *Instrumentation and Controls Ann. Prog. Rep. July 1, 1957*, ORNL-2480, p 46.

The fact that the Berkeley unit is paralyzed when more than 10% of the light is interrupted means that the counter has a dead time and that statistical corrections should be applied to the data. These corrections to the pulse data were made in much the same manner as Geiger tube counting is corrected. Results from a number of tests with various physical mountings of the Berkeley unit demonstrated that the photoelectric method would be suitable for a glass column, especially in the lower resin rates. Higher rates could be handled, but some refinement in technique would be required.

Particle counting by conductivity depends on the fact that the total electrolytic conductivity of a resin particle is somewhat higher than that of the surrounding aqueous medium in the wash section of the Jury column. The basic principle of particle counting by the conductivity method can be understood by reference to Fig. 25. The conductivity bridge (excited by dc) was constructed with one leg made up of a pair of electrodes embedded in the throat of a venturi. As a resin particle traversed the electrode region a pulse was produced at the output of the bridge. Conventional amplification, indication, and totalization were provided for readout.

Some early tests made by simply inserting a pair of electrodes in the return leg of the column with spacings of approximately 1/32 in. indicated that such a simple counting technique might be feasible. However, a poor signal-to-noise ratio, due in part to the low particle velocity, prompted development of the venturi technique. The venturi could, if desired, be the same unit used as the prime mover in the Jury column. Counting the total number of particles and counting these at the greatly increased velocity afforded by the venturi resulted in a much improved signal-to-noise ratio. The limiting counting rate was approximately 600 particles/sec, apparently due to particle coincidence at the throat of the venturi. Metering only a fraction of the total resin stream or altering the venturi design might overcome this limitation.

It is felt that both the photoelectric and conductivity methods of particle counting can be further improved. The experiments described here were performed to establish the feasibility of the measuring techniques.

UNCLASSIFIED
ORNL-LR-DWG 33787A

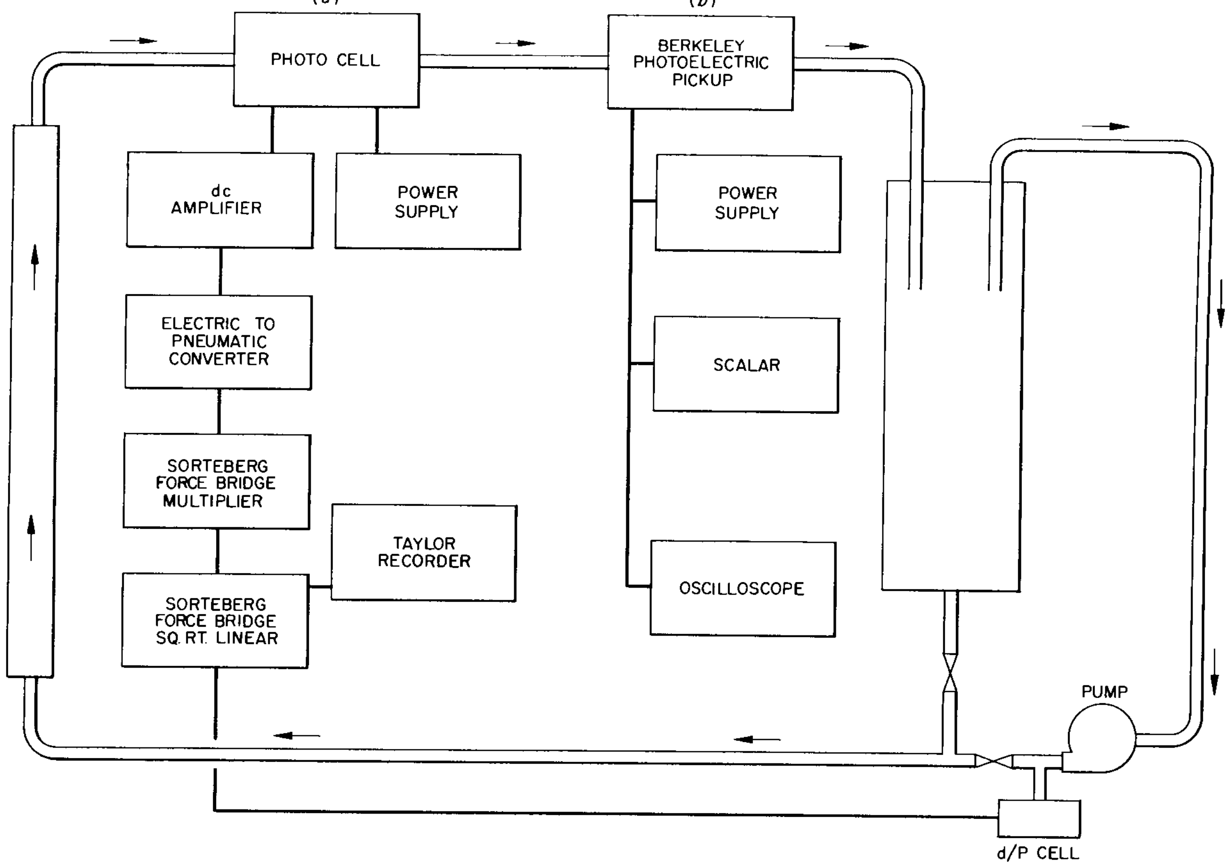

Fig. 24. Resin Loop. (*a*) Mass rate determination. (*b*) Particle counting with light interruption.

UNCLASSIFIED
ORNL-LR-DWG 33786A

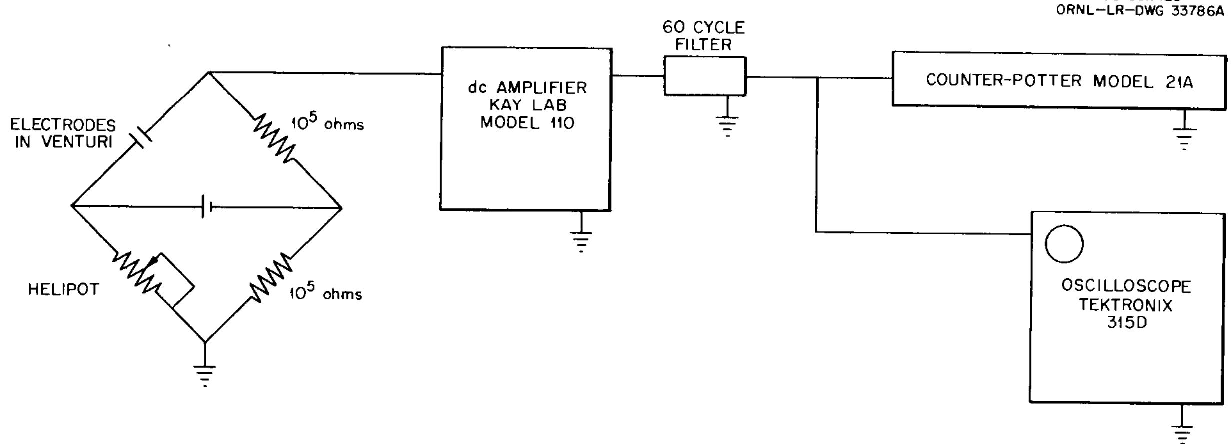

Fig. 25. Resin Particle Counting by Conductivity.

RADIATION EFFECTS ON PLATINUM vs PLATINUM-10% RHODIUM THERMOCOUPLES

M. J. Kelly

The use of platinum vs platinum-rhodium thermocouples is attractive for projected in-pile experiments at temperatures in excess of 2000°F, where the space available for the measuring element is both inaccessible and restricted in size. In laboratory service they are unquestionably better than base-metal couples at high temperature from the standpoint of both service life for the same wire size and stability of the emf output at constant temperature. For experimental measurements in nuclear reactors their use has been avoided since the rhodium component has a large nuclear cross section (150 barns) and converts to palladium, whose thermal emf to platinum is opposite to that of rhodium. Experimental data have not been available on the magnitude of this effect as a function of neutron exposure.

In cooperation with the Solid State Division, irradiation experiments were placed in the LITR, the ORR, and the MTR to experimentally determine the magnitude of these changes with thermal neutron flux exposure.

Short thermocouples (15 to 18 in.) were fabricated and placed in aluminum tubes. These assemblies were then irradiated for a chosen number of reactor cycles. When the individual tubes were removed they were set aside until the short-lived isotopes had decayed. Both the platinum and the rhodium were of extremely high purity; the only gamma emitter remaining after a few weeks of decay was Ir^{192}. The irradiated thermocouples were then recalibrated, an unirradiated thermocouple made from the same spools of wire being used as a control. No change in the platinum wire was observed, but the platinum-rhodium alloy wire showed a decrease in thermal emf at a given temperature due to the transmutation of the rhodium to palladium. The magnitude of the change vs exposure is shown in Fig. 26.

The thermocouples were irradiated in three different reactors. The data are plotted as observed percentage errors at 1900°F vs neutron exposure, nvt. Data from the LITR and the ORR will be extended, since additional couples with greater nvt exposure will be available for calibration later.

The horizontal spread of individual points represents the maximum uncertainty of integrated flux. The flux data were obtained from other workers at the same locations.

A complete report on this project will be issued when the data on higher exposure times are available from the ORR.

UNCLASSIFIED
ORNL-LR-DWG 36659

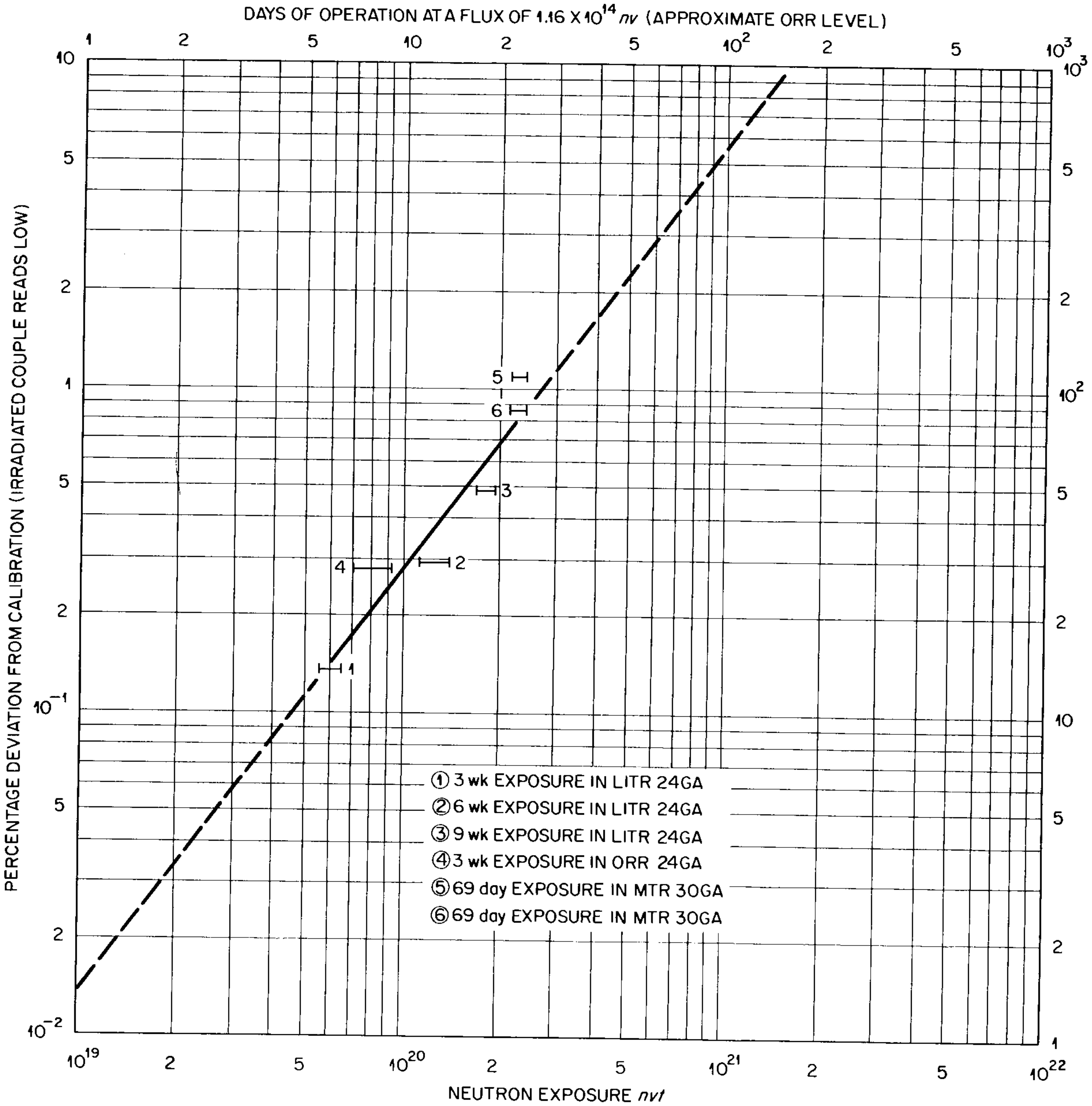

Fig. 26. Effect of Neutron Exposure on Platinum vs Platinum–10% Rhodium Thermocouples.

ANODIC DECONTAMINATION FOR INSTRUMENT SENSING ELEMENTS

M. J. Kelly

In a program to develop in-line radioactivity monitors for continuously measuring the level of radiation of process streams, the plating out of radioactive particles on the pipe or sample container causes the background radiation to increase to a level which precludes accurate measurement of the stream activity. This is particularly true in cases where widely fluctuating stream activity levels are encountered. If an activity excursion in excess of ten times normal occurs, the sample container may retain a background count far in excess of the count contribution of the normal sample. Accurate determination of the sample's contribution becomes difficult if not impossible.

In order to improve this situation, experiments were performed to determine whether the plated-out particles could be removed by electrochemical treatment while the sample cell remained in place. Since most of the fission products in solution are positively charged ions, and also since the application of a positive or anodic potential to the cell surface results in that surface passing into solution, anodic treatment appeared the most practical.

A series of experiments were conducted in which coupons of types 304 and 316 stainless steel were immersed in contaminated solutions of process type. Electropolishing the coupons was found to greatly inhibit the rate of buildup of plated-out material from the contaminated solutions. All further experimental work was done on electropolished samples. In the static test systems, one coupon was made the anode and two coupons were made the cathodes. Usually one additional coupon was immersed as a control (no potentials were applied to it).

Because of the equilibrating characteristics of the unprotected and anodically protected samples, the only decontamination factors which have a useful meaning are those which refer to samples that came to equilibrium in a particular solution concentration. This concentration is definitely lowered when anodic protection is applied to a surface, and, in fact, decontamination is readily possible. Increasing the current density increases the equilibrium decontamination factor and also hastens the approach to equilibrium. Unfortunately, increasing the current density also raises the corrosion rate. The corrosion rate for an equilibrium decontamination factor of 5 or more approaches 50 mpy. The cathodic surface becomes very contaminated over long periods of time and therefore must be well shielded from the radiation detector. There is a tendency for insoluble $U_3O_{10} \cdot 2H_2O$ to form in low acid solutions. This does not represent a problem in a flow system.

In general the contacting solution contained 4.86×10^5 gross gamma counts per minute per milliliter, uranium, and dilute HNO_3. A normal equilibrium count for a coupon was 6000 counts/min at constant geometry. A current density of 1.0 ma/cm^2 for several hours resulted in a count of less than 2000 counts/min. The associated corrosion rate is about 40 mpy.

The static test results were confirmed in a flow cell consisting of a pump, an electropolished section of 1/4-in. type 316 stainless tubing as the anode, stainless steel cathodes, and two polyethylene spacers. The contaminated solution was pumped around the system until the anode section was in equilibrium with the solution. An anodic current of 2.1 ma/cm^2 was then applied.

The results are shown below:

Time (hr)	Activity of Anode Section (counts/min)
0	3348
0.7	1472
2.7	1008
7.7	642
8.8	791

All the results of these tests indicate that the background of a stainless steel sample cell can be kept low enough by anodic current application to permit the cell to be used in the determination of the radioactivity level of the process solution passing through it.

AUTOMATIC KELVIN BRIDGE RESISTANCE RECORDER

R. K. Adams

In the study of metallurgical crystal structure changes induced by temperature, measurement of the resistance of the specimen gives valuable information about such structural transformations. To assist the Metallurgy Division in studies of this kind, an instrument was developed which measures and records low resistance by using the principle of the Kelvin double bridge.

This instrument is unique because it not only <u>records</u> low resistance values (0.010 to 0.110 ohm) without lead resistance effects, but it also does this over ten linear ranges by means of an automatic range-changing mechanism. Figure 27 shows a front view of the instrument.

Figure 28 shows a simplified measuring circuit of the instrument. The circuit is that of the standard Kelvin double bridge, modified by the use of the Speedomax recorder as the detector and the inclusion of an additional slide-wire, S_3, for linearizing the balancing action of the servo-driven slide-wires. From the development of the Kelvin bridge equations of balance, the resistance R_x of the unknown may be determined from the following relationship:

$$R_x = \left[R_{std} + (1 - M)\ S_3\right] \frac{A_6 + S_1 M}{B_7 + S_1\ (1 - M)} \ ,$$

when $A_5 = A_6$, $B_4 = B_7$, and $S_1 = S_2$.

Fig. 27. Front View of Automatic Kelvin Bridge Resistance Recorder.

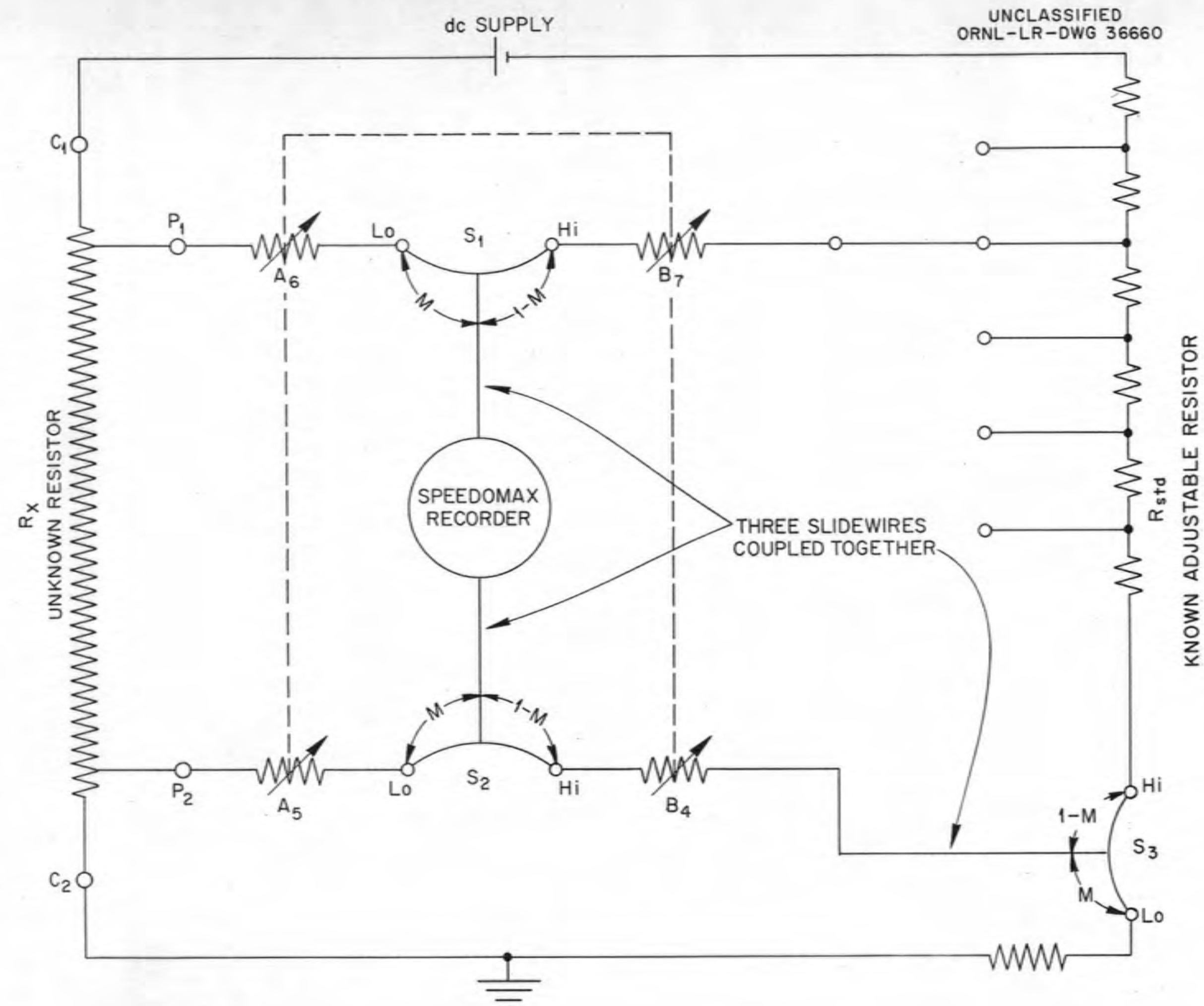

Fig. 28. Simplified Measuring Circuit of Automatic Kelvin Bridge Resistance Recorder.

Also, it may be proved that the inclusion of the linearizing slide-wire, S_3, permits values for A_6, B_7, S_1, and S_3 to be chosen so that the position of the slider on the slide-wires will be a linear function of the unknown resistance R_x over a chosen range, and hence the recorder scale will be linear. Note that without the linearizing slide-wire the recorder scale would be a ratio device.

As previously noted, the total span of the instrument was chosen to be from 0.010 ohm to 0.110 ohm, divided into ten ranges of 0.010 ohm each. To facilitate range changing, the scale length was shortened to allow approximately 2% (0.0002 ohm) overtravel at each end of the scale.

The range resistors A_5, A_6, B_4, B_7 and the standard known resistor R_{std} are switched into the circuit by a high-quality multipoint selector switch, which is powered by a rotary solenoid stepping motor. Limit switches actuated by cams on the recorder slide-wire shaft (Fig. 29) activate the range-stepping switches to select the next higher or lower range when the recorder pen reaches the end of the scale.

Figure 30 is a view of the rear of the range-selection chassis, showing the rotary solenoids and other control equipment for the range-changing mechanism. Range identification is made by a marker pen which inks a coded set of pips on the edge of the chart to represent the specific range which the instrument is recording. Information for the marker pen is obtained from the range selector switches and four motor-driven cams.

Figure 31 shows a sample of chart that illustrates the range identification feature.

Special construction of the three slide-wires in the recorder is shown in Fig. 32. Also shown is the damping tachometer, which was found necessary to achieve good dynamic balancing characteristics.

To cancel thermal emf's due to temperature gradients along the specimen, which may appear superimposed on the resistance measurement emf, the bridge current is periodically reversed by a motor-driven timer. If thermal emf's are present in the signal, the average of the recorder readings for the two current directions will be the true resistance.

The physical layout of the circuits necessary to accomplish the polarity reversal (both bridge current and recorder input must be reversed) may be seen in Fig. 33. To eliminate spurious recording spikes when the current reversal is made, one phase of the recorder balance motor is opened shortly before the reversal is made and closed shortly afterward.

To supply the bridge current for operation of the circuit, the power supply pictured in Fig. 34 was built. The storage batteries are used as filters. The supply is designed to have an output of up to 3 amp at 2 v.

Calibration of the completed instrument (by a Leeds & Northrup precision Kelvin bridge, model 4300-4320) showed, after eight months' use, that it had retained its recording precision of better than ±0.00005 ohm and a calibration accuracy of better than $\begin{pmatrix}+0.0003\\-0.0006\end{pmatrix}$ ohm. Expressed in per cent of the full scale range of 0.110 ohm, these are ±0.05% precision and $\begin{pmatrix}+0.3\\-0.5\end{pmatrix}$ % calibration accuracy.

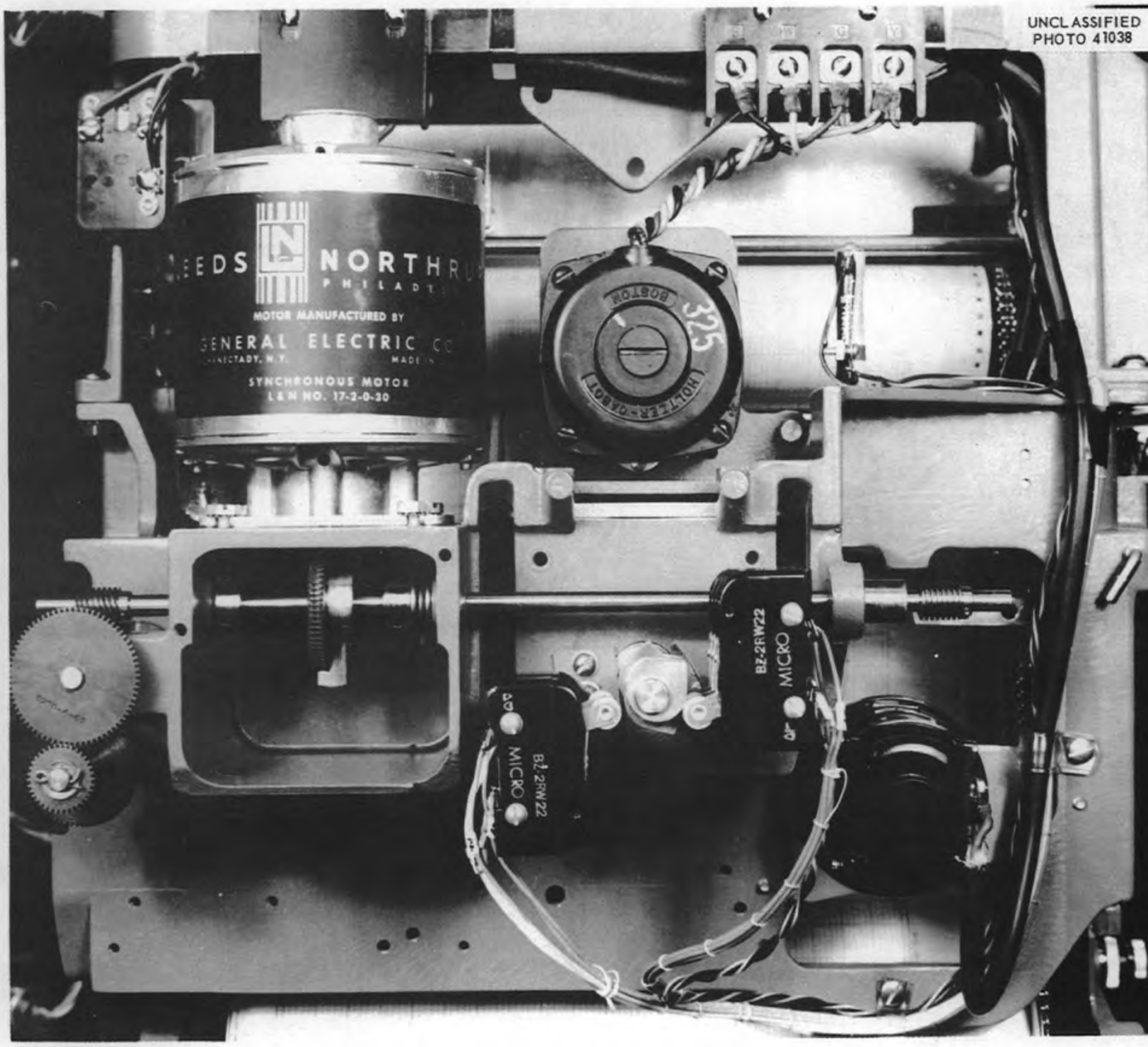

Fig. 29. Rear View of Recorder Unit.

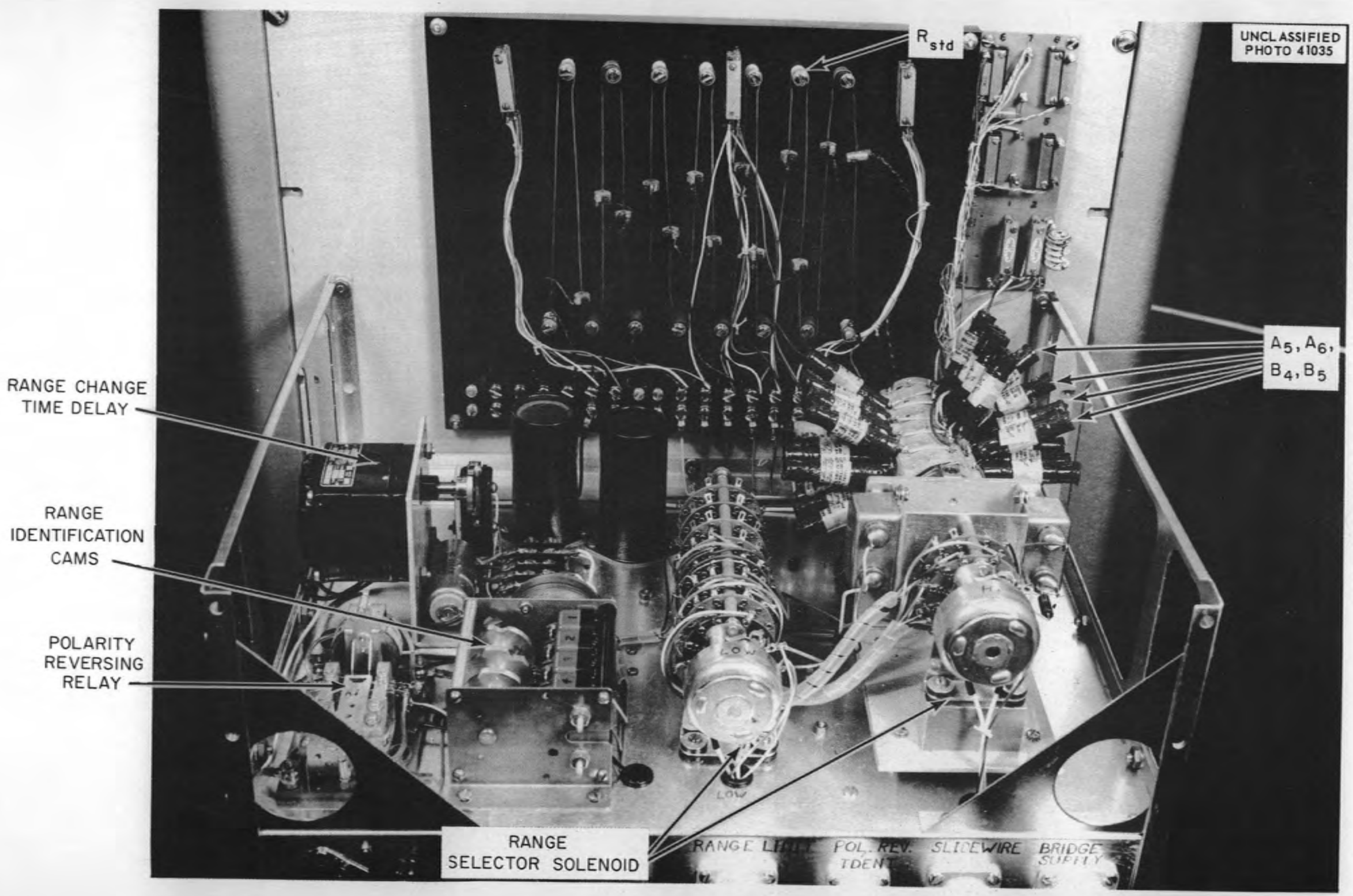

Fig. 30. Rear View of Range Selection Chassis.

UNCLASSIFIED
ORNL-LR-DWG 36665

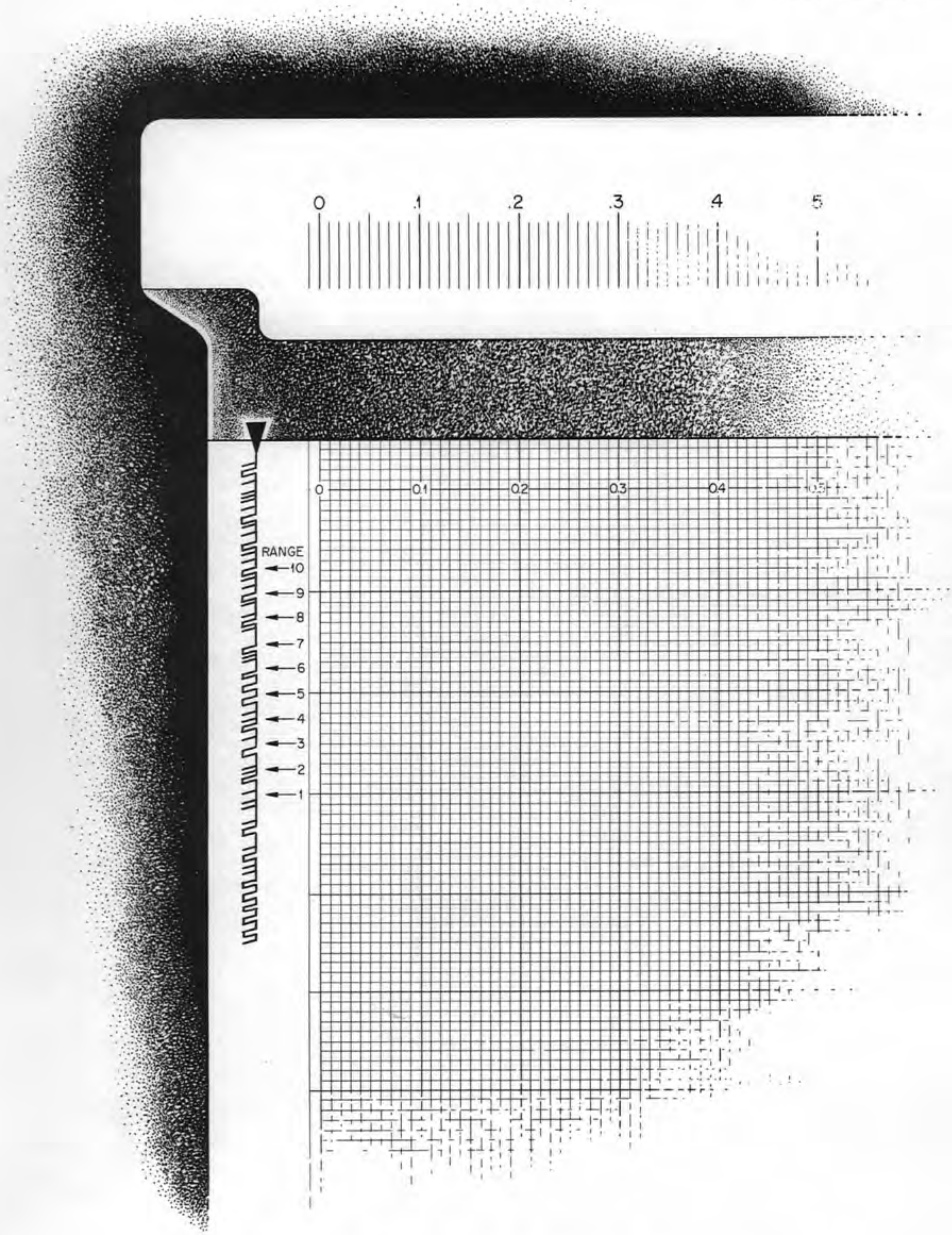

Fig. 31. Sample of Chart, Showing the Range Identification Feature.

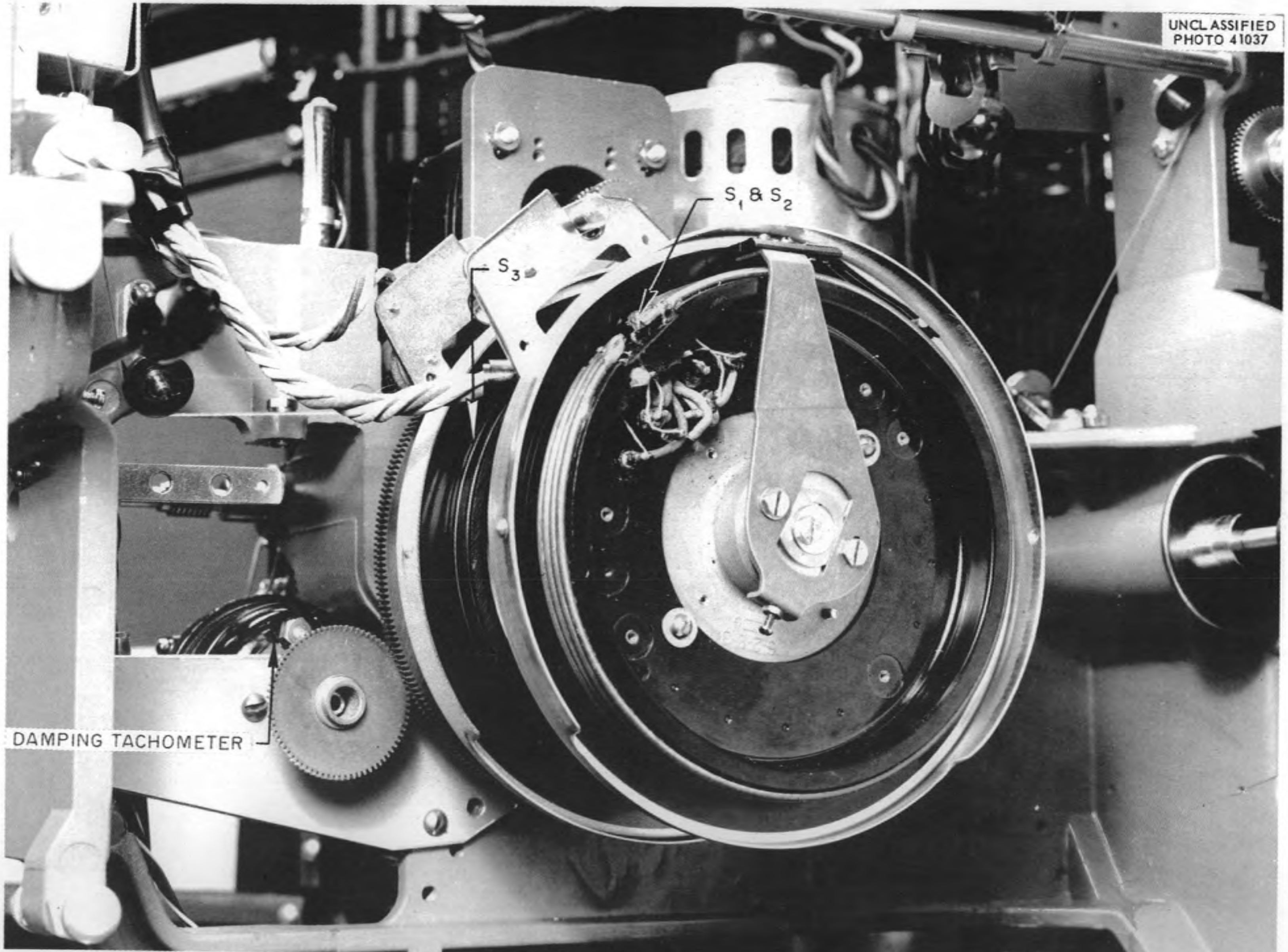

Fig. 32. Inside Front View of Recorder Unit.

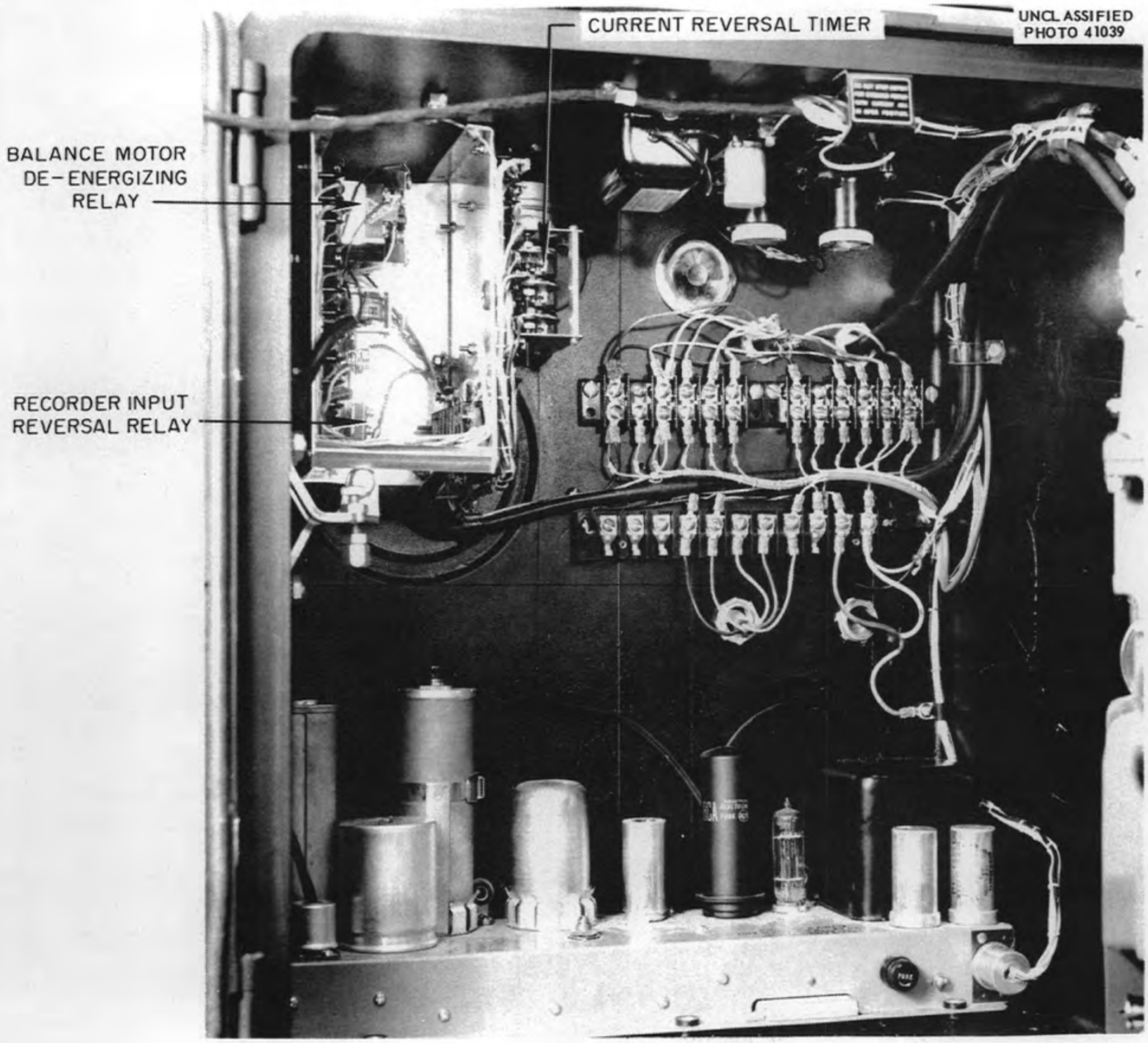

Fig. 33. Interior of Recorder Case.

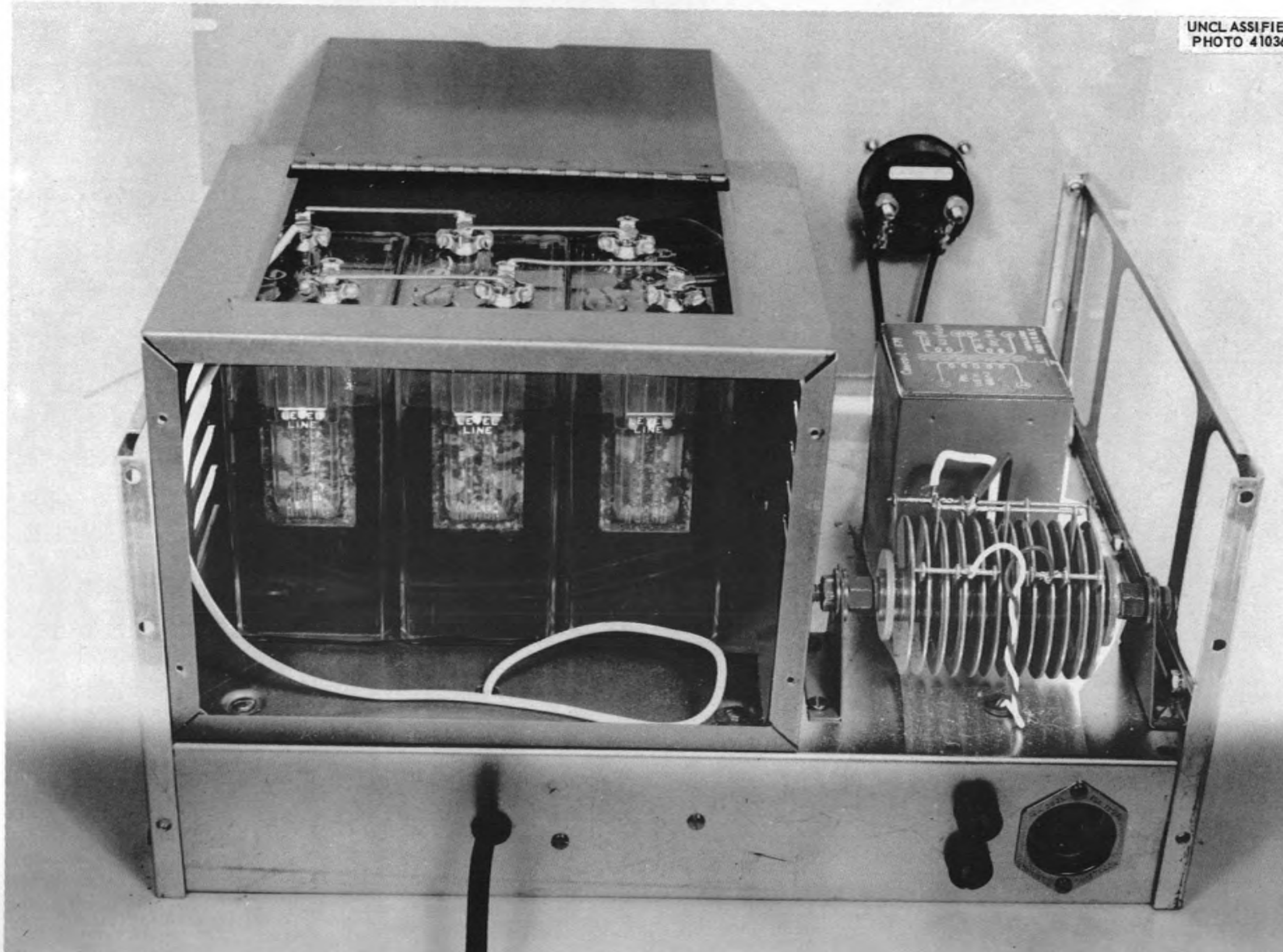

Fig. 34. Power Supply for Kelvin Bridge Circuit.

INSTRUMENTATION FOR THE METALLURGICAL CREEP-TESTING LABORATORY

R. K. Adams

A new metallurgical creep-testing facility was installed and instrumented in Building 2000.

As shown in Fig. 35, the creep frame, furnace, and instrumentation are completely integrated into a compact, easily operable unit. This is largely the result of the use of the standard Q-1699 power-panel assembly, previously reported,[1] and the use of the door of the creep frame as

[1]R. K. Adams, Instrumentation and Controls Ann. Prog. Rep. July 1, 1957, ORNL-2480, p 52–53.

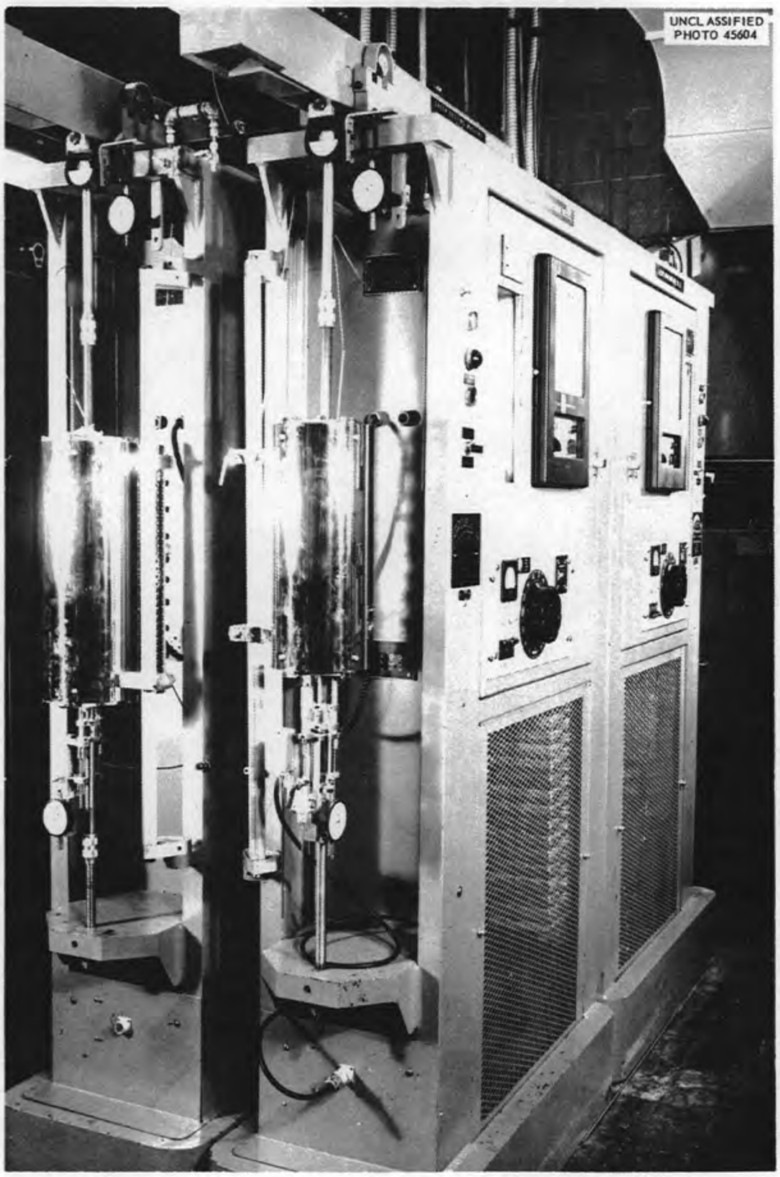

Fig. 35. Creep Testing Facility.

the instrument mounting panel. As shown, four of the creep frames are assembled as a unit. Thermocouple and power lines are brought into each unit from overhead ducts. Figure 35 also shows the thermocouple jacks near the furnace, which provide convenient access to the control instrumentation (Speedomax H, DAT) and the expanded-scale emf recorder unit, shown in Fig. 36. This recorder consists of a -0.5 to 0 to +0.5 mv recording potentiometer, used in conjunction with a stable, calibrated d-c bucking voltage and reference thermocouple cold junction. By using the expanded-scale emf recorder it is possible to select and monitor any one of the 16 creep-test furnaces.

The bucking supply and calibrating panel may be seen in Fig. 37. The calibrating adjustments are provided with a locking device to prevent inadvertent calibration changes. The expanded-scale recorder is capable of a sustained accuracy of better than ±15 μv over a range of 0–50 mv. This represents approximately ±0.4°C between 0 and 1250°C when a Chromel-Alumel thermocouple is used.

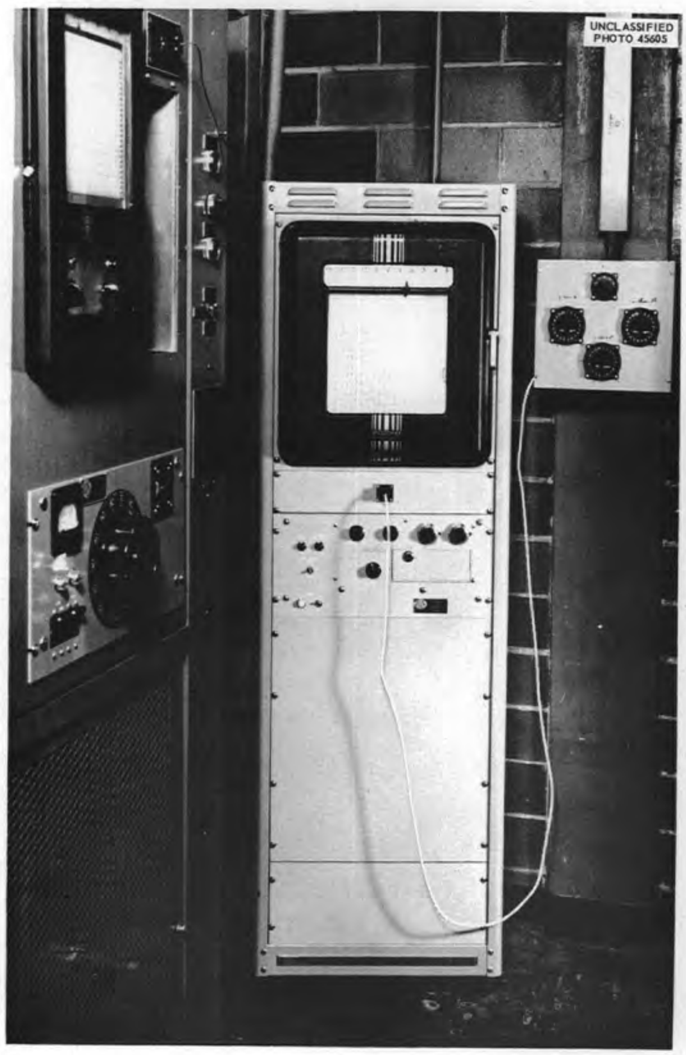

Fig. 36. Expanded-Scale EMF Recorder Unit.

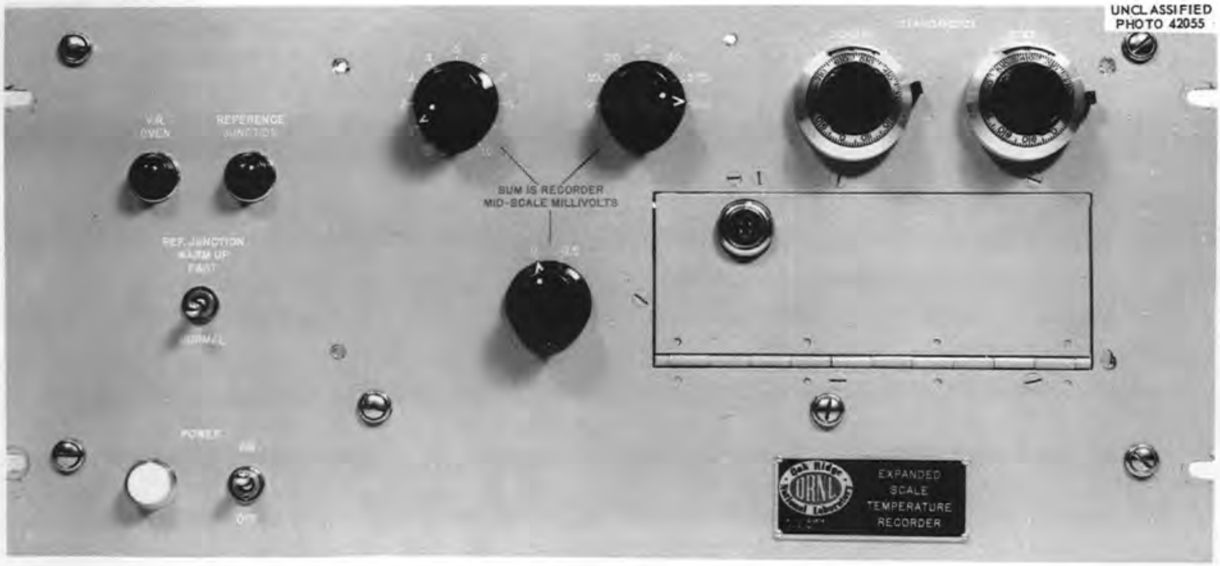

Fig. 37. Bucking Supply and Calibrating Panel.

LOGARITHMIC RESPONSE GAMMA RADIATION MONITOR

J. L. Blankenship

A radioactivity monitor was developed to meet the requirements of most gamma radiation level monitoring for reactor and in-pile loop systems. The design was intended to provide high reliability, good calibration stability, and rapid maintenance. The probe is less than 1 in. in diameter and 8 in. long, and it can be located up to 500 ft from the electronics. No preamplifier is used. The scale indication on the monitor is proportional to the logarithm of the radiation level over a three-decade span and has ±2% linearity with respect to full scale. Full-scale indication may be either 100 or 1000 mr/hr depending on the size of the input resistor. An upscale electronic alarm is provided. The alarm level may be set to any point over the readout range, and the alarm point may be read on the meter while the setting is being made without tripping the alarm circuit.

The basic design is illustrated by the block diagram of Fig. 38. The gamma radiation detector is a 900-v halogen-quenched Geiger-Mueller tube. However, the radiation level is determined from the average current through the tube rather than from the pulse rate. Intense radiation fields cause the tube to conduct continuously, producing an upscale indication. Since the tube is used as a d-c device, no preamplifier is needed for long cable runs. The tube serves to quantize the current for each event; a series resistor (of the order of a few megohms) may be used to develop the signal voltage. Such a low-impedance voltage source does not require electrometer techniques. The G-M tube is independent of gamma energy, and a true dose rate is not read out except for a particular gamma energy. The energy of any gamma activity is usually well known in reactor process loops and in-pile loops; conversion to dose rate for energies of gamma rays other than the calibration spectrum (usually Co^{60}) is easily made.

The voltage signal from the shunt resistor in the G-M tube probe is smoothed and then applied to an amplifier whose transfer function is approximately logarithmic. The actual amplifier response is shown in Fig. 39. The method of obtaining this response is shown schematically in Fig. 40. Feedback from the output of the amplifier is attenuated by a system of resistors and diodes and is subtracted from the input signal by a high-gain difference amplifier. The over-all logarithmic transfer characteristic is the composite of a series of linear regions, each of which is bounded by the conduction levels of two adjacent diodes. This characteristic, when displayed on the semilogarithmic graph of Fig. 39, appears as a series of "scallops," the discontinuities occurring where the diodes begin conduction and change the effective gain of the amplifier.

The output of the logarithmic amplifier is referenced to ground, has a low source impedance, and produces signals in the range of 0–60 v. Output indication is by a 0–10 mv strip-chart recorder, a panel meter, and an upper-limit alarm indicator. The panel meter may also be used to indicate the alarm set point by depressing a switch. This does not disturb the readout of the radiation level through the strip-chart recorder or the alarm indicator. The alarm set point may be changed while it is being observed on the panel meter without causing the relay contacts of the alarm indicator to open, unless the set point is dropped below the radiation level.

Figure 41 shows the plug-in modular construction typical of this unit. Modules may be replaced in less than a minute. Figure 42 is a top view of a three-channel unit. The power supplies are located along the back of the chassis. A single-channel radiation monitor is also available. A probe and an interconnecting cable assembly are shown in Fig. 43.

Two units of an earlier model have been in use at the ORR on two process water lines since February 1958. No maintenance or repairs were necessary during the nine months following installation.

UNCLASSIFIED
ORNL-LR-DWG 31166A

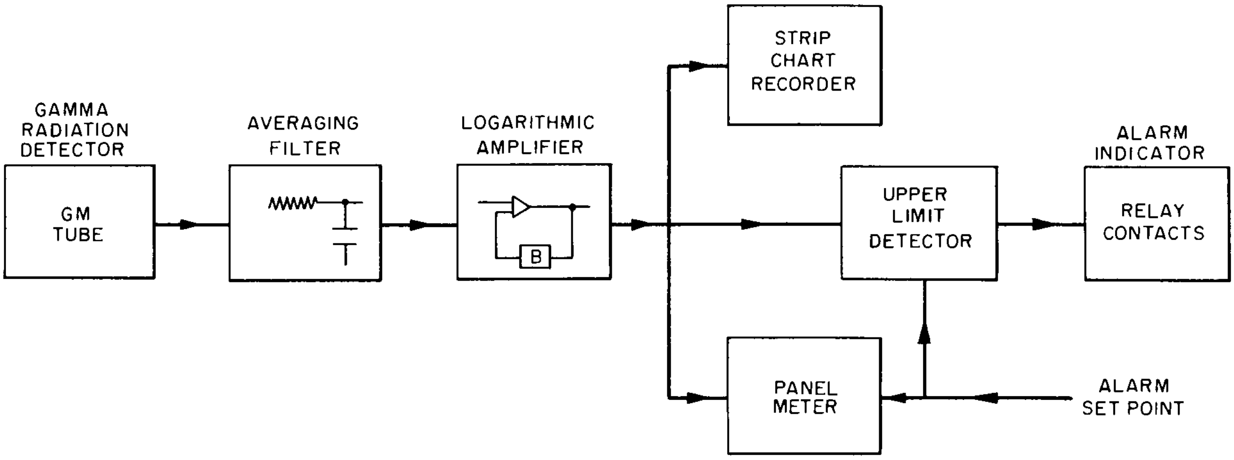

Fig. 38. Block Diagram of Q-1916, Logarithmic Response Gamma Radiation Monitor.

UNCLASSIFIED
ORNL-LR-DWG 31172A

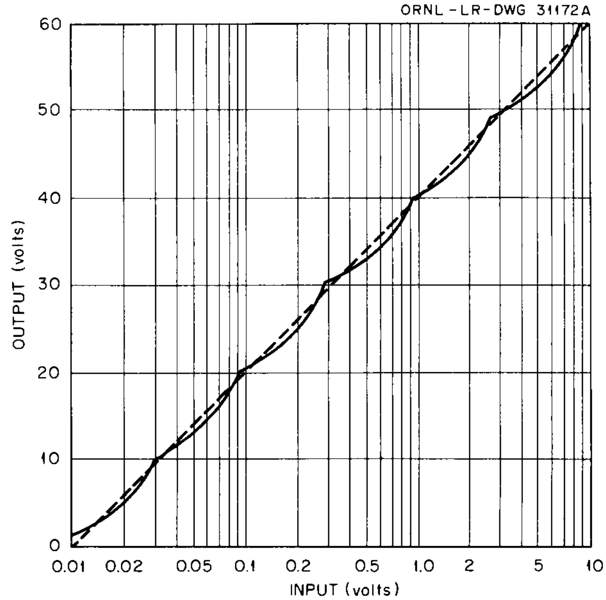

Fig. 39. Logarithmic Amplifier Response.

UNCLASSIFIED
ORNL—LR—DWG 31165A

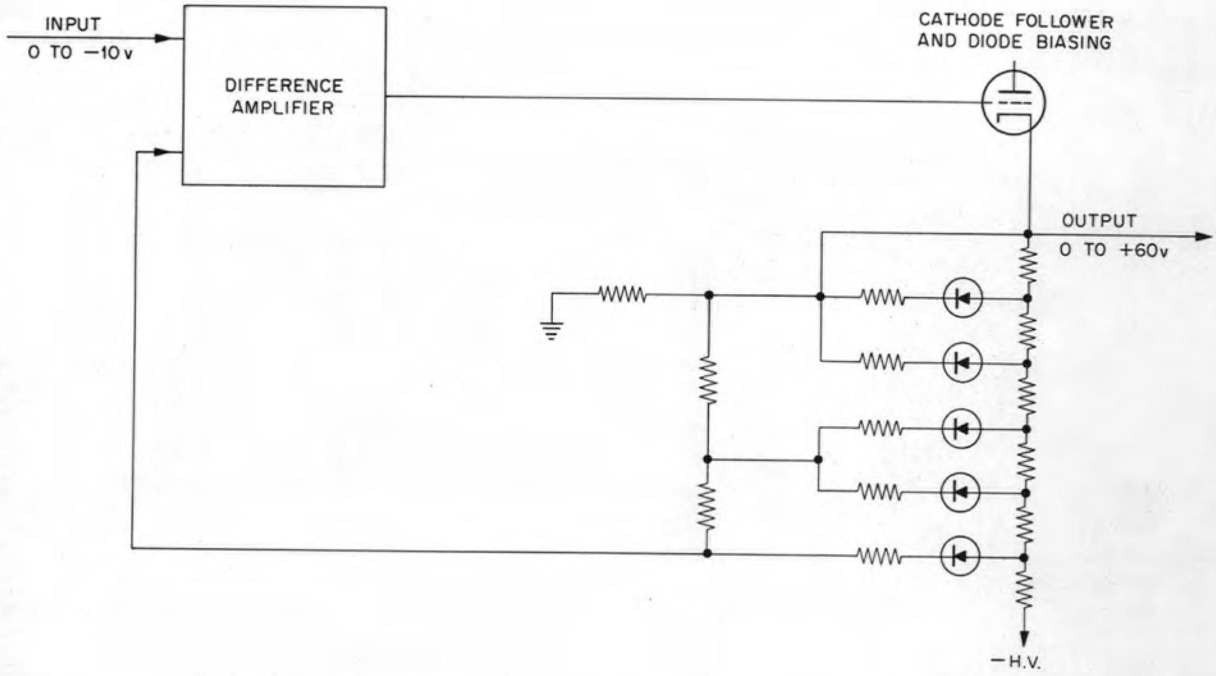

Fig. 40. Logarithmic Amplifier Using Nonlinear Feedback.

UNCLASSIFIED
PHOTO 44394

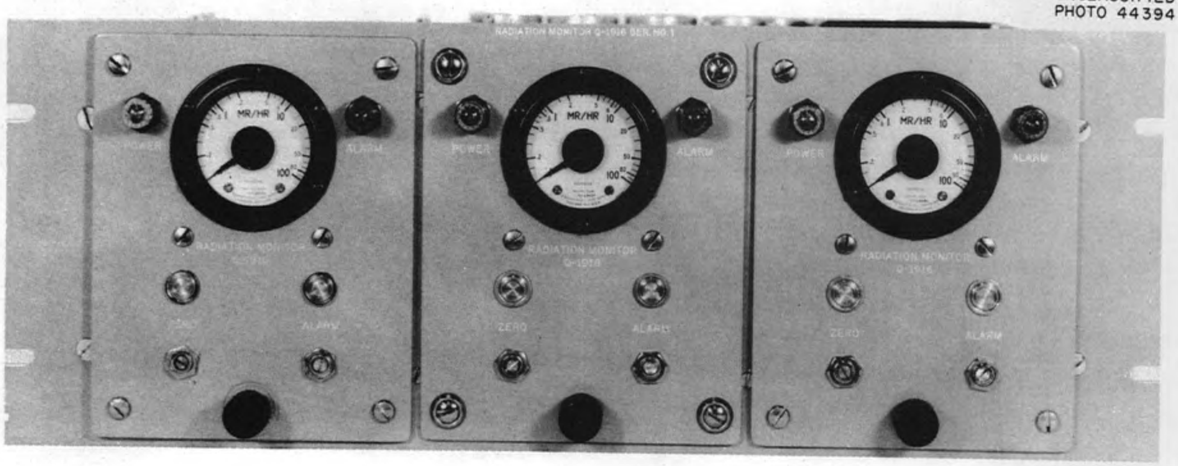

Fig. 41. Front View of Radiation Monitor, Showing Modular Construction.

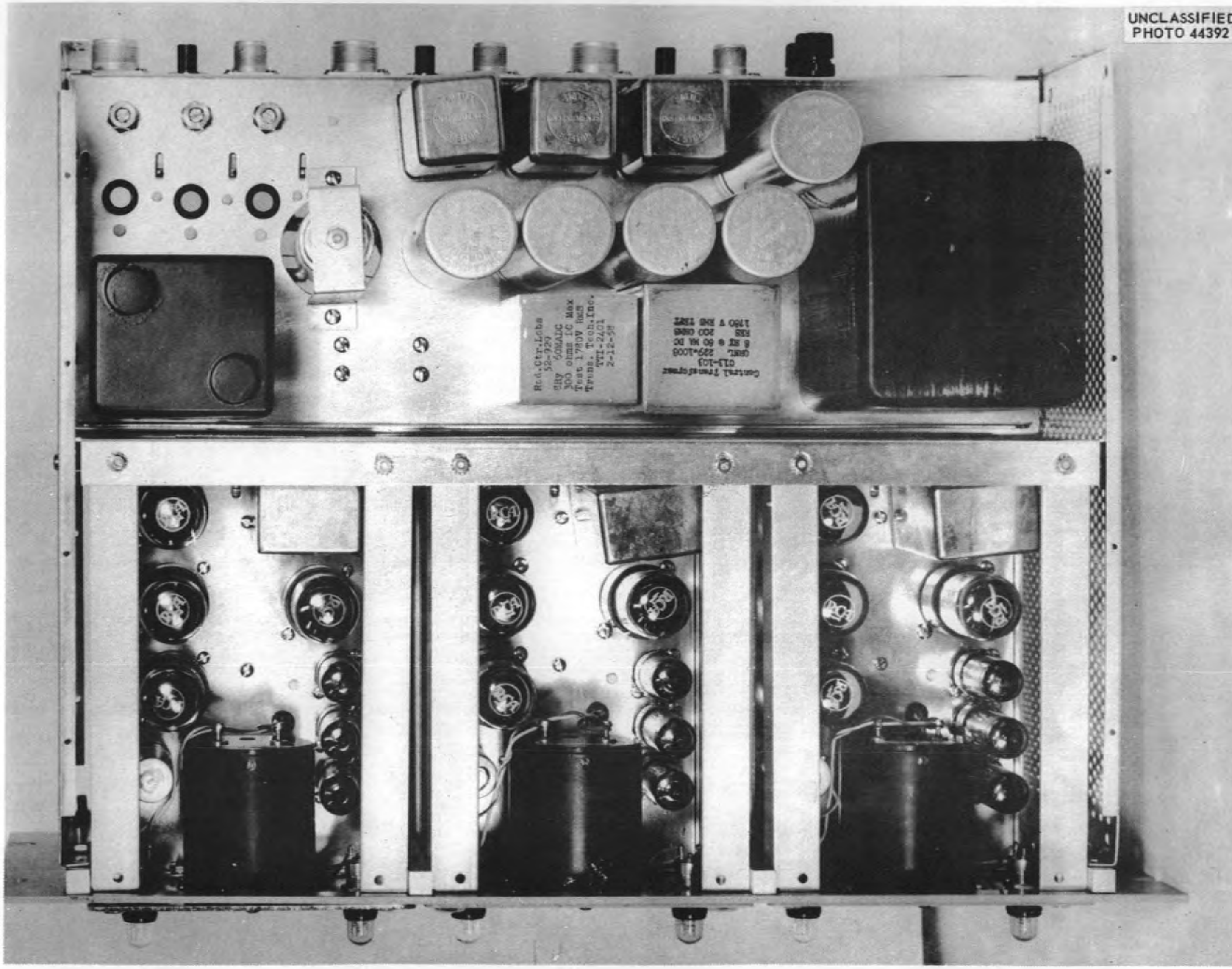

Fig. 42. Top View of Radiation Monitor, Showing Power Supply.

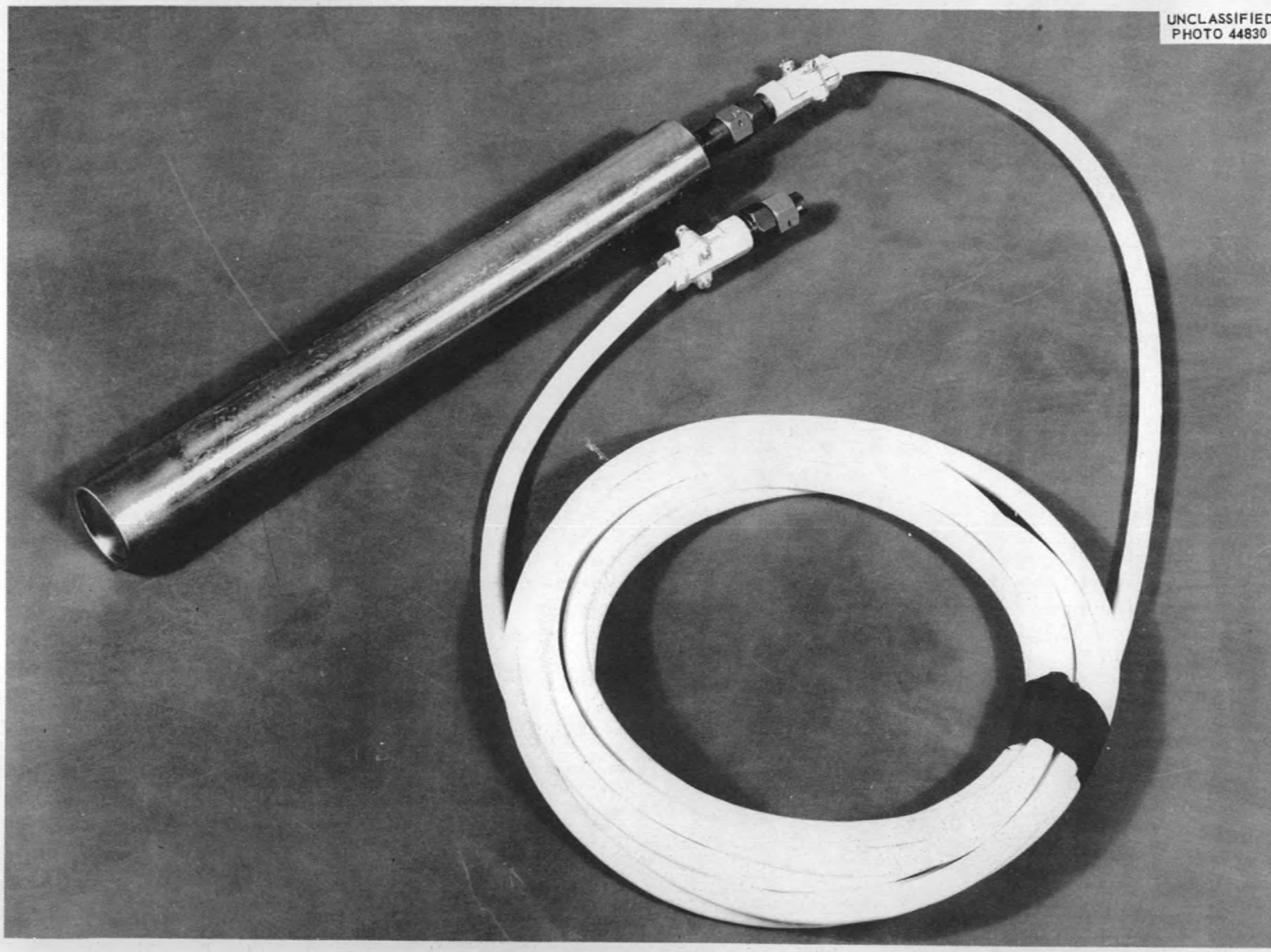

Fig. 43. Detector and Cable for Radiation Monitor.

AVALANCHE DIODE REGULATED POTENTIOMETER CURRENT SUPPLY (Q-1931-4)

J. L. Blankenship

A precision potentiometer makes a convenient voltage reference in regulated magnet supplies. In one such application, it was required that the drift in reference voltage not exceed 0.01% per month. If a battery is used as the working current supply of the potentiometer, frequent readjustments of the working current and occasional battery rechargings are necessary. To improve this situation, an avalanche diode regulated supply was designed and built to replace the working battery. Table 2 permits a comparison between the avalanche diode and other sources of working current. It is evident that the avalanche diode possesses several advantages over other power sources.

The supply as built is power line operated and capable of furnishing 11 ma to a Rubicon type B potentiometer. The supply is sufficiently stable so that adjustment once a week provides 0.01% stability. The circuit is shown in Fig. 44. The Sola transformer and three stages of avalanche diode regulators stabilize the output against line voltage changes. The temperature coefficients of the avalanche diode regulators are consistent with the improvement factor of each regulator stage. The last two diode regulator stages and the Manganin resistors are immersed in an oil bath to minimize rapid temperature changes.

A 10% change in line voltage produces less than 0.002% change in output current. The power supply has a temperature coefficient of less than ±0.001% per degree C, which is smaller than that of an unsaturated standard cell. Peak noise and drift over a 1-hr period do not exceed ±0.001%. The actual performance of the supply referenced against a standard cell is given in Table 3. The data were reduced from a strip chart recorded at 2 in./hr for 12 weeks.

The average drift per week shows an aging process which stabilizes after the third week. The peak deviation from the average drift is probably a temperature effect depending on the sum of the temperature coefficients of both the standard cell and the reference diode. The variations are periodic; daily and weekly patterns are apparent.

Table 2. Comparison of Power Sources or Regulators Suitable for Furnishing Working Current to a Potentiometer*

Voltage Reference	Temperature Coefficient (per degree C)	Drift Coefficient (per hour)	Total Drift (parts in 10^5)	
			100 hr	1000 hr
	$\times 10^{-5}$	$\times 10^{-5}$		
Mercury cell (13,000 ma-hr)	20	3-6	300	**
Lead-acid cell (45 amp-hr)	20	5	500	**
Nickel-cadmium cell (45 amp-hr)	20	0.4	40	**
Silver-zinc cell (45 amp-hr)	20	< 1	< 1	**
85A2	5-20	~ 1	5-100	100
IN430A avalanche diode	1	1-3	5	5

*All batteries are furnishing 11 ma.
**Beyond one charge life.

Table 3. Drift Characteristics of an Avalanche Diode Potentiometer Current Supply

Parts in 10^5

Week	Average Drift During Week	Peak Deviation from Average Drift	Total Drift over Four Weeks
1	+8	±3 1/4	+14 1/2
2	2 1/2	3 1/2	
3	4	3	
4	0	2 3/4	
5	1 1/2	2 1/2	5 3/4
6	2	2 1/4	
7	0	2 1/4	
8	2 1/4	2 3/4	
9	2	2 1/2	4 1/4
10	2 1/4	2 1/2	
11	0	2 1/2	
12	0	1 1/2	

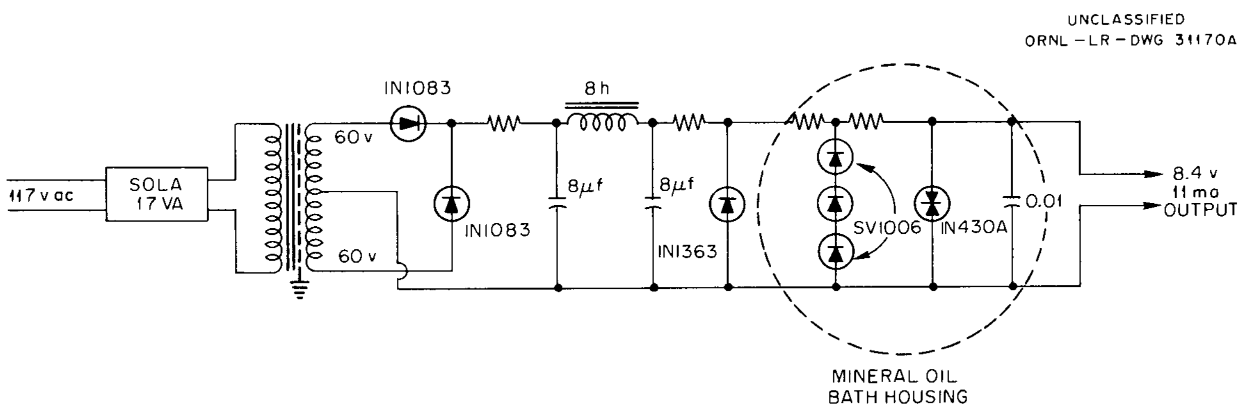

Fig. 44. Avalanche Diode Regulated Power Supply Q-1931-4.

BROAD-BAND, TRANSISTORIZED FIELD CURRENT SUPPLY

J. L. Blankenship

A broad-band power supply for a generator field was needed. This field supply is part of a 78-kw power supply for the analyzer magnet in H. W. Schmitt's fission fragment experiment. Four amperes through the 50-ohm field winding produces full generator output, and this field current is controlled by 12 power transistors in a circuit which limits the voltage across the transistors to a safe value. The output voltage responds faithfully to a demand signal to beyond 14,000 cps.

Figure 45a illustrates a system for controlling voltage or current into a load R_L by varying a resistance R_c. Physically, R_c may be a tube or a transistor. If a transistor is used as a practical control resistor R_c, then a scheme of blocking diodes and center-tapped transformers must be used. This circuit is shown in Fig. 45b. The current I_L flowing through the load will be proportional to the current through the transistor and therefore proportional to I_b, the base current. A three-phase system, as shown in Fig. 46, possesses several advantages over a single-phase system. One of these advantages is that the load voltage E_L has only 4% ripple, with the ripple frequency having a fundamental component six times that of the power line frequency. Another advantage is that the effective band width of the system is in the kilocycle range. This is so because at least one phase is always in conduction, allowing continuous control of the output. The transfer function of the three-phase system shown in Fig. 46 is essentially that of the transformers and the power transistors. This band width permits the use of negative feedback, which in turn reduces the already small ripple voltage, improves the gain stability, and linearizes the transfer function.

Figure 47 shows the front of the power supply. The two lower relay rack panels contain the transformers. The panel with the meter contains the transistors and associated control circuitry, and the blower which forces air past the heat sinks that cool the power transistors is located behind the grill below this panel.

Figure 48 is a top view of the chassis that contains the relays, the rectifiers, and the power transistors, which are mounted on heat sinks. A plenum chamber, attached to the blower, is mounted below this chassis and directs the air flow over the heat sinks. This chassis may be removed without disturbing the plenum chamber and blower.

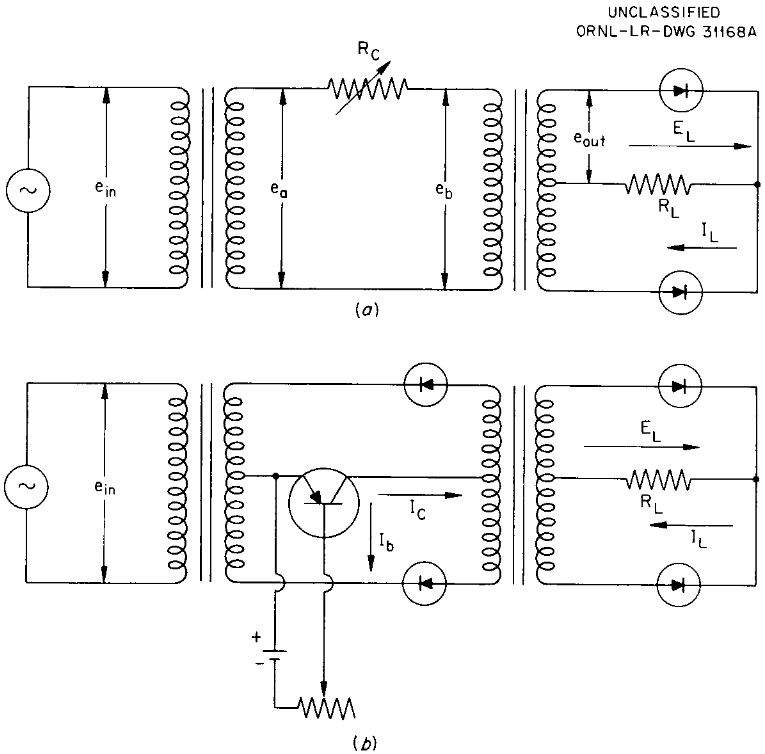

Fig. 45. A Simple Control System. *(a)* Schematic Diagram. *(b)* System using a transistor.

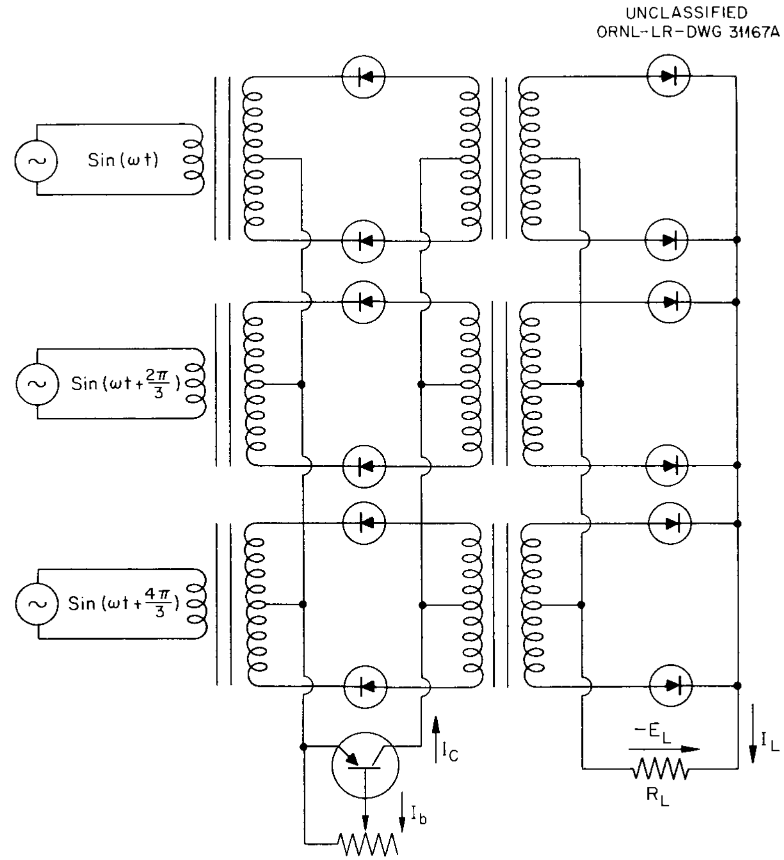

Fig. 46. A Three-Phase Control System Using Transistors.

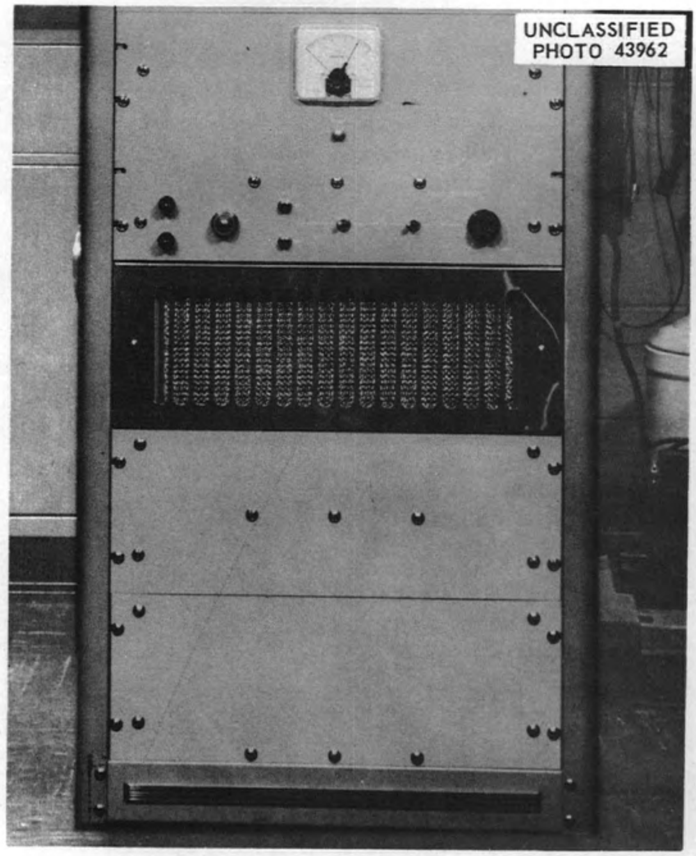

Fig. 47. Front View of Power Supply.

UNCLASSIFIED
PHOTO 43961

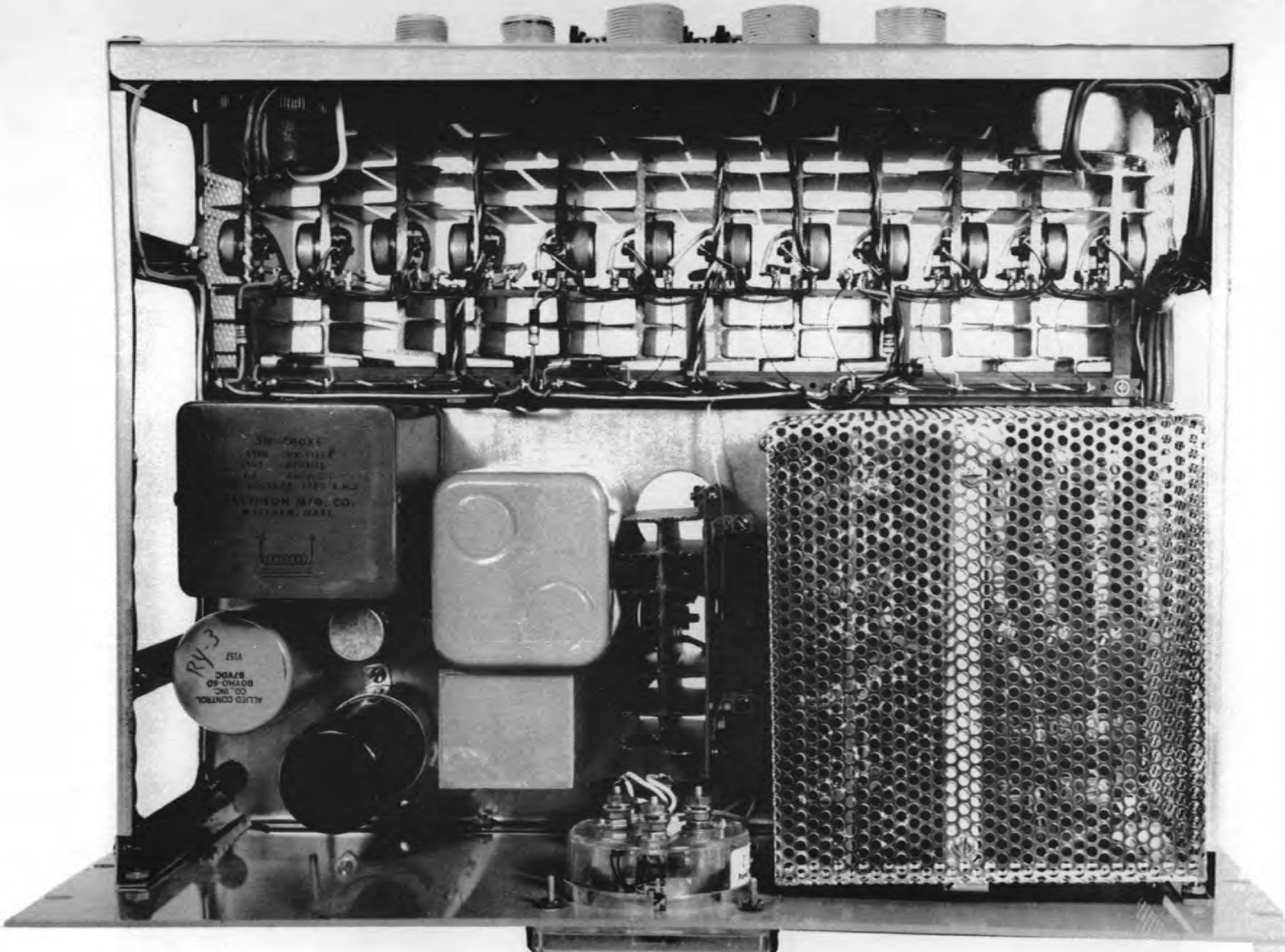

Fig. 48. Top View of Chassis, Showing Transistors.

MAGNETIC FLOWMETER TEST AND CALIBRATION

G. H. Burger

The magnetic flowmeter tests and calibration previously described[1] were continued until November 1957. At that time a total of 20 flowmeters had been calibrated, ten 2-in. units and ten 3 1/2-in. units. The remaining four units of the original 24 were installed without calibration. At the close of the tests the units had operated a total time as follows:

2-in. Units		3 1/2-in. Units	
Number	Time (hr)	Number	Time (hr)
4	1038	4	770
4	1916	4	2368
2	2935	2	3138

During the calibration and test of the units, fluid temperatures up to 1500°F were reached with flows in excess of the normal operating requirements[1] (300 gpm for the 2-in. units and 1200 gpm for the 3 1/2-in. units). With the curves obtained from the calibration data the calibrated units can be used with an accuracy of 1% over the normal operating ranges.[1] The linearity and reproducibility of the units were better than 1% over the ranges tested. The temperature effects upon the units were as expected and can be predicted with good accuracy if the magnet assembly is properly designed and installed. It is advisable to periodically monitor the magnet flux. Care should always be used in handling and installing the units, since irreversible changes in magnet flux can occur with careless handling, such as hitting or dropping the magnets and storing or installing the units close to magnetic materials. The long-term reliability of the units should be very good after initial installation and aging of the magnets. However, it is still advisable to monitor the flux, since the units were not operated long enough to obtain long-term reliability data. A discrepancy of approximately 8% was observed between the theoretical flow equations and the measured equation, making calibration necessary where accurately known flow rates are desired. The effect of oxide in the flowing fluid (wetting) causes errors at low temperature on initial startup, but after several hours of operation at low temperature and after a few minutes at temperatures above 600°F no wetting effects are observed.

In summary, it appears that the use of magnetic flowmeters for measurement of liquid metal flow is satisfactory if proper precautions are taken in the design, handling, installation, and flux monitoring of the units. They are extremely reliable, and infinite life may be expected.

---

[1]G. H. Burger and C. L. Pearce, Jr., Instrumentation and Controls Ann. Prog. Rep. July 1, 1957, ORNL-2480, p 87.

For high accuracy, however, calibration is still necessary, since the data obtained from the units calibrated are not sufficient to alter the theoretical flow equation or establish a new one.

A complete report[2] of the tests has been issued.

---

[2]R. G. Affel, G. H. Burger, and C. L. Pearce, Calibration and Testing of 2" and 3 1/2" Magnetic Flowmeters for High Temperature NaK Service, ORNL CF-58-9-31 (Sept. 29, 1958).

HIGH-TEMPERATURE TURBINE FLOWMETERS

G. H. Burger

A test of two redesigned 1-in. turbine flowmeters[1] was terminated in February. The tests were conducted with NaK in a gas-fired, forced-circulation 1-in. test loop. One of the two test units is shown in Fig. 49. The two units in the initial test were designated as No. 4–rev 0 and No. 5–rev 0.

These units are of the same general design as the units reported earlier.[1] However, the over-all assembly method was changed and the bearing assembly enlarged for added strength. Also, in the initial test of the No. 4 and No. 5 units, the No. 4 unit contained only five turbine blades and No. 5 ten blades; this was done in order to determine the effect of end thrust upon the bearings.

After the initial startup of the test loop the two units were under test for a total of 644 hr, from room temperature to 1200°F, before the loop was dumped for replacement of pressure-measuring units under test in the same loop. At the time of shutdown the two turbines were removed, since one was not operating properly. The units were examined, and it was found that the bearing shaft had worn off on the downstream end, allowing the end of the rotor to drag on the bearing housing face. This was corrected on both units by decreasing the bearing journal length.

No further damage to the units was found. The No. 5 unit was modified to a five-blade unit; then both units were assembled and reinstalled in the loop and labeled as No. 4–rev 1 and No. 5–rev 1.

The second test of the two modified units was terminated after a total loop operating time of 2204 hr due to bearing seizure on both units.

The tests were conducted at temperatures up to 1560°F. Above 1460°F the units operated erratically, finally stopping at 1560°F. However, as the temperature was dropped both units resumed normal operation. At no time during the tests did the units "freeze" or self-weld even after having been stopped at temperatures above 1400°F for several hours.

---

[1]G. H. Burger, Instrumentation and Controls Ann. Prog. Rep. July 1, 1957, ORNL-2480, p 99.

Each unit operated a total of approximately 2000 hr, mostly above 1200°F, before failure, at which time it appeared that the units did seize.

The units were removed from the loop and sent to W. H. Cook of the Metallurgy Division for examination. The No. 5 unit after removal from the loop is shown in Fig. 50, the bearing shaft in Fig. 51, and the upstream positioner in Fig. 52.

Upon examination of the bearing surfaces with a metallographic microscope the polished surface, shown in Fig. 51, was found to be normal bearing material K-152B (TiC); however, the ridges were found to contain broken TiC particles embedded in a matrix of metal. The grooves were found to be clean of this material and appeared to be normal material.

The mechanism causing the loose TiC material in the bearing ridges is not known, but it is suspected that foreign material (metal) contained in the fluid was swept in between the shaft and journal. Subsequent grinding caused the damage.

The reason why the units ceased to rotate is shown in Fig. 52. It is seen that the bearing journal is actually protruding beyond the positioner face, causing the turbine to lock.

The cause of this failure is not known, since the sleeve was rolled in (the rolled material can be seen in Fig. 52). It is suspected that the thermal cycling of the loop probably caused the sleeve to be driven out of the positioner body.

Further examination of the bearings failed to disclose any abnormal wear or corrosion. The oxidation and wear of the bearings were low and were considered to be satisfactory under the test conditions. However, it was the opinion of W. H. Cook that bearing materials containing less metal and more cermet would prove to be even more satisfactory, particularly for use in both molten salts and liquid metals.

The operational characteristics of the units were approximately as previously reported,[1] with accuracy approximately 1% and linearity slightly poorer due to increased bearing friction.

UNCLASSIFIED
PHOTO 40854

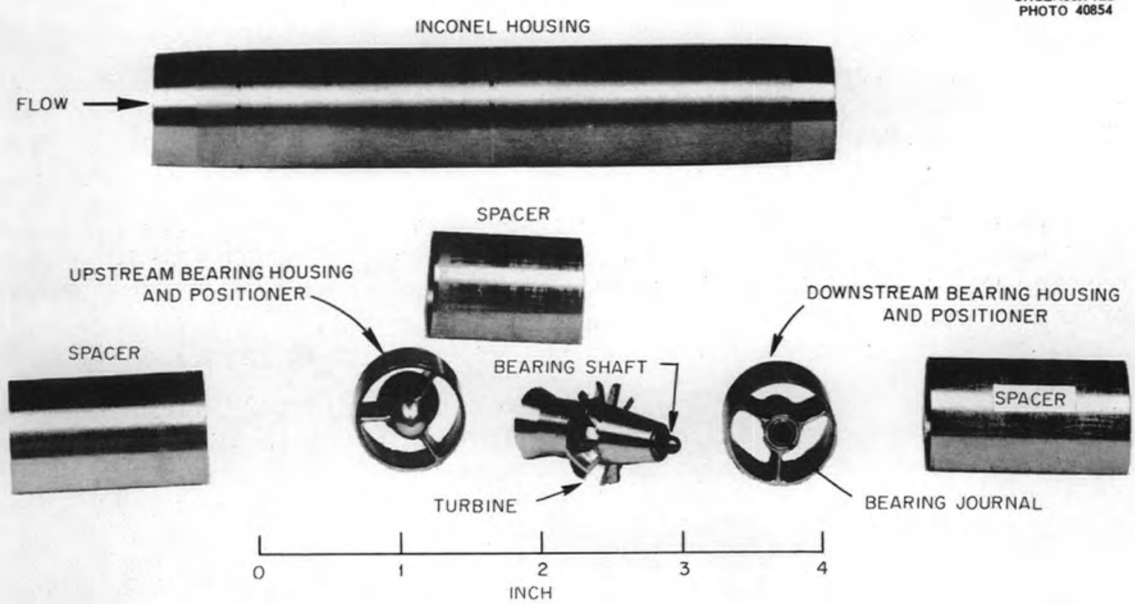

Fig. 49. High-Temperature Turbine Flowmeter.

UNCLASSIFIED
Y-25341

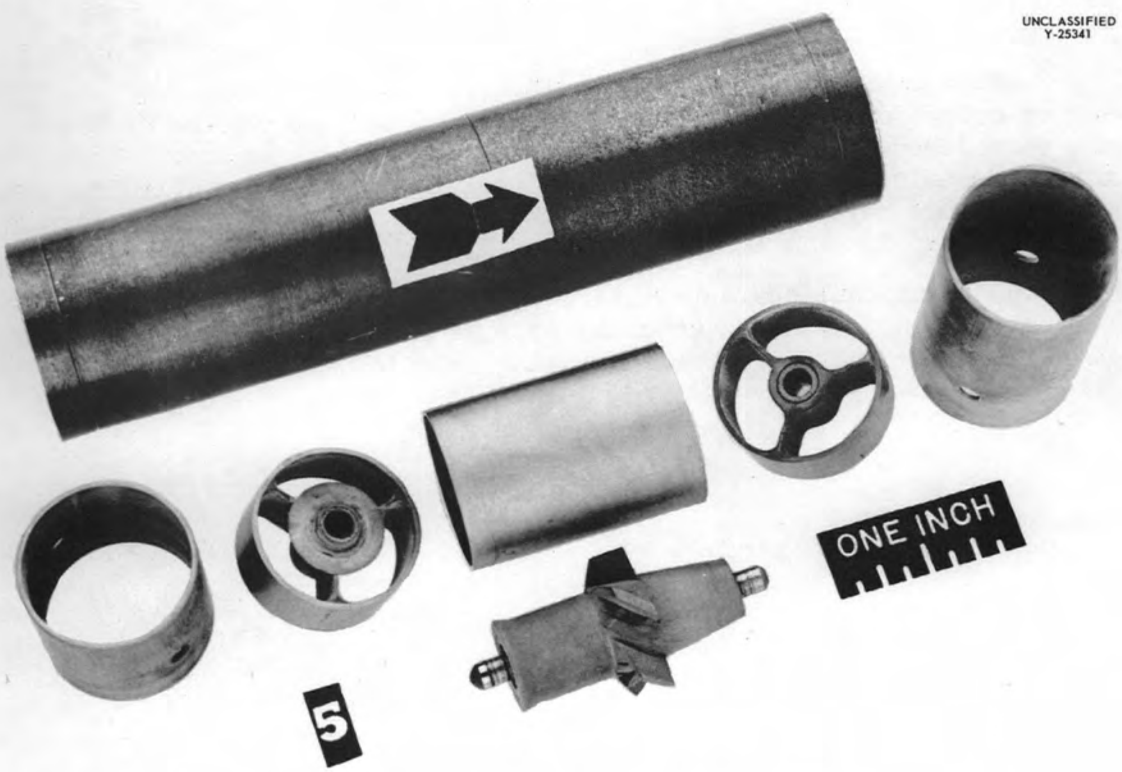

Fig. 50. Test Unit No. 5 After Removal from Loop.

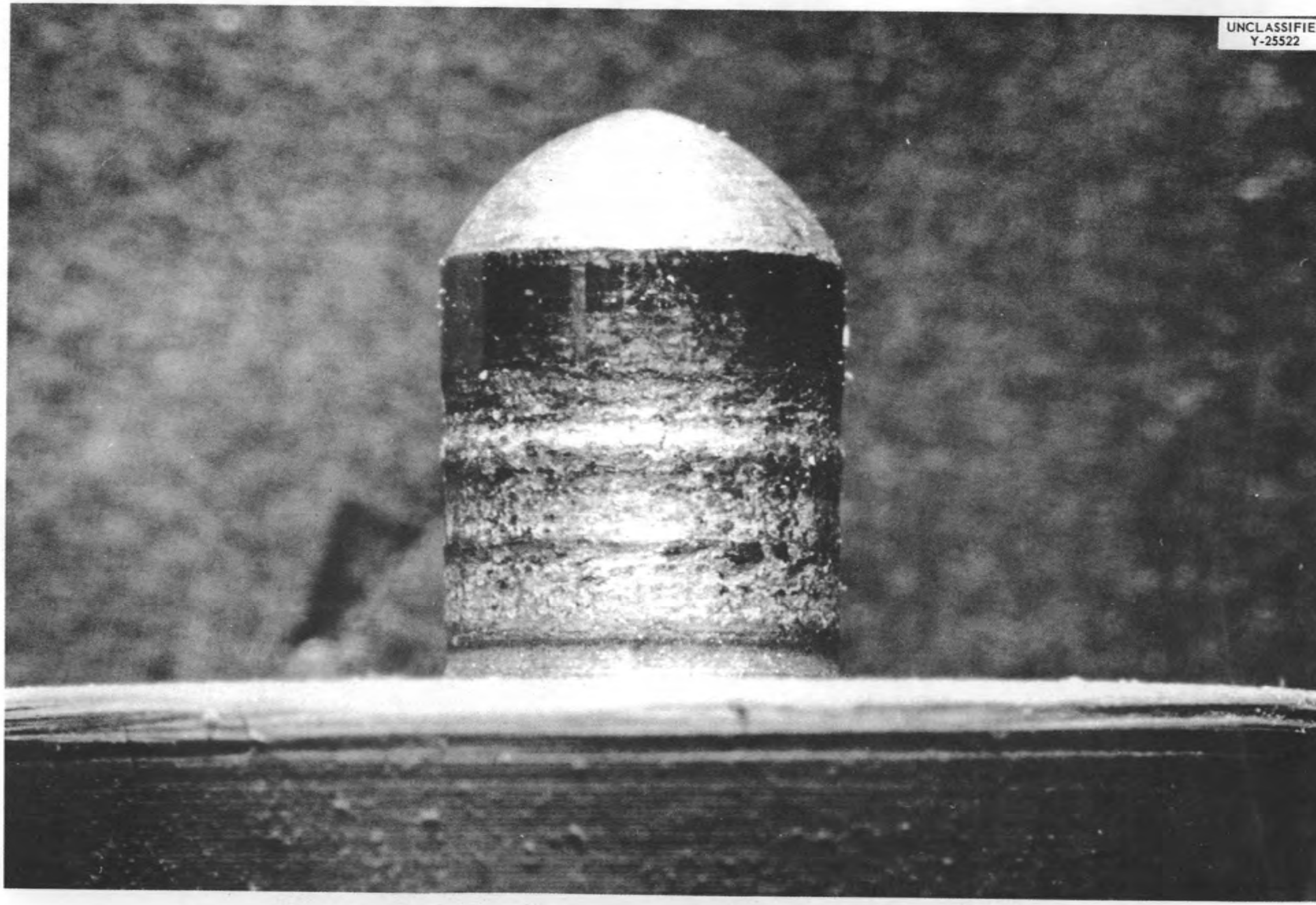

Fig. 51. Bearing Shaft.

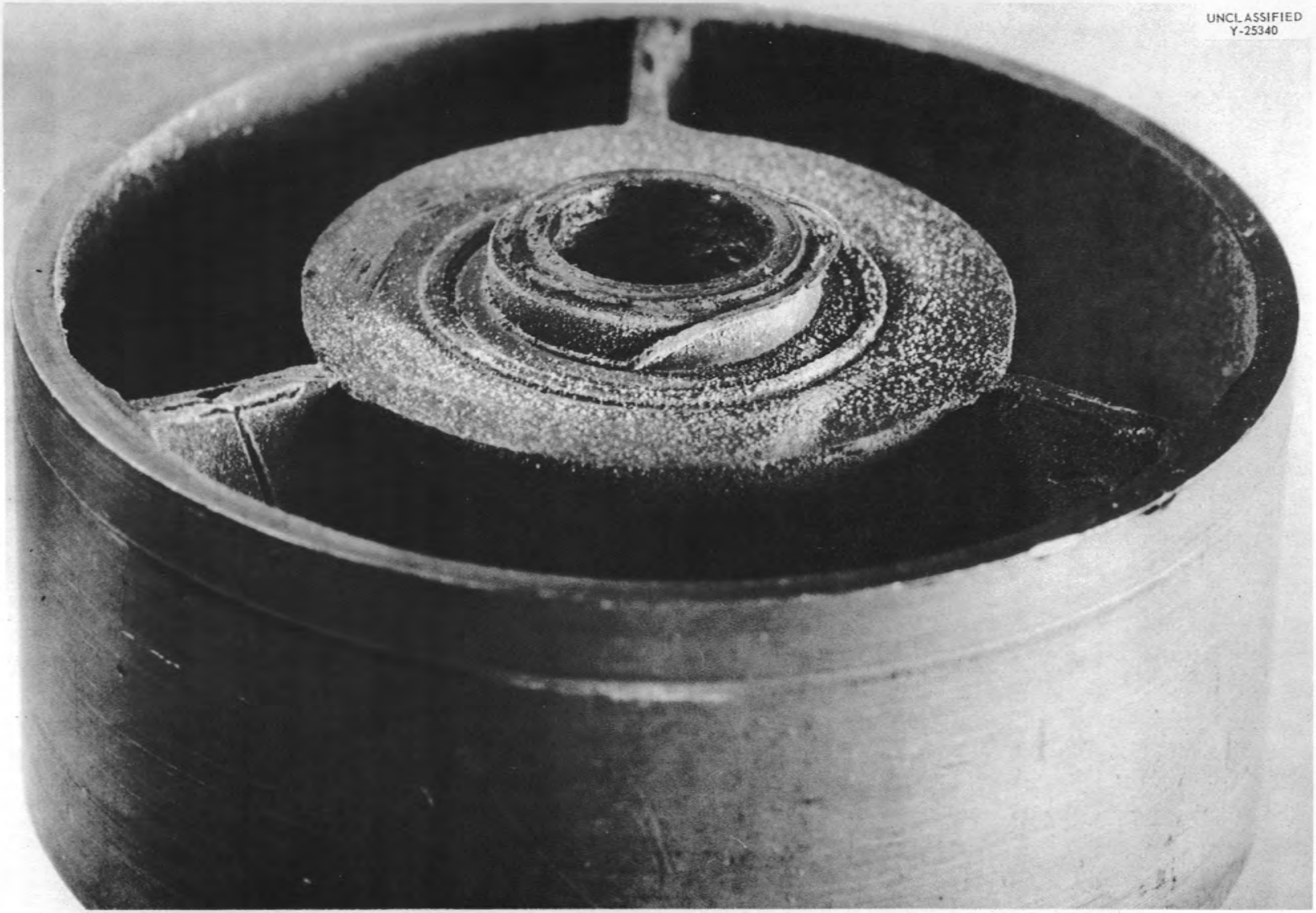

Fig. 52. Upstream Positioner.

LIQUID METAL LEVEL TRANSDUCER TESTS

G. H. Burger

Tests of previously designed and fabricated resistance-type level transducers were continued.[1] Units were tested in both NaK and sodium. The units were tested for accuracy, temperature effects, wetting effects, and operating life at temperatures up to 1400°F. At present seven units are under test in the level-cycling test rigs. Three units are in operation in the No. 1 NaK test rig; two of these have now operated better than 9000 hr and another over 4600 hr at 1200°F and above.

The No. 2 NaK test rig was drained and filled with sodium in June 1958 in order to determine wetting effects in sodium. Previously the units had operated 1440 hr in NaK. Tests to date indicate that, at the higher temperatures and using the probes previously wet by NaK, the wetting effect in sodium is approximately the same as that in NaK. Tests using other probes will be continued to more fully determine the effect of wetting in sodium, since sodium is a widely used reactor heat exchanger fluid.

Life tests on all units will continue following completion of the wetting tests.

A complete report on the liquid metal level development and test program is being prepared.[2] The report covers the entire development and testing of all the resistance-type level probes for liquid metal service through November 1957.

---

[1]G. H. Burger and R. E. Pidgeon, Instrumentation and Controls Ann. Prog. Rep. July 1, 1957, ORNL-2480, p 104.

[2]R. G. Affel, G. H. Burger, and R. E. Pidgeon, Liquid Metal Level Transducers, ORNL CF-58-8-19 (Aug. 11, 1958).

DATA HANDLING

G. H. Burger

A data handling system was purchased from G. M. Giannini & Co. in order to evaluate the use of such a system in reactor instrument and controls systems and related reactor development work.

The system is constructed to record automatically in digital form the millivolt inputs of ten 12-point Brown strip-chart recorders, a total of 120 points plus a time reference. The information is recorded on an automatic typewriter which has a tape punch for recording the data in Oracle code. In addition, all information is displayed by a lamp bank simultaneously with the recording on the typewriter. Controls are included in the system to enable automatic logging cycles to be made at regular time intervals. The system is capable of logging 120 points in

4 to 8 min, depending on the Brown recorders. It is to be noted that the system is not limited to the use of Brown recorders only, since the initial digitizing of the analog input signal is accomplished by the use of an encoder mounted on the rotating shaft of the recorder. The only requirement of the primary detecting instrument is that the initial signal be converted to a rotary motion or a shaft position.

The initial installation and checkout of the system was completed in March 1958. A number of recorders being used in instrument tests were connected to the system and the initial operation was begun. Since that time the system has operated a total of 469 hr. While there has been trouble in the system it was generally due to initial design mistakes which are now being corrected by the vendor. In general, the system has operated in a satisfactory manner, and it is expected that, with the final corrections to be made to the system, it will prove to be satisfactory for the use for which it was intended. It is expected that the system will soon be put into use in the kind of development work that requires a large amount of data to be recorded. This type of operation will serve as a final test of the system and will help to complete the objective as originally stated.

FUSED SALT CONTINUOUS LEVEL ELEMENT

T. V. Blalock R. F. Hyland

The widespread interest at the Laboratory in a fused salt mixture known as composition 30 (50 mole % NaF, 46 mole % ZrF_4, 4 mole % UF_4) led to a need for a simple, reliable level element that would measure level continuously at temperatures ranging from the melting point of the salt, 977°F, to a maximum temperature of 1600°F. An element of all-welded design was preferred in order to avoid a possible seal leakage problem which could cause salt contamination and/or corrosion of the salt container and level element.

An all-welded Inconel unit meeting these specifications, which uses a ceramic sleeve as a high-temperature insulation medium, was developed and preliminary tests have been completed.

The operation of this element depends on a fluid resistance change that is a function of level. A schematic electrical diagram of the measuring system is shown in Fig. 53. The operation is as follows:

In Fig. 53, R is the current-adjusting potentiometer, R_L is the lead resistance, R_c is a temperature-compensation resistance, R_f is the fluid resistance between the Inconel rod and the 1 1/2-in. Inconel pipe (Fig. 54), R_t is the Inconel tube resistance, r_f is a resistance representing the shorting-out effect of the fluid on the Inconel tube, and R_T is the total input resistance of the parallel section of the level element.

UNCLASSIFIED
ORNL-LR-DWG 27023A

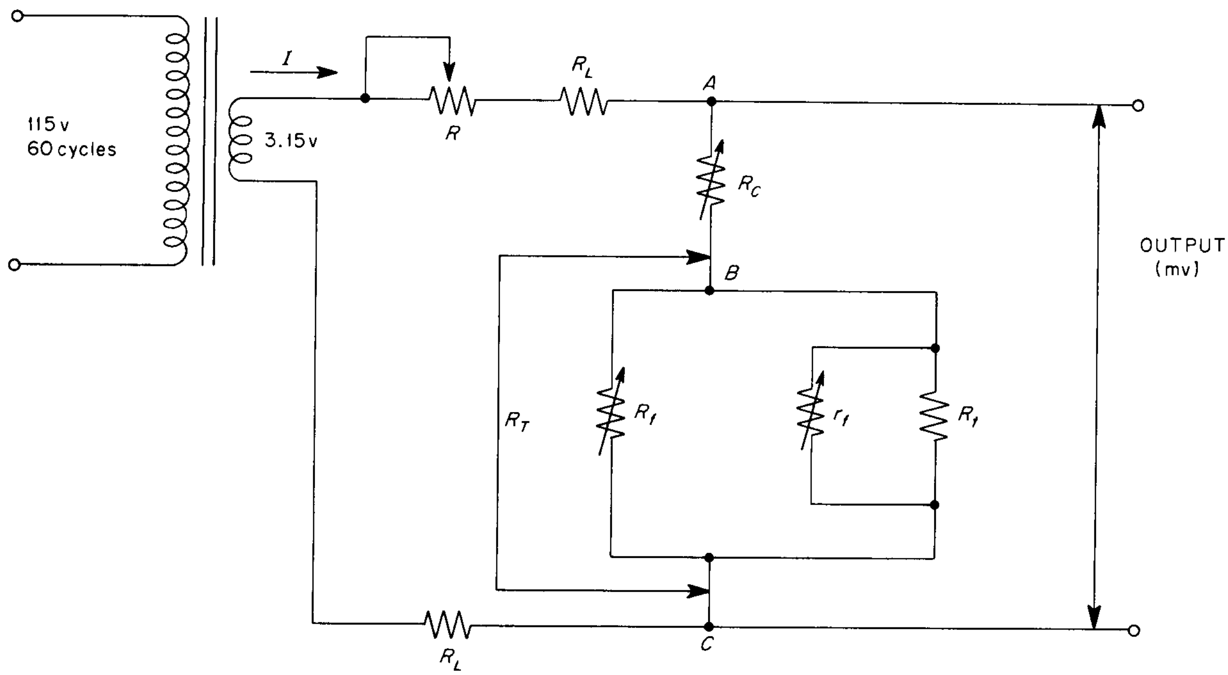

Fig. 53. Fused Salt Continuous Level Element. Schematic electrical diagram of measuring system.

In reference to Fig. 53, if $R \gg 2R_L + R_T$, the current I will depend primarily on R, and therefore the level element can be supplied with a constant current. The output voltage must be measured with an instrument having an input impedance at least as high as that of a Brown recorder. The current flows from the source through the compensating resistance R_c to junction B. From this junction the current has three parallel paths. The first path is through the Inconel rod, the fluid, the 1 1/2-in. pipe, and the 1/4-in. plate to junction C; the second path is through the Inconel tube and the 1/4-in. plate to junction C; and the third path is through the fluid, the Inconel tube, and the 1/4-in. plate to junction C.

As the fluid level rises, the current flow through the fluid between the Inconel rod and the 1 1/2-in. pipe will control because of the increase in the flow-path cross-sectional area. At zero level the element output will be given by the product of the supply current and the Inconel tube resistance, since the resistance R_f will be infinite

UNCLASSIFIED
ORNL–LR–DWG 27024

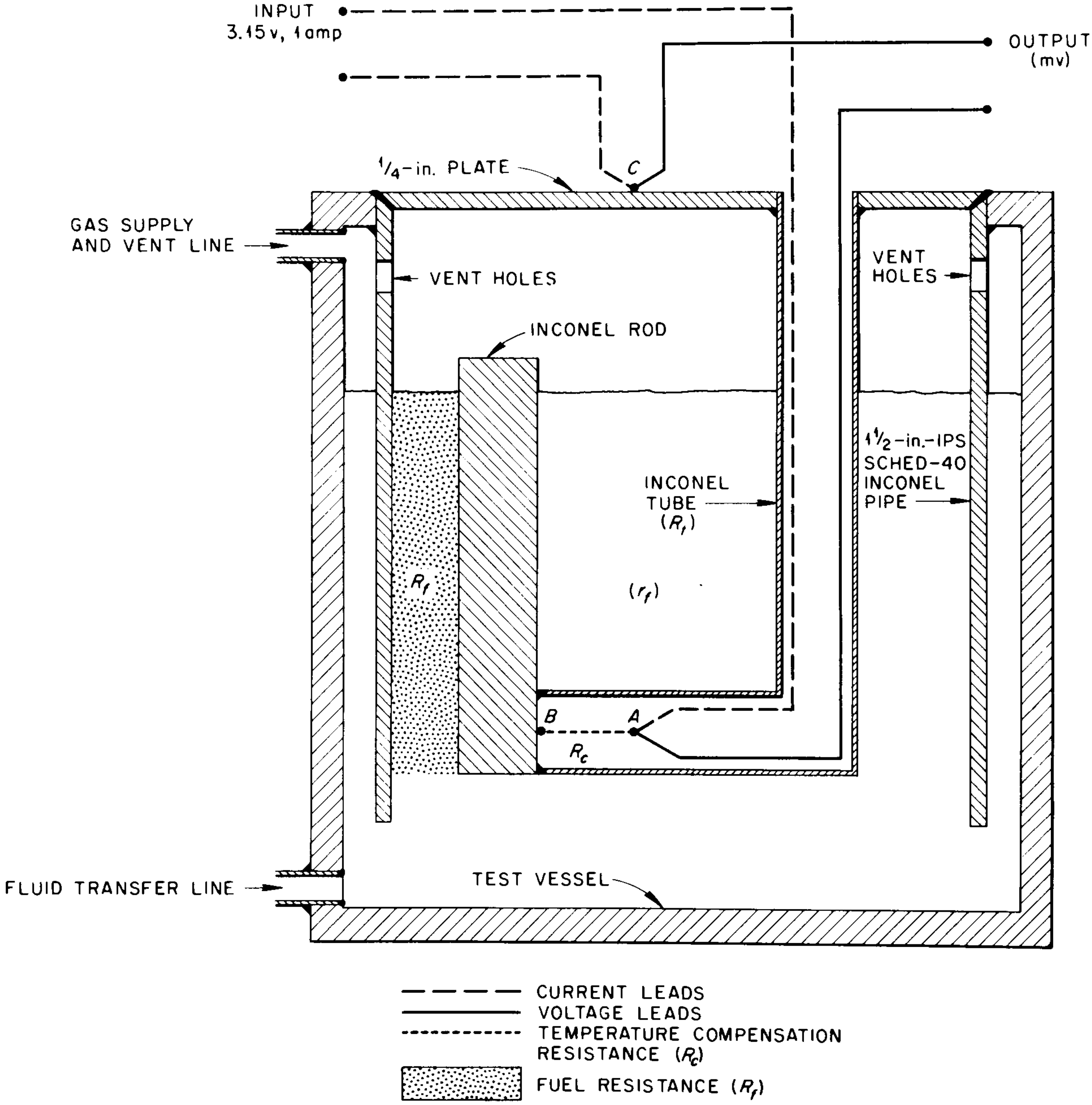

Fig. 54. Fused Salt Continuous Level Element. Schematic diagram.

for nonimmersion. The maximum output will occur at zero level, and the output will decrease as the level increases. The resistance R_c is a function of temperature only, and R_f and r_f are functions of both temperature and level.

The resistivity of the fluid mixture has a negative temperature coefficient. The resistivity of Inconel is almost constant over the temperature range under consideration, and therefore R_t can be assumed to be constant. It follows then that R_T will be a function of R_f and r_f and will decrease with increasing temperature.

An increase in fluid temperature will have the same effect on the output as an increase in level if the system is not temperature-compensated. One method of temperature compensation is described below. The element is to be compensated at a fluid height h, so that a temperature excursion from T_1 to T_2 will produce no change in output. If the compensating resistance R_c is placed in series with R_T, the temperature-compensation criterion will be satisfied if

$$\frac{V_{R_{c_1}} - V_{R_{c_2}}}{T_1 - T_2} = - \frac{V_{R_{T_1}} - V_{R_{T_2}}}{T_1 - T_2} \quad , \qquad (1)$$

or, for $\Delta T = T_2 - T_1$,

$$\frac{\Delta V_{R_c}}{\Delta T} + \frac{\Delta V_{R_T}}{\Delta T} = 0 \quad . \qquad (2)$$

As stated previously, $\Delta V_{R_T}/\Delta T$ is negative, and therefore $\Delta V_{R_c}/\Delta T$ must be positive and the resistivity curve of the compensating resistor must have a positive slope.

A short length of grade "A" nickel wire can be used for R_c, and its dimensions can be arrived at as follows:

$$V_{R_c} = IR_c = I \frac{\rho_c}{A_c} \ell_c \quad ,$$

$$V_{R_T} = IR_T \quad ,$$

$$V_{R_{c_1}} = I \frac{\ell_c}{A_c} \rho_{c_1} \text{ at temperature } T_1 \quad ,$$

$$V_{R_{c_2}} = I \frac{\ell_c}{A_c} \rho_{c_2} \text{ at temperature } T_2 \quad ,$$

$$V_{R_{T_1}} = IR_{T_1} \text{ at temperature } T_1 \quad ,$$

$$V_{R_{T_2}} = IR_{T_2} \text{ at temperature } T_2 \quad ,$$

$$I \frac{\ell_c}{A_c} \rho_{c_1} - I \frac{\ell_c}{A_c} \rho_{c_2} = - (IR_{T_1} - IR_{T_2}) \quad ,$$

$$\frac{\ell_c}{A_c} = \frac{R_{T_1} - R_{T_2}}{\rho_{c_2} - \rho_{c_1}} \quad , \tag{3}$$

where

ρ_c = specific resistance of compensating wire,

ℓ_c = length of compensating wire,

A_c = area of compensating wire.

Two resistance-type level elements without temperature compensation were fabricated (Figs. 55 and 56) and were used to experimentally determine the resistance-level characteristics of the element and to observe polarization and other effects not included in the design calculations. Calculated performance curves for these elements, both temperature-compensated and uncompensated, are shown in Fig. 57. These curves are based upon a constant current of 1 amp through the measuring element.

A test rig designed to test two level elements simultaneously was fabricated in accordance with the flow diagram shown in Fig. 58. The liquid level was varied by a helium-forced exchange of fluid between the two vessels. The initial readout of the level signal was accomplished with a Hewlett-Packard model 400H vacuum-tube voltmeter. A variable probe which completed a lamp circuit when contacted by the fluid was used for calibration.

Preliminary experimentally determined performance characteristics of an uncompensated element are shown in Fig. 59. The actual performance of the probe was in reasonable agreement with the calculated performance. However, this work was discontinued before detailed performance characteristics of the probe could be studied.

A new requirement for a continuous level element for the Molten Salt Power Reactor program reactivated an interest in the existing element. The fused salt of interest in this program is known as composition 130 (62 mole % LiF, 37 mole % BeF_2, 1 mole % UF_4). The temperature range will be from its melting point to 1300°F. An improved type of level element was designed (Fig. 60) which eliminated some of the fabrication and assembly problems associated with the earlier model. Also, due to the increased fluid contact area, the new design should allow a greater output voltage change per unit level change. The element was inserted in a cylindrical vessel. The level was varied by a helium-forced exchange of salt between the vessel and the well. Calibration was accomplished by a variable probe which completed a lamp circuit when contacted by the fused salts.

The initial tests were performed with an uncompensated element, and typical data are summarized in Table 4. The results indicate that there is a calibration drift as a function of time for constant temperature. However, more data must be accumulated before any conclusions can be drawn. The effects of polarization and surface tension as well as the effects of higher or lower input current amplitudes and frequencies will be determined. Various methods of temperature compensation will be explored. Although the data accumulated to date are inconclusive, the probe appears promising.

UNCLASSIFIED
PHOTO 29725

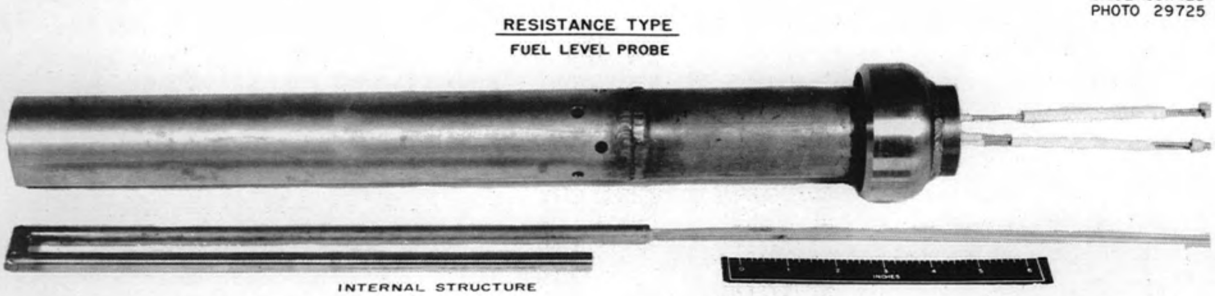

Fig. 55. Resistance-Type Fuel Level Probe Without Temperature Compensation.

UNCLASSIFIED
PHOTO 29726

Fig. 56. Resistance-Type Fuel Level Probe Without Temperature Compensation. Lower end.

UNCLASSIFIED
ORNL-LR-DWG 27025

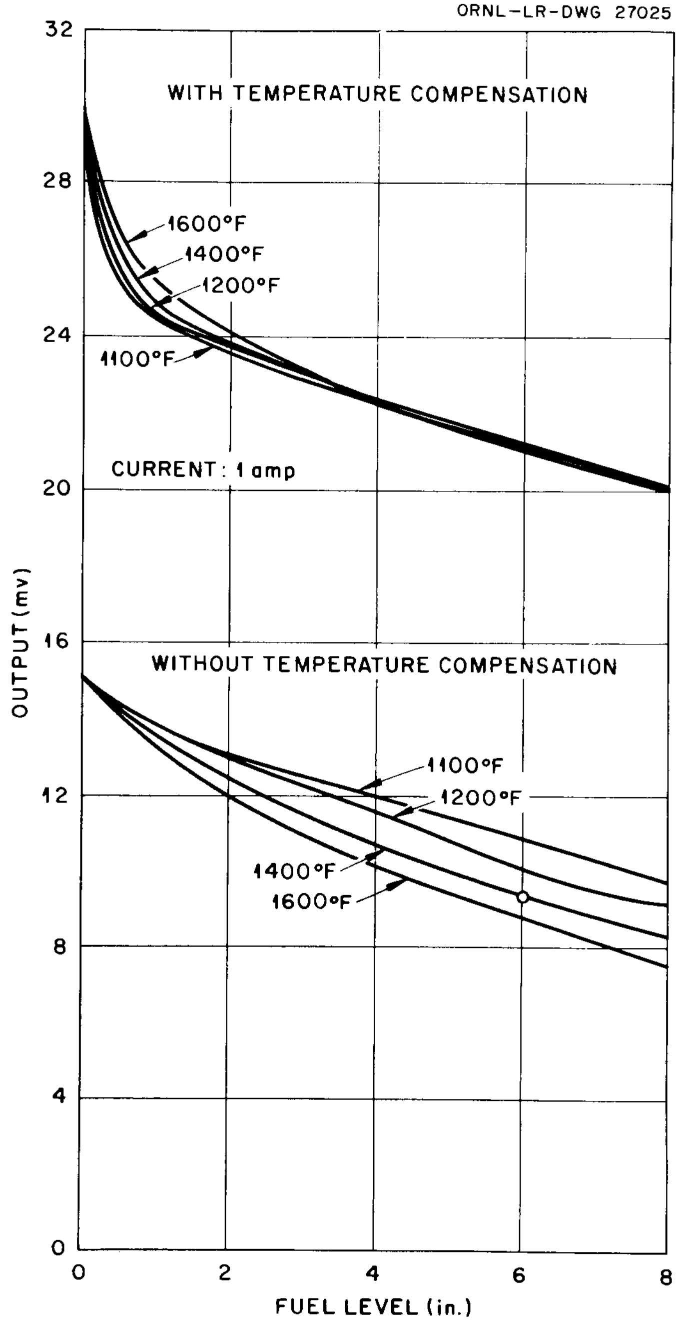

Fig. 57. Calculated Performance Curves for Resistance-Type Fuel Level Probe.

UNCLASSIFIED
ORNL-LR-DWG 27026

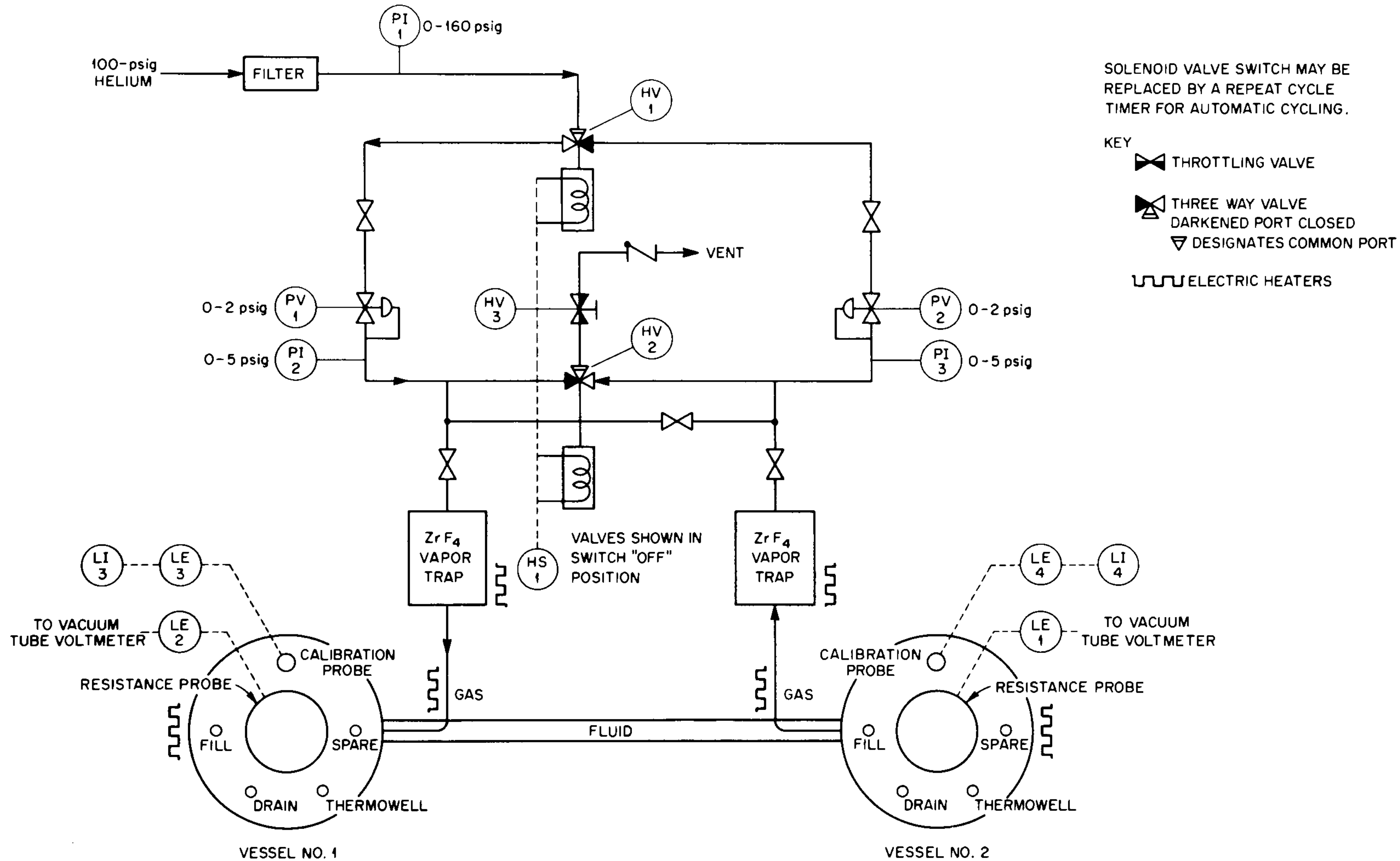

Fig. 58. Flow Diagram of System for Testing Fuel Level Elements.

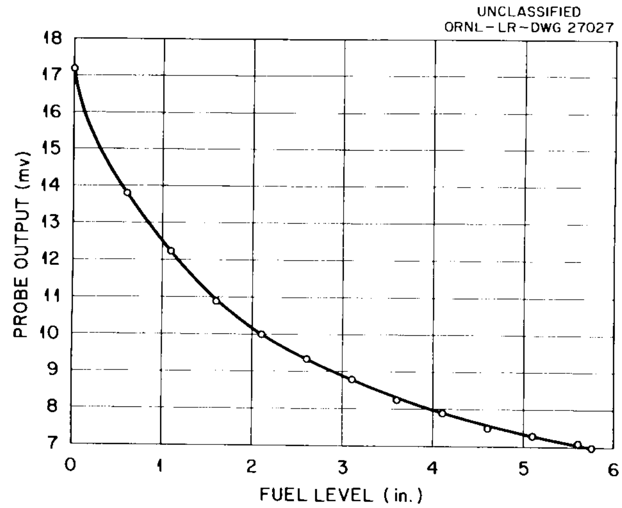

Fig. 59. Experimentally Determined Performance Curve for an Uncompensated Fuel Level Element.

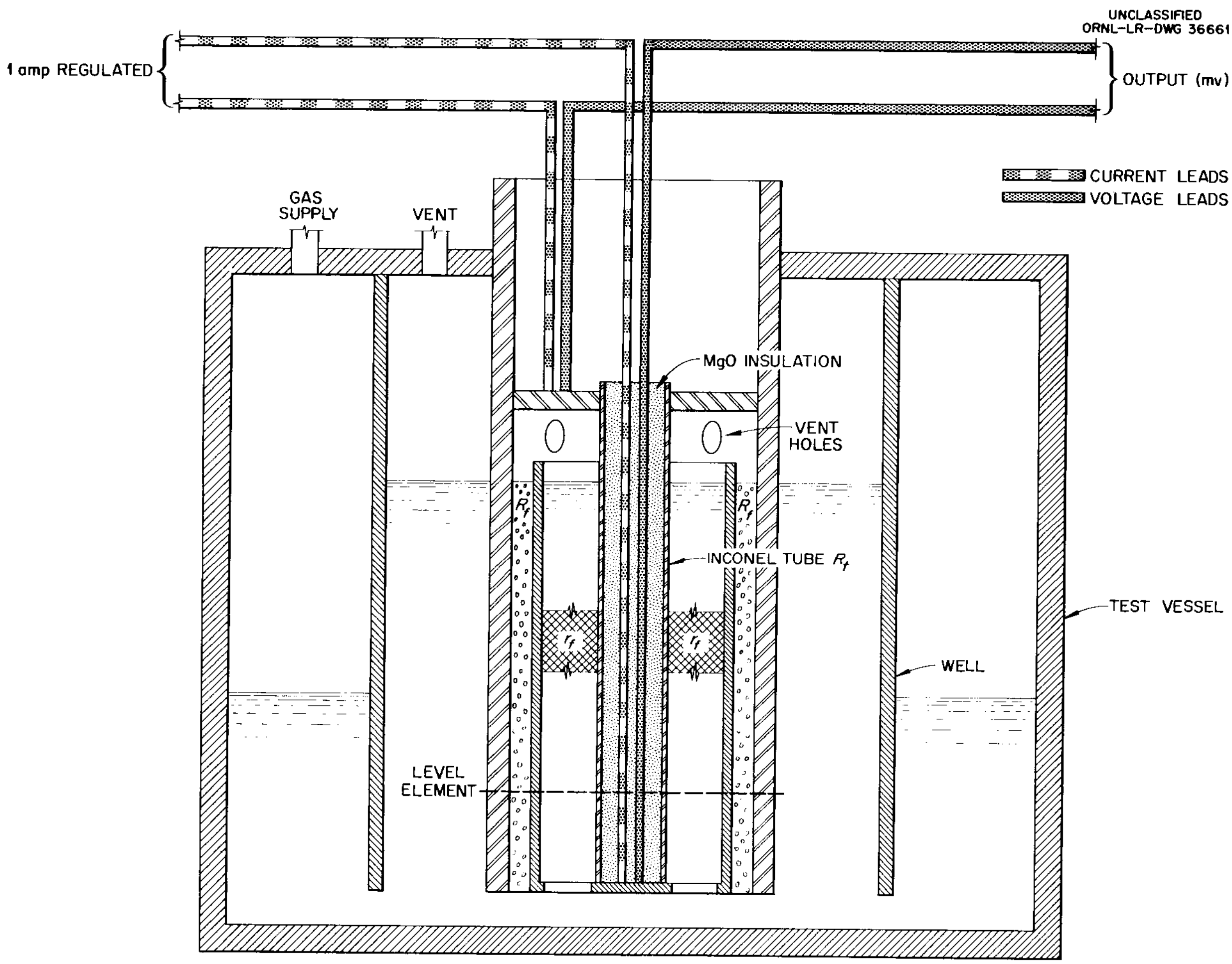

Fig. 60. Improved Level Element for Fused Salts. Schematic diagram.

Table 4. Summary of Data from Tests of Resistance-Type Fuel Level Probes

Probe supply voltage (regulated): 3.4 v ac
Probe supply current (constant): 1.0 amp
Frequency: 60 cps
Readout device: Hewlett-Packard model 400H vacuum-tube voltmeter
Fluid: composition 130 (62 mole % LiF, 37 mole % BeF_2, 1 mole % UF_4)

Run No.	Date (1957)	Test Temperature (°F)	Level Range (in. of fuel 130)	Probe Output at Zero Level (mv)	Zero to Maximum Level Probe Output Range (mv)	Probe Output Span (mv)
1	7/29	1000	0–6	15.7	15.4–12.0	3.4
2	9/2	1000	0–6	15.7	14.9–8.0	6.9
1	8/5	1100	0–6	15.7	15.2–11.5	3.7
2	8/22	1100	0–6	15.7	14.2–6.0	8.2
1	8/11	1200	0–6	15.7	15.5–12.2	3.3
2	8/22	1200	0–6	15.7	14.6–7.0	7.6
1	8/20	1300	0–6	15.7	14.8–7.4	7.4
2	9/9	1300	0–6	15.7	14.7–7.1	7.6

HRP INSTRUMENTATION AND CONTROL

D. S. Toomb

S. J. Ball	P. G. Herndon
E. H. Bell	R. L. Moore
A. M. Billings	R. M. Pierce[1]
J. R. Brown	J. L. Redford
D. G. Davis	J. A. Russell
G. W. Greene	K. W. West
J. D. Grimes[1]	H. D. Wills

INSTRUMENT DEVELOPMENT

A program is under way to instrument a proposed slurry reactor. In this program emphasis is being placed on electric transmission from primary elements.

A complete instrumentation system contains a number of individual loops, each of which has an input and an output end. These ends (sensing elements and actuators, respectively) are inside the reactor containment vessel, but the intermediate instrumentation is outside the vessel. The choice of components used for the sensing and actuating elements is primarily determined by the reliability of the components and the type of seal which must be made in the walls of the containment vessel. Experience has shown that the sensing elements should convert the measured quantities to electrical signals to permit the use of static seals – as opposed to dynamic seals, which are subject to leaks and blockages and which require line blocking valves – while actuators should be limited to pneumatic-powered bellows, despite the fact that dynamic seals are necessary for such actuators. The block diagram of a typical reactor instrument loop based on this philosophy is shown in Fig. 61. The remainder of this report is devoted to descriptions and test results of components and instruments which make up these loops.

Transistorized Electropneumatic Converter

The existing converter, operated by six vacuum tubes and powered from a 15-v a-c supply, has proved to be a weak link in the control loop. In an attempt to improve this situation, a contract with the University of Virginia Engineering Experiment Station was initiated to develop a transistorized electropneumatic converter which could be powered from the battery-energized system used in most power plants. This instrument converts a low-level millivolt a-c output from such devices as differential transformers, inductance bridges, and strain gages to proportional 3- to 15-psi pneumatic pressure signals and operates from a 48-v d-c supply.

The transducer is shown in block diagram form in Fig. 62. Operation is as follows:

1. A 3-v, 1000-cps signal is supplied to the primary of a differential transformer from an oscillator.

---

[1]On loan from TVA.

UNCLASSIFIED
ORNL-LR-DWG 36662

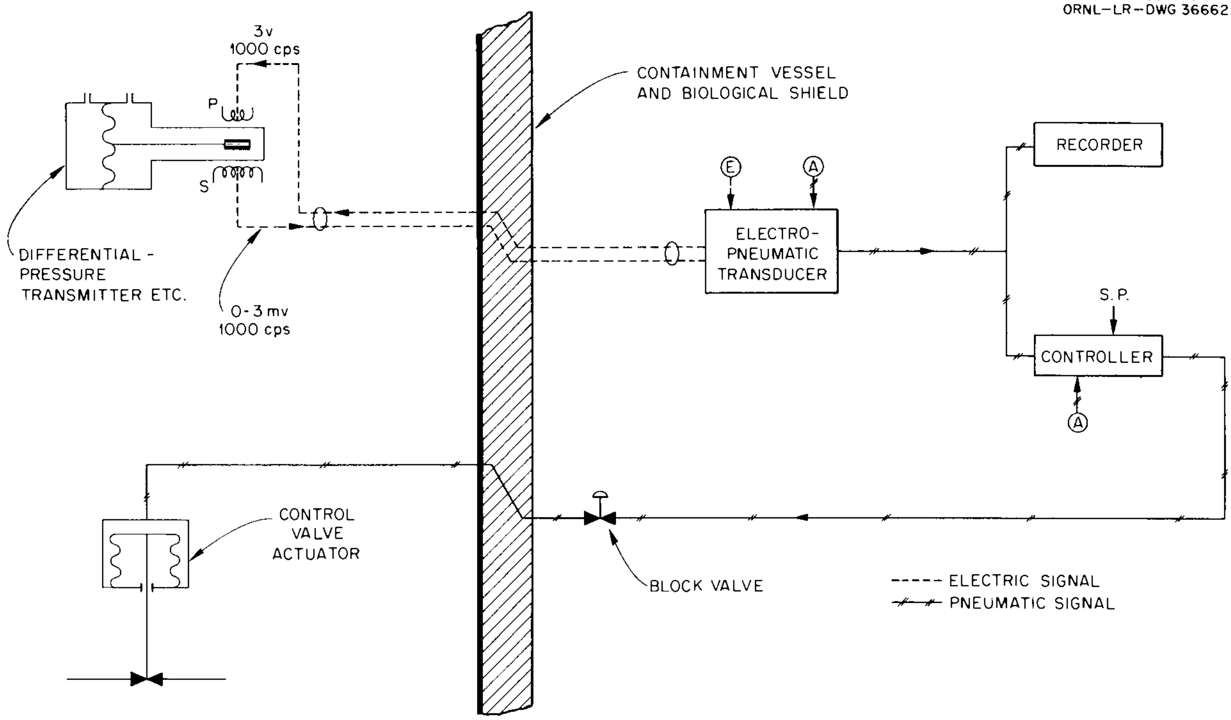

Fig. 61. Typical Reactor Instrumentation and Control Loop.

UNCLASSIFIED
ORNL-LR-DWG 36663

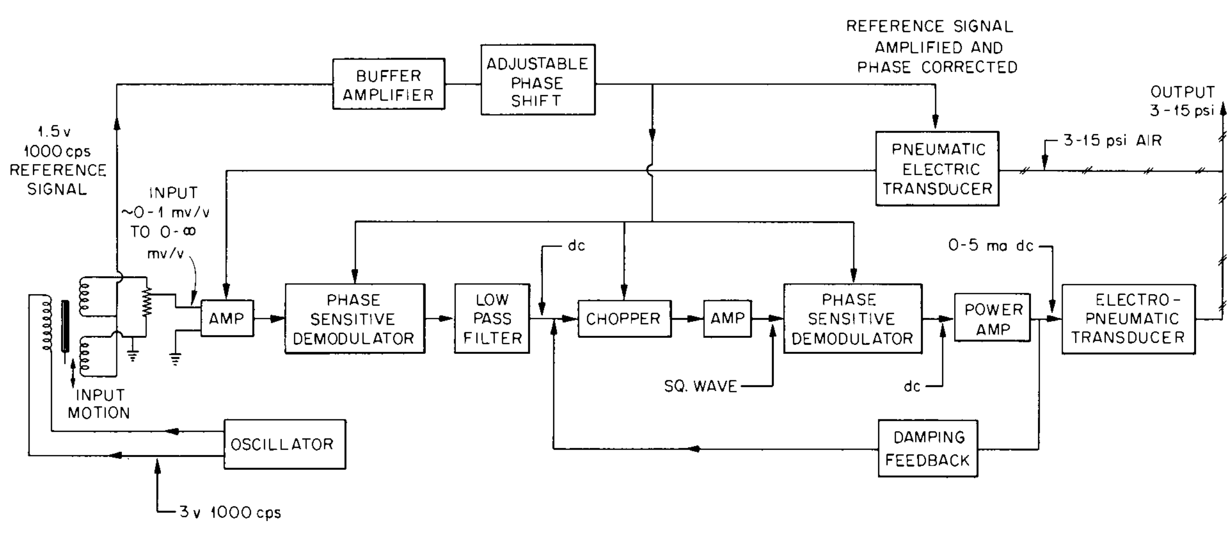

Fig. 62. Transistorized Electropneumatic Converter.

2. The output of the linear variable differential transformer is a 1000-cps signal having an amplitude proportional to the linear displacement of the ferrite core slug which is positioned by the instrument sensing element.

3. This signal is amplified and converted to a d-c voltage by a phase-sensitive demodulator.

4. The d-c output of the first stage is passed through a low-pass filter to remove frequencies above 1 cps. This eliminates signals caused by vibration or turbulence in primary elements which might saturate the amplifier.

5. After filtering, the d-c signal is amplified by a d-c amplifier consisting of a 1000-cps transistor chopper, an a-c amplifier, and a phase-sensitive demodulator.

6. The amplified d-c voltage is used to control a power amplifier stage which supplies a d-c current of 0–5 ma to a commercial electromechanical electric-to-pneumatic transducer giving a 3- to 15-psi proportional output signal.

7. The output also supplies a pneumatic-to-electric converter, the output of which is a 1000-cps signal which is proportional to the pneumatic signal and which is in phase opposition to the input signal. This signal is fed back to the input amplifier to provide over-all feedback around the instrument. This feedback stabilizes the instrument and increases linearity.

8. An adjustable d-c feedback loop is also provided around the d-c amplifier to provide damping and prevent oscillation of the instrument.

9. The reference voltages for the phase-sensitive demodulator and transistor chopper and the primary voltage for the feedback transducer are supplied via phase-shift and buffer amplifiers from one secondary of the transmitting differential transformer. This method of phasing eliminates the attendant reduction in signal amplitude experienced when phasing is accomplished by phase-shifting the signal voltage.

Unusual features of this instrument include

1. the use of over-all electric-to-pneumatic feedback to provide stability and linearity,
2. the use of a two-stage amplifier with d-c filtering at low levels to prevent saturation of the amplifier by noise and stray pickup voltages or by spurious signals resulting from vibrations in the transmitting device,
3. the elimination of the necessity for phase-shifting the input signal and the automatic phase-shifting which results from deriving the reference voltage from the differential transformer secondary rather than directly from the oscillator.

The power requirements of the instrument are 250 ma at 48 v dc. It is estimated that the instrument could be duplicated at a cost of about $1000, which is about the cost of vacuum-tube equipment. The instrument utilizes 26 transistors to replace six vacuum tubes (really ten tube functions). Experience in test operation to date has not been conclusive. In an effort to minimize the package size and afford modular construction, the unit was built on modular printed circuit boards. Condenser leads were bent on too short a radius and have been giving intermittent trouble. It is hoped that reliability can be proved and that perhaps the circuitry can be simplified in the future.

Figure 63 shows the amplifier chassis. The components are mounted on printed circuit boards which plug into side-mounted connectors. Figure 64 shows the aluminum heat-dissipating fins for the output transistors and the chassis connector. Figure 65 shows the electric-to-pneumatic output stage and the pneumatic-to-electric feedback assembly.

Differential Pressure Transmitter for Slurry Systems

A survey of pressure and differential pressure instruments suitable for a reactor slurry system has been made to aid in the planning of an instrument development program.[2] Commercial instruments presently available require connecting lines which are subject to plugging, incorporate fluid fills not compatible with the reactor fluids or piping, or lack a secondary seal behind thin members. It is desired that an instrument system be developed which does not require an auxiliary source of purge water. A transmitter of the type shown conceptually in Fig. 66 is now being constructed by The Foxboro Company on a best-effort basis.

This transmitter has a diaphragm flush with the slurry-filled pipe wall to avoid plugging. The diaphragm is mechanically coupled to range springs and the core of a differential transformer by a rod. The core motion is sensed through a pressure housing to provide an all-welded seal. The back side of the diaphragm will be reference-connected to a system vapor space or to a source of constant gas pressure.

Instrument Alarm-Scanner

A process variable instrument alarm-scanner manufactured by Taylor Instrument Companies to ORNL specifications was placed in service. This alarm-scanner affords a means of satisfying a dual requirement encountered in instrumenting in-pile loops. Periodic loop operation for data acquisition requires precision readout of pressure, and operational safety requires continuous monitoring of temperatures and pressure to ensure that the variables are within safe limits. A block diagram of the system is shown in Fig. 67. This instrument is designed to select in sequence one variable per second and compare it with a preselected high and low limit. If the system is outside the limits, an audible alarm is sounded and a visual indication of its high or low condition is displayed. Means for manually checking the lamps and the high-low limit operation are built into the instrument. Precision readout is accomplished by manually

---

[2]H. D. Wills, Survey of Pressure and Differential Pressure Instrument Types for Possible Application to HRE-3 Slurry Systems, ORNL CF-57-10-88 (Oct. 25, 1957).

UNCLASSIFIED
PHOTO 31566

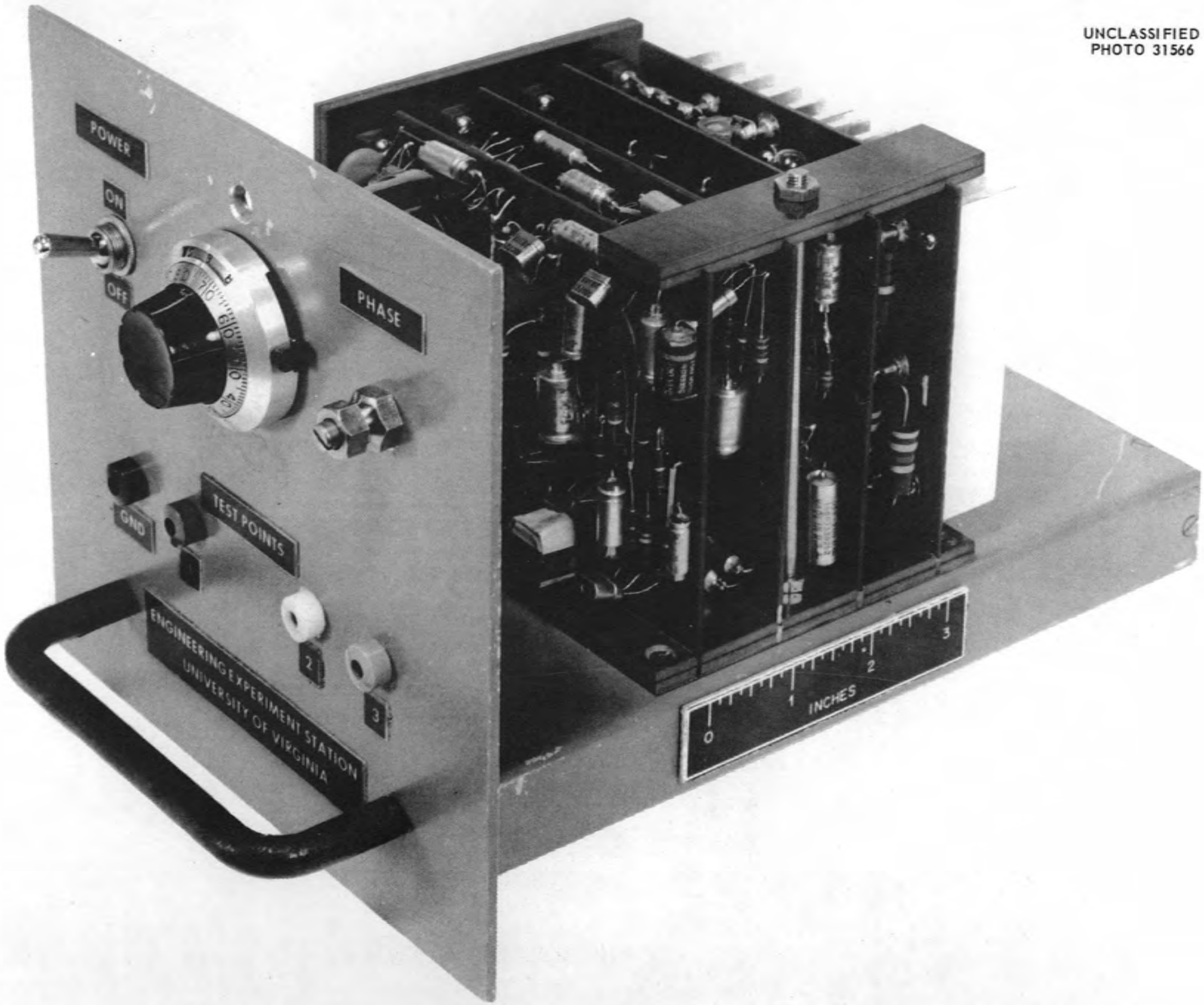

Fig. 63. Transistorized Electropneumatic Converter Chassis. Front view.

UNCLASSIFIED
PHOTO 31569

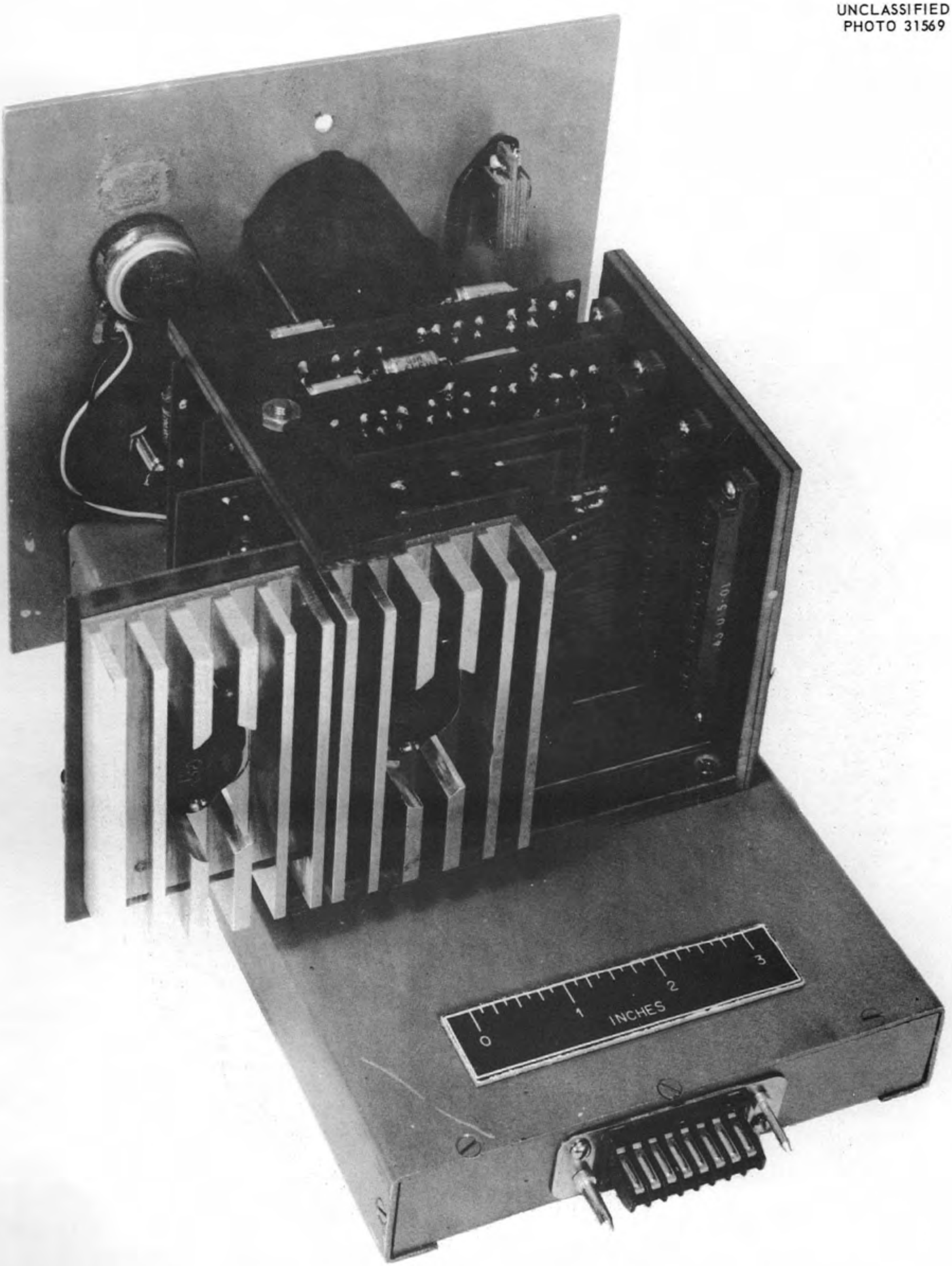

Fig. 64. Transistorized Electropneumatic Converter Chassis. Back view.

UNCLASSIFIED
PHOTO 31567

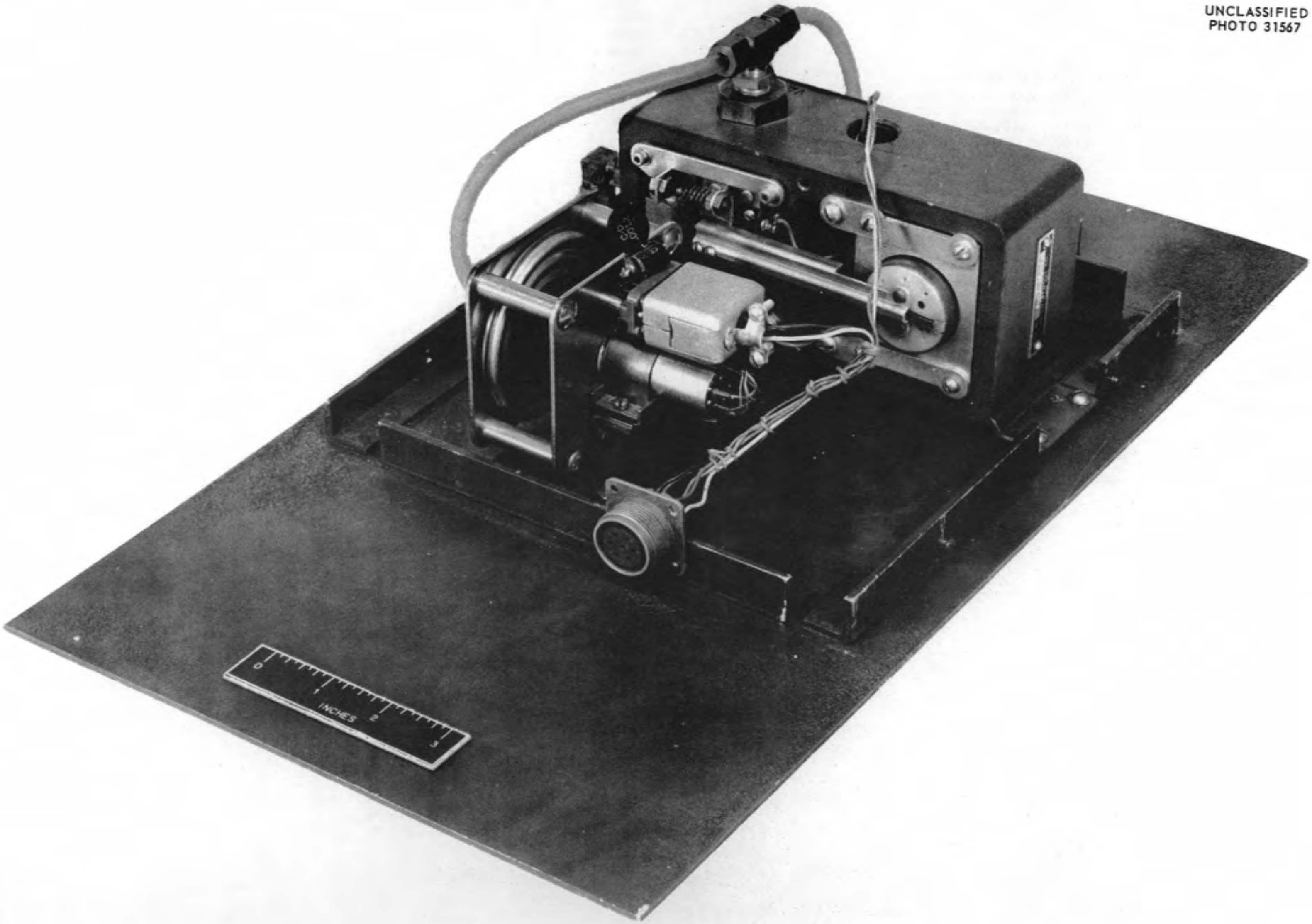

Fig. 65. Transistorized Electropneumatic Converter – Electric-to-Pneumatic Output Stage and Pneumatic-to-Electric Feedback Assembly.

UNCLASSIFIED
ORNL-LR-DWG 25323

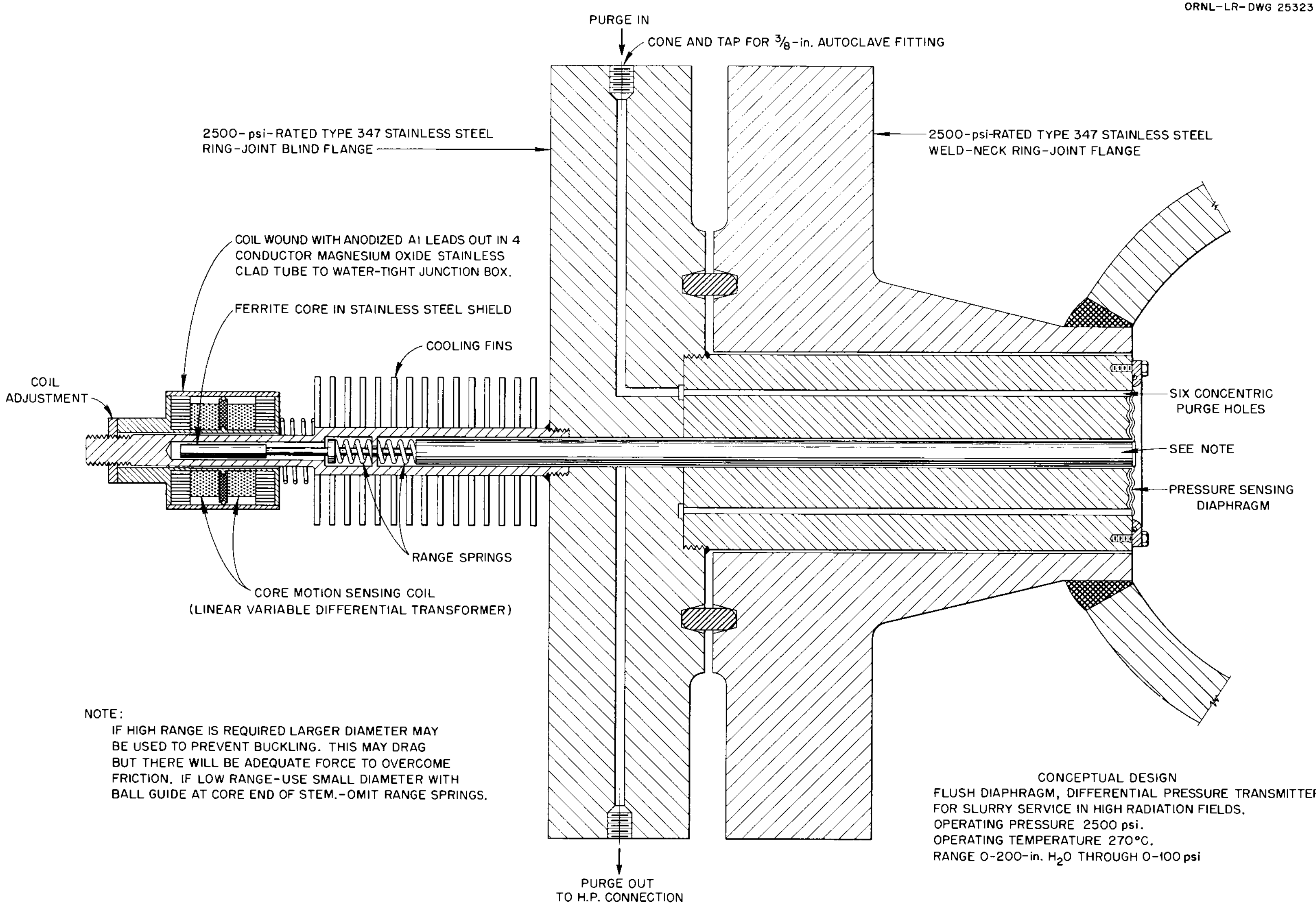

Fig. 66. Flush Diaphragm Differential Pressure Transmitter – Conceptual Design.

UNCLASSIFIED
ORNL-LR-DWG 28348

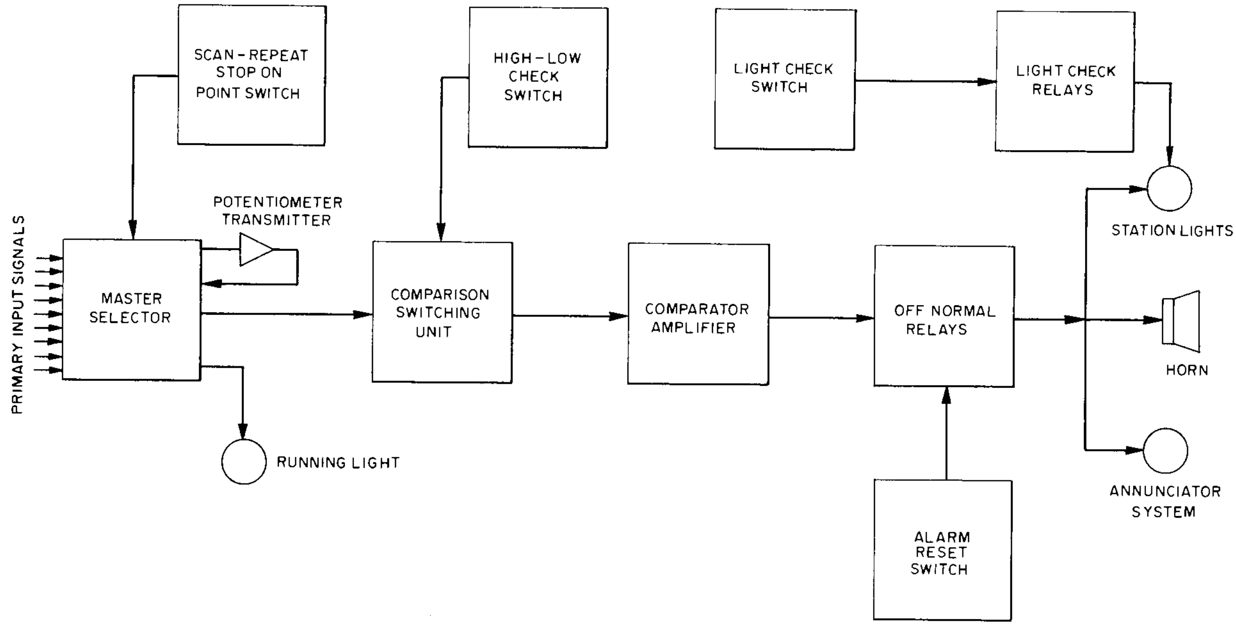

Fig. 67. Instrument Alarm-Scanner. Block diagram.

switching the variable to an expanded-scale self-balancing precision potentiometer.

Figure 68 shows the scanner and indicator mounted in a standard ORNL modular instrument cabinet. The bottom section contains auxiliary power supplies and Transet potentiometer-transmitters for converting signals from strain-gage-type pressure transmitters to millivolt signals compatible with the scanning system. Temperature signals from thermocouples are fed directly into the scanner.

While most of the system is wired to scan 20 variables, indication was provided for only 14 of these. Each of the variables is designated by a number marked on a circular Lucite block; the blocks are arranged in two rows at the top of the panel. Each block has two indicating lamps mounted within, an amber light indicating an off-normal low condition and a red light indicating a high condition. Another amber lamp flashes once per second as the variables are scanned.

The eight electronic chassis, the lamp and manual switch bank, and the high-low limit setting are shown in Fig. 69. The separate chassis are interconnected with Varicon connectors so that any unit may be easily removed from the cabinet for maintenance.

Control Valve Stem Position Transmitter

A control valve position-indicating system utilizing a differential transformer for a transmitting element was developed and installed on the HRT mockup letdown valve for testing. The transmitter, shown mounted on a valve actuator in Fig. 70, was designed to withstand the HRP reactor

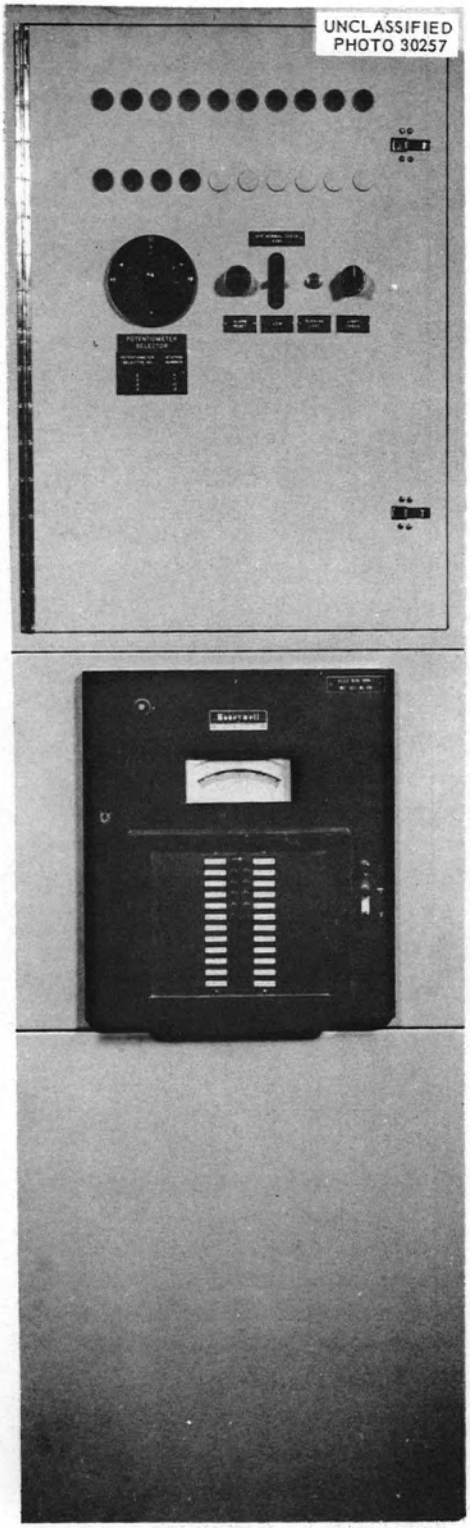

Fig. 68. Instrument Alarm-Scanner. Front view.

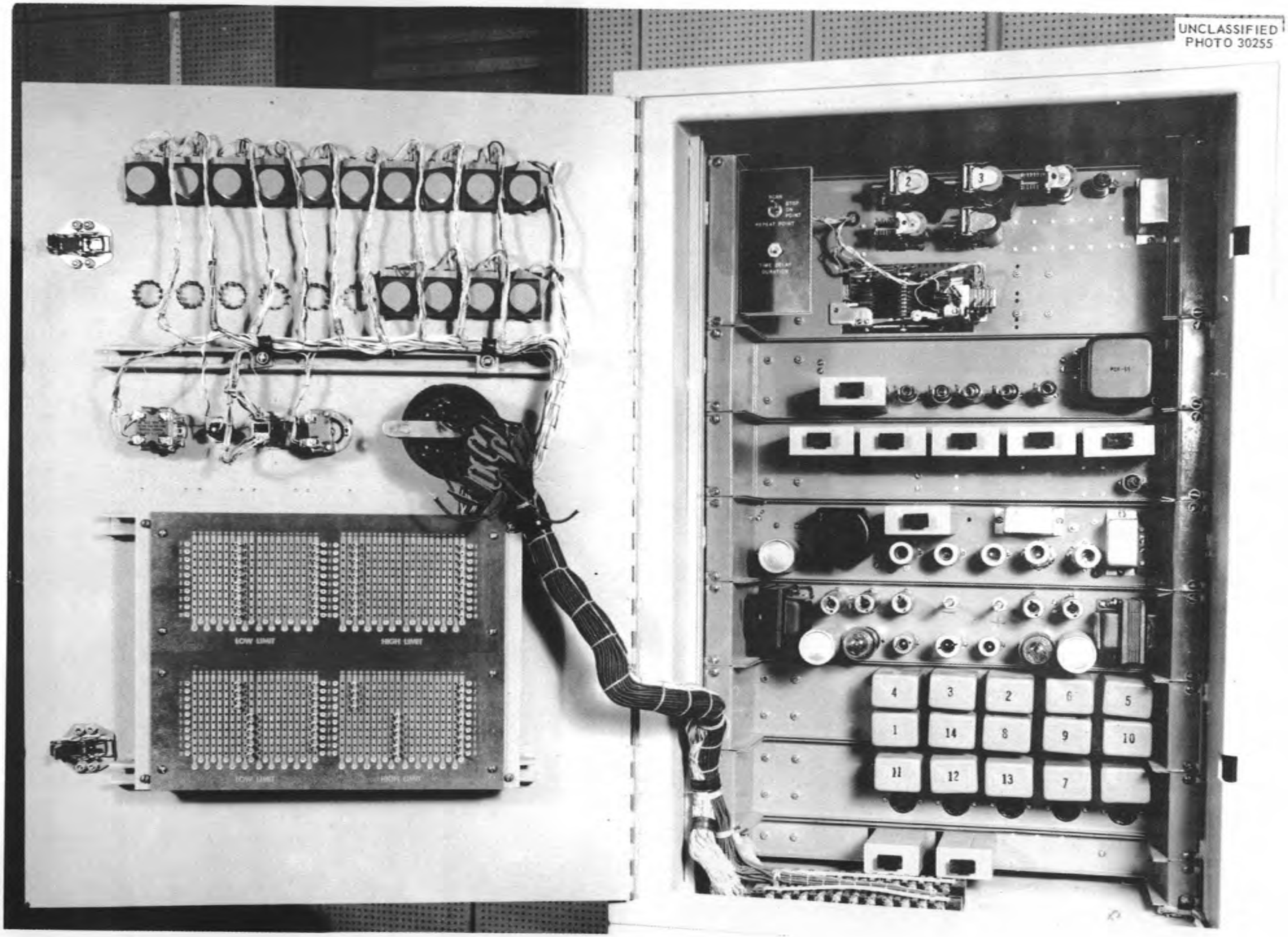

Fig. 69. Instrument Alarm-Scanner. Back view of chassis.

UNCLASSIFIED
ORNL-LR-DWG 28326

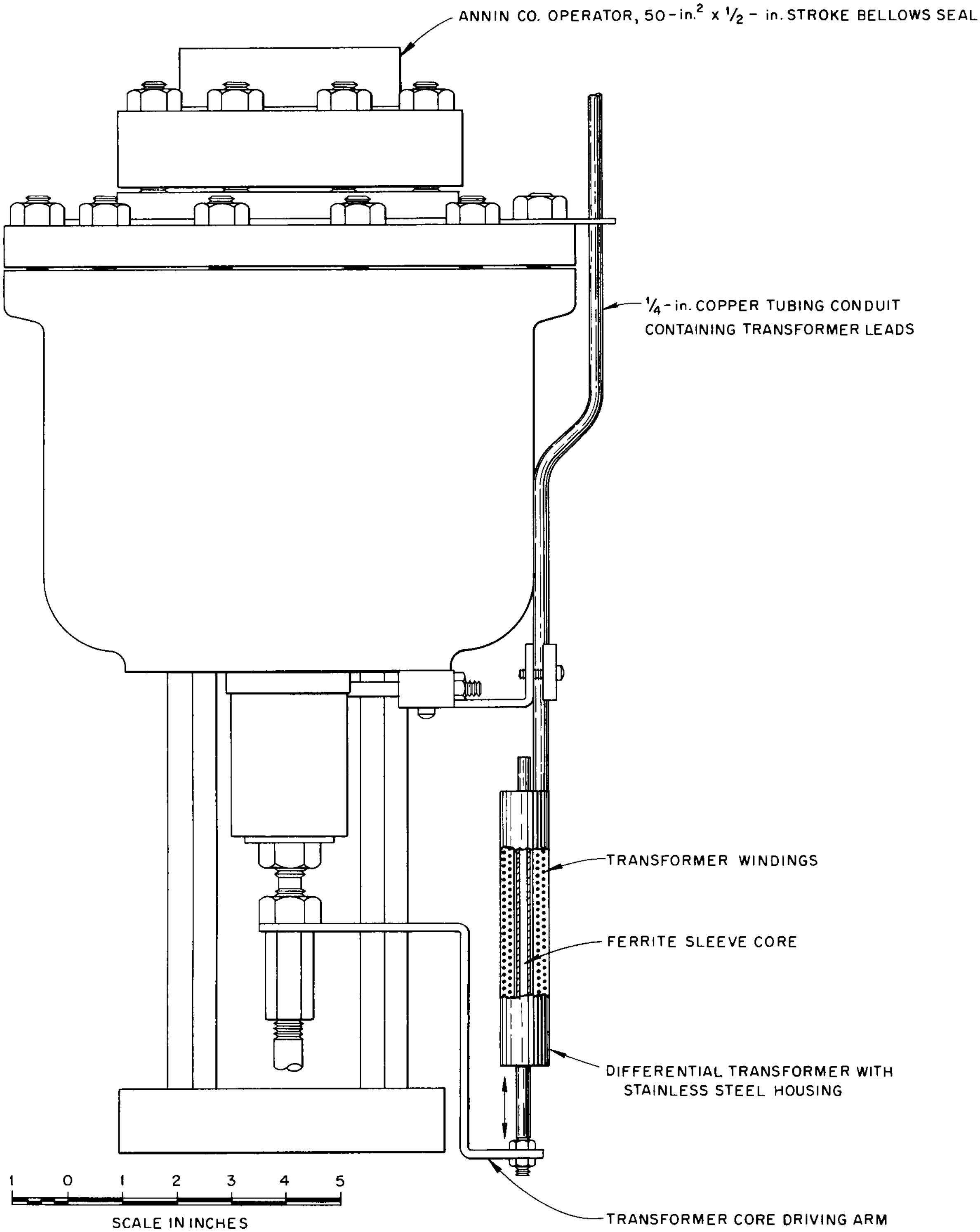

Fig. 70. Control Valve Stem Position Transmitter.

cell environmental conditions. These include a 140°F ambient temperature, possible water flooding, and high levels of radiation. The differential transformer is an Automatic Temperature Control Company model 6206-K with a linear range of 0 to 1/2 in., a linearity of 2%, and an output of 0.1 v for 1/2-in. core travel with 60-cps primary excitation. The Fiberglas-insulated lead wires leave the waterproof transformer housing in a 1/4-in. copper tube conduit.

A simple electropneumatic transducer system for the 60-cps signals from the above linear variable differential transformers was developed using standard modular elements. The system shown in Fig. 71 employs three vacuum tubes in the controller and is used to derive a pneumatic signal proportional to the valve position for indication and alarm. Performance tests indicate a linearity of 0.5%, no change in output signal with supply pressure changes from 15.5 to 25 psi, and freedom from zero drift with electric supply changes from 95 to 125 v.

A transmitting flowmeter of the variable-area type was purchased to evaluate its suitability as a primary element for the measurement of the very low purge-water flow rates which exist in the pressurizers and circulating pumps of HRP systems. The prototype design shown in Fig. 72 is superior to that incorporated in a higher-flow-range transmitter tested earlier[3] because the in-line flow connection avoids stagnant areas which

[3] D. S. Toomb *et al.*, Instrumentation and Controls Ann. Prog. Rep. July 1, 1957, ORNL-2480, p 74.

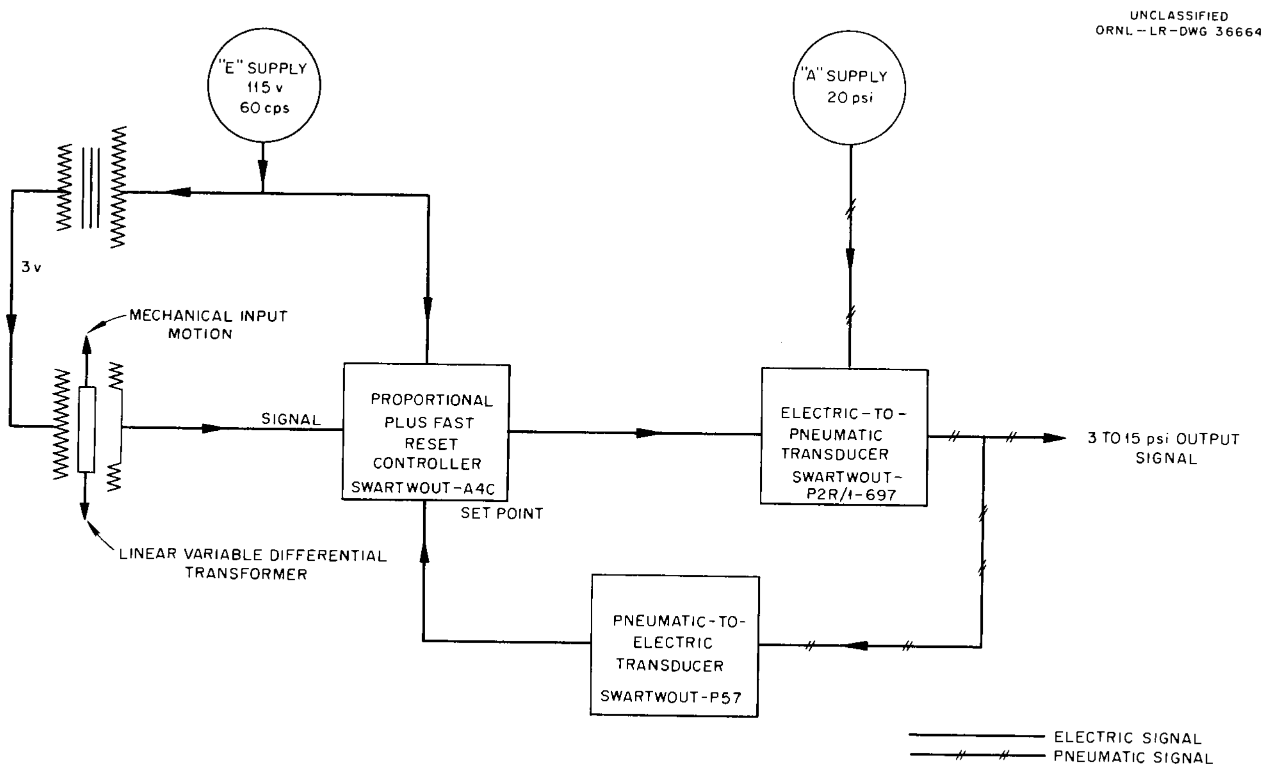

Fig. 71. Transducer System for Linear Motion to Pneumatic Signal. Block diagram.

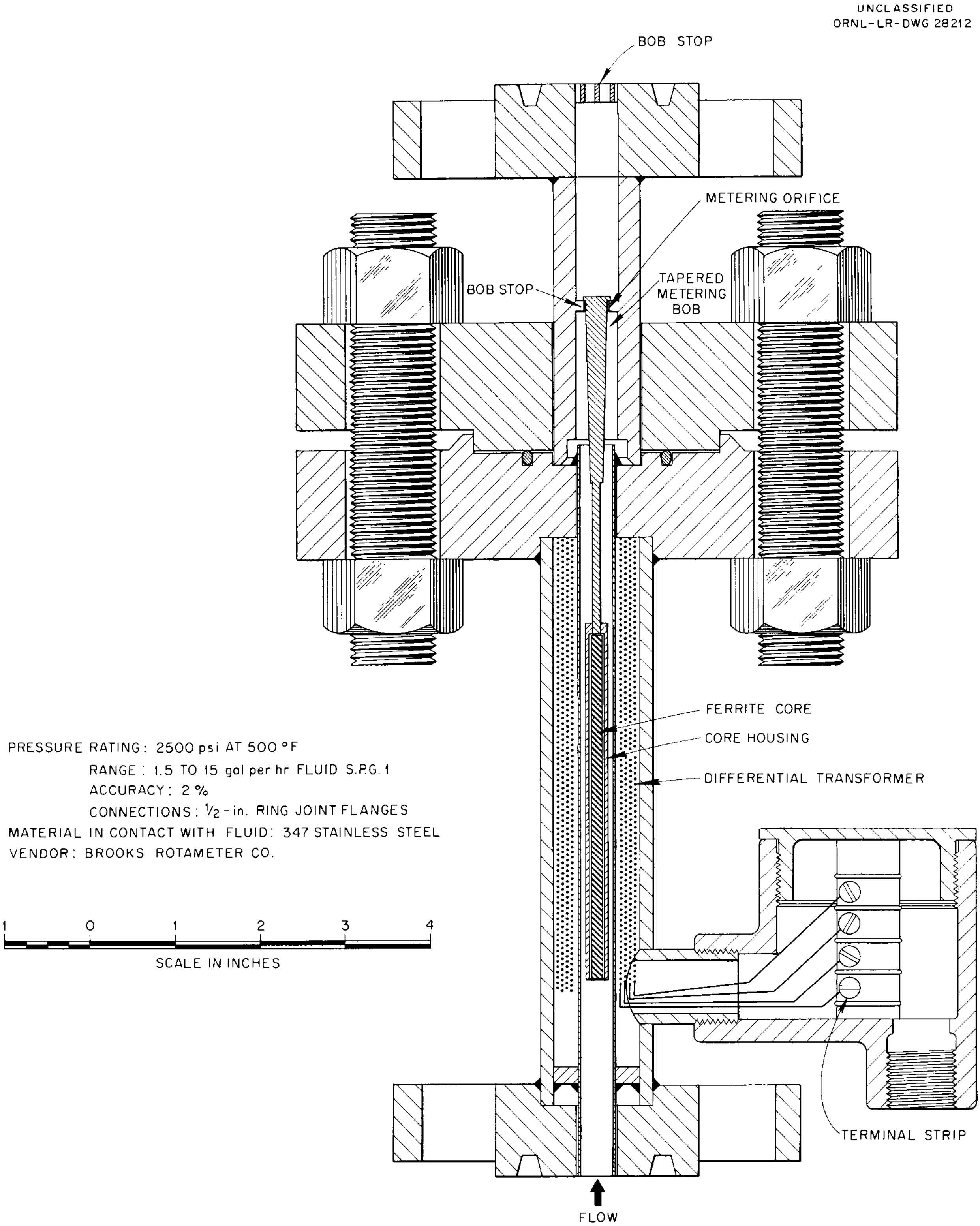

Fig. 72. Low-Range Transmitting Variable-Area-Type Flowmeter.

might fill with sediment. Other features of this meter include the linear output signal necessary to produce a true average of the pulsing flow (when damped by a suitable filter) and a low head loss, which allows the transmitter to be used in the low-pressure suction line of the pumps.

A similar but higher-range transmitter purchased for feed pump output flow measurements is shown in Fig. 73. The undesirable mid-section flange was not used in this design.

Heated-Thermocouple-Probe Liquid-Level Sensor

A heated-thermocouple probe of the type shown in Fig. 74 is being used as a static low-liquid-level sensor in a high-pressure boiler. The sensor contains a thermocouple which is heated at a constant rate by a Nichrome heating element. When the liquid level drops below the thermocouple junction, the reduced heat transfer from the probe to the surrounding vapor causes the temperature of the probe to rise. The resulting increase in thermocouple output closes a contact-making millivoltmeter which pilots an alarm or safety relay. In preliminary tests, the probes were operated for 1 1/2 months at 300°C in air with no change in insulation resistance noted.

The probes are an improvement over a previously described type[4] in that the heating is localized at the thermocouple junction, resulting in an increased sensitivity to liquid-level changes and a shorter response time. The electrical insulation, being completely inorganic, is not subject to radiation damage.

Pressure Transmitters

The pressure transmitter shown in Fig. 75 was developed for the Navy by the Swartwout Company. The transmitter is being evaluated for its suitability in HRP reactor environments. This transmitter has twin Bourdon tube sensing elements, a containment pressure housing, and a motion-to-electrical-signal transducer. The transducer is a differential transformer which senses the primary element motion through the pressure housing. Figure 76 shows the rugged construction of this instrument.

CONTROL VALVE AND ACTUATOR DEVELOPMENT

A continuing program is being carried on for the development of improved valves and actuators to control the flow of fluids and slurries in the HRP.

Slurry-Service Valves

The prototype of a pneumatically actuated sampling valve was constructed for slurry test-loop service. The valve, shown in Fig. 77, has a bellows stem seal and a replaceable plug and seat. A type 17-4 PH

---

[4]D. S. Toomb, A. M. Billings, and H. D. Wills, HRP Quar. Prog. Rep. July 1, 1956, ORNL-2148, p 67.

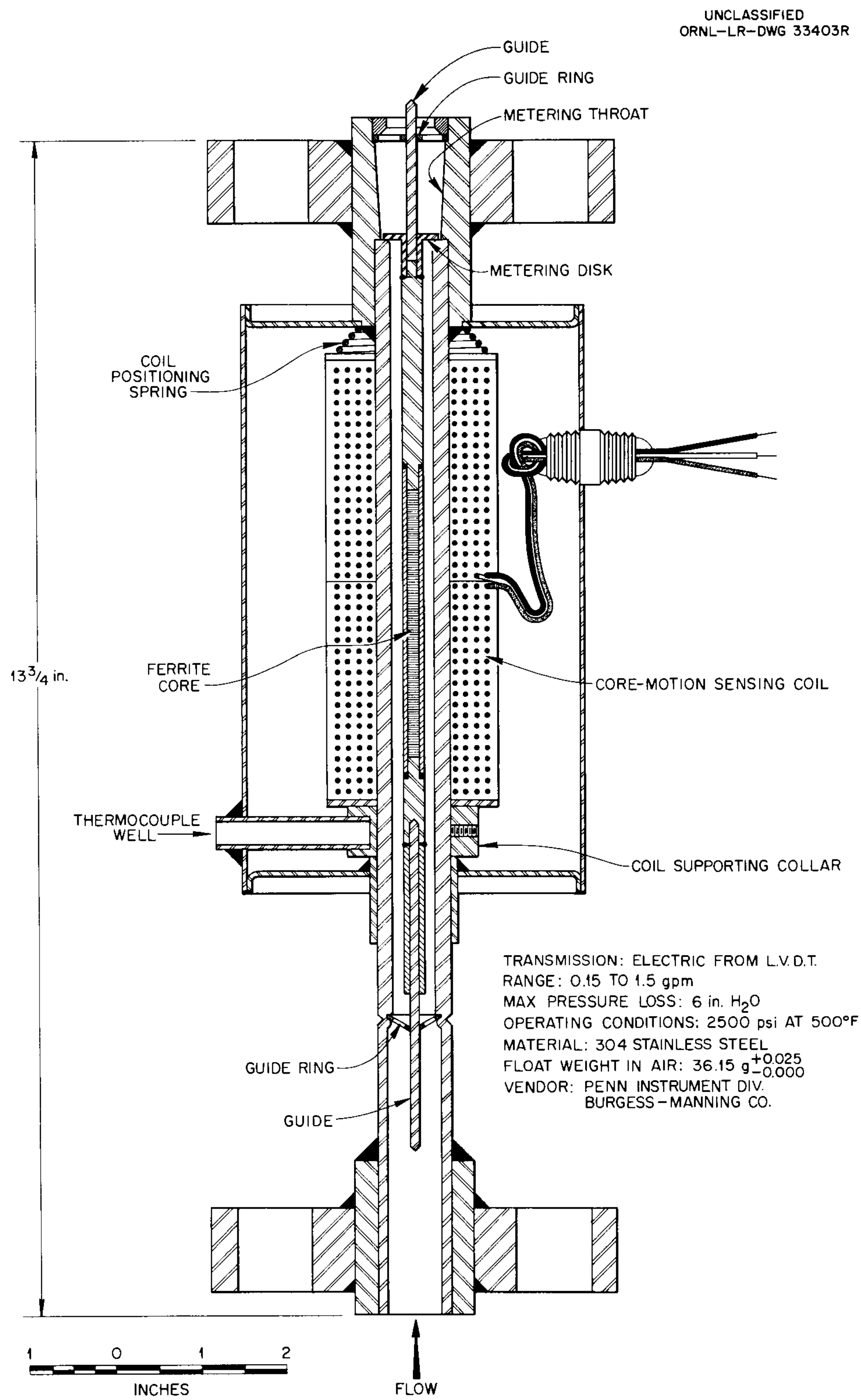

Fig. 73. High-Range Transmitting Variable-Area-Type Flowmeter.

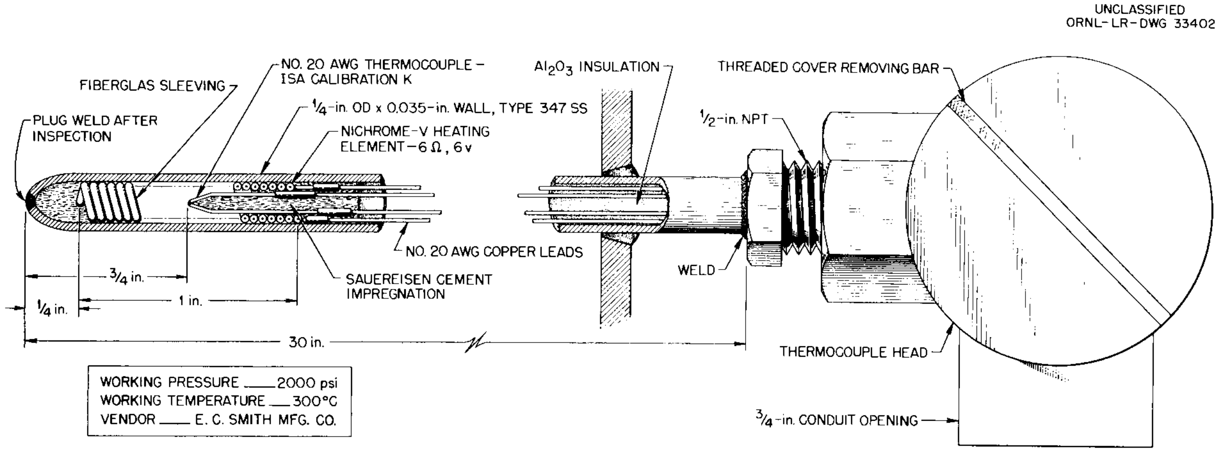

Fig. 74. Heated-Thermocouple-Probe Liquid-Level Sensor.

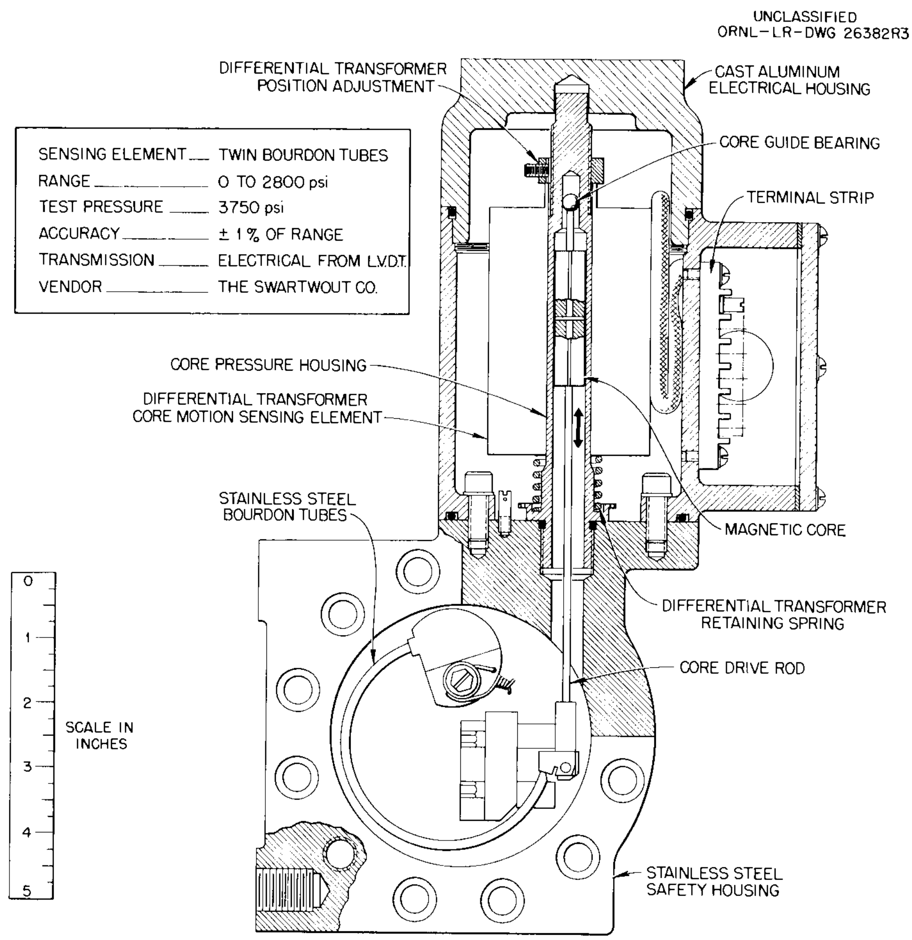

Fig. 75. Pressure Transmitter with Safety Housing.

UNCLASSIFIED
PHOTO 31577

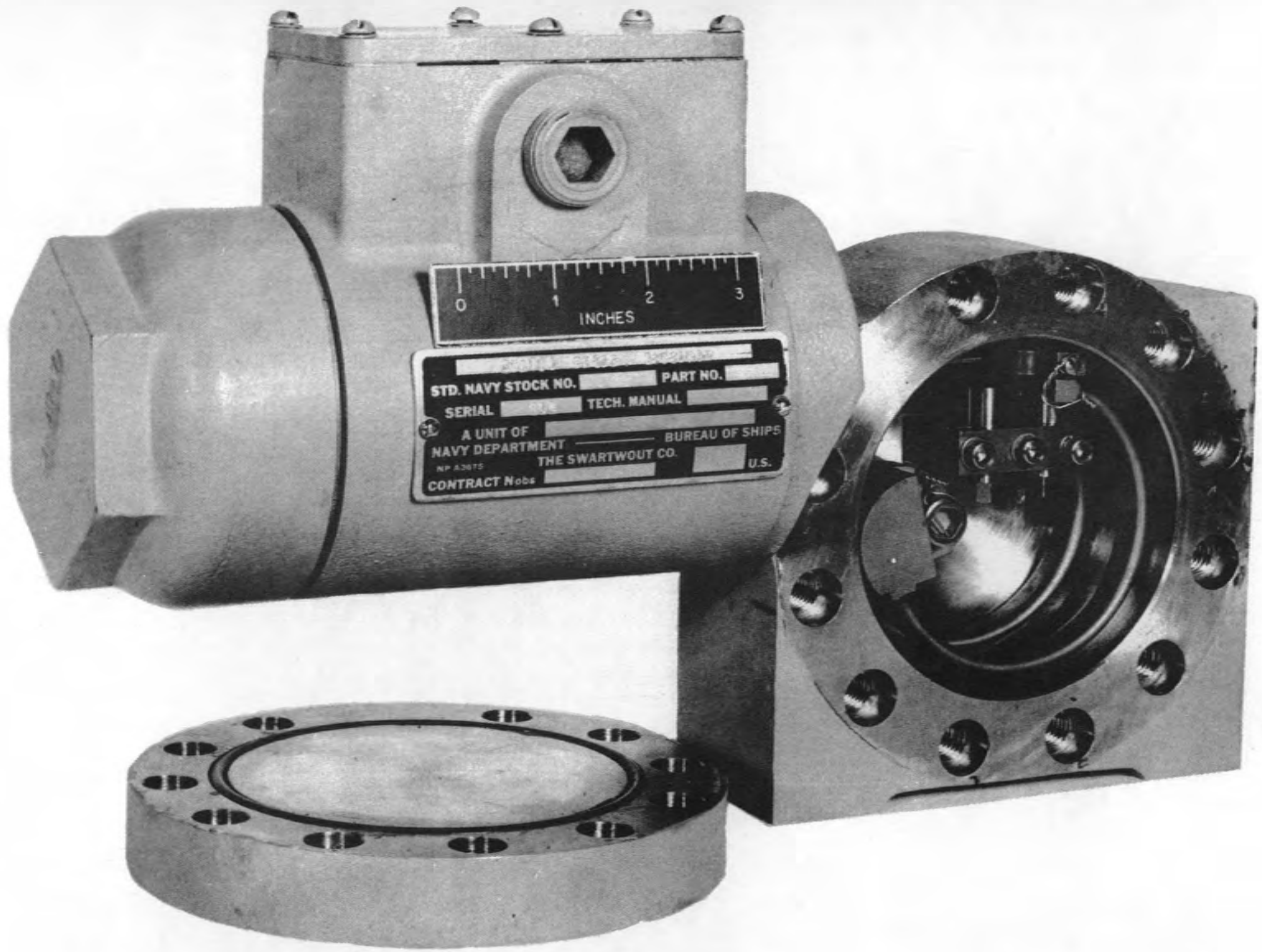

Fig. 76. Pressure Transmitter with Safety Housing. View of element housing.

UNCLASSIFIED
ORNL-LR-DWG 33407

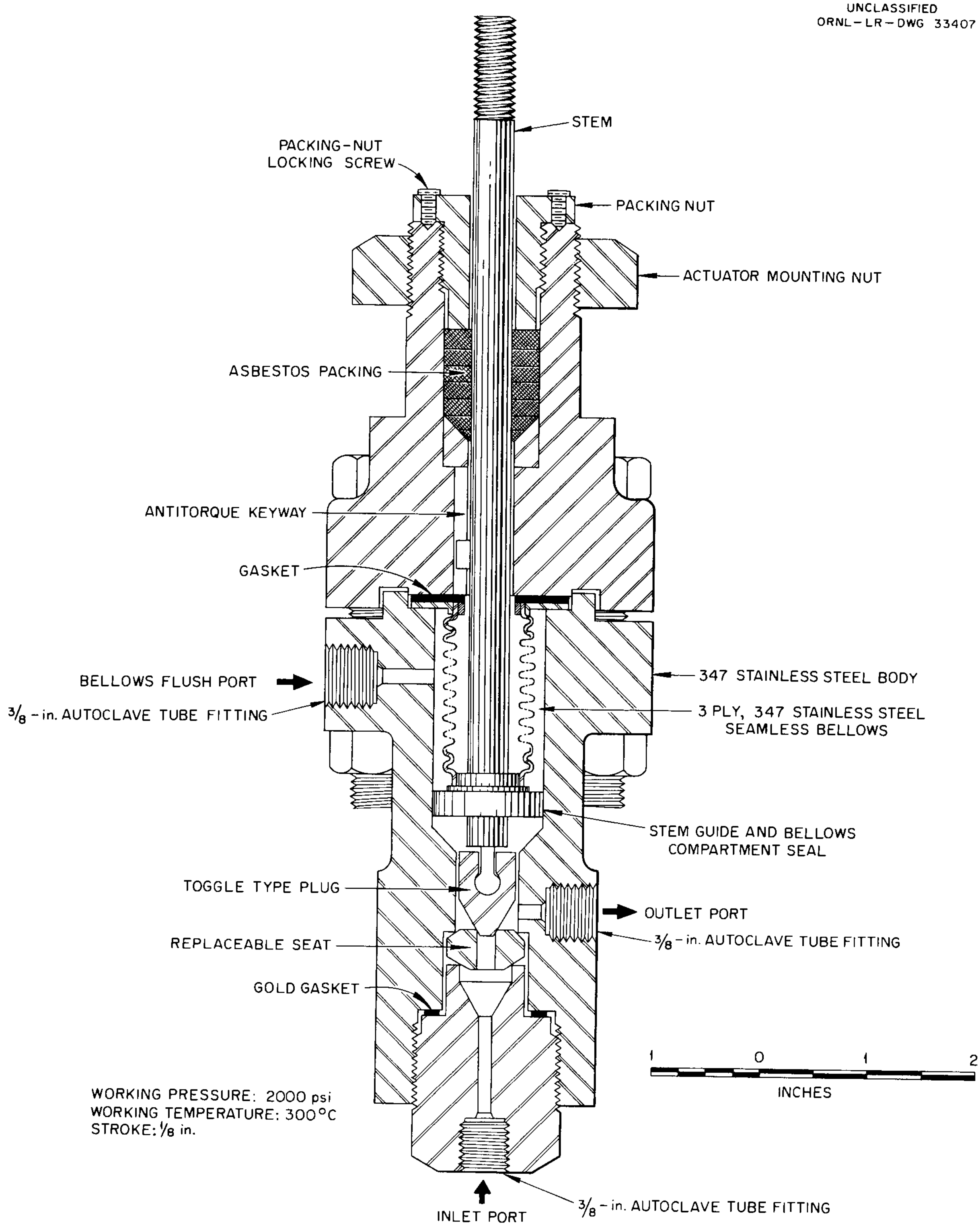

Fig. 77. Slurry Sampling Valve.

stainless steel plug and seat will be tested initially. Since the replacement of the plug and seat is simple, several other materials will be tried at a later date.

A bellows-sealed pneumatically actuated control valve installed as a flow control element in the 30-gpm slurry loop was removed after 907 hr of service. The valve design, shown in Fig. 78, incorporates a bellows compartment flushing connection and angle body design; tungsten carbide was used for the plug, seat, and plug guide.

Upon disassembly, the tungsten carbide plug and plug guide were found to be bound so tightly that movement of the plug was impossible. Also, the plug guide was cracked and displaced by 1/4 in. from its press fit in the stainless steel holder. A thin layer of slurry was visible in the annulus between the plug and plug guide. After removal of the plug from its guide, a thick green and blue scale was found on the portion of the plug which was frozen in the guide. The plug and guide (after removal) are shown in Fig. 79.

Service to which this valve was subjected was as follows:

Valve wide open	825 hr
Valve 40% open (50% flow)	75 hr

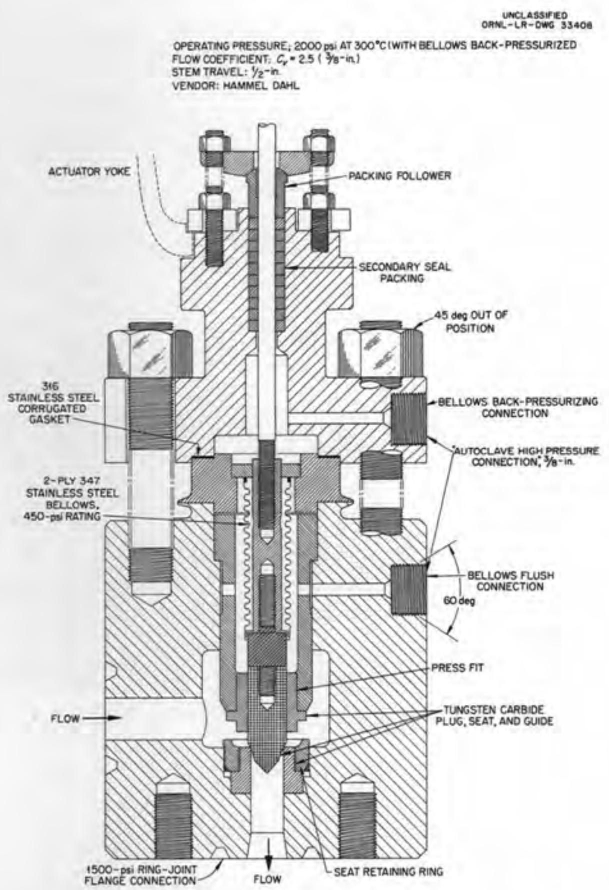

Fig. 78. High-Pressure Slurry Control Valve.

Fig. 79. Plug and Guide Assembly from High-Pressure Slurry Control Valve.

Flow, wide open	40 gpm
ΔP across valve	5 to 10 psi
Loop pressure	1650 psig
Loop temperature	280°C
Direction of flow in valve	From top of seat
Slurry concentration	450 g of Th per kg of H_2O

The replacement valve for this application uses a chromium carbide plug and seat and a tungsten carbide guide. For subsequent loop operation, the condensate purge of the bellows compartment will be increased as a precaution against plugging of the guide-to-plug passage.

A valve especially constructed for slurry use was obtained from the Hammel-Dahl Company and will be installed in the 200B slurry loop. The valve, shown in Fig. 80, incorporates a long-radius-bend body configuration to minimize erosion by the slurry. The bellows compartment can be purged to prevent slurry from entering through the annulus between the Stellite No. 6 stem guide pads and the Colmonoy hard-faced stem. As the two-ply type 347 stainless steel bellows used in this valve is rated at only 450 psi, provision is made to back-pressurize the bellows when the valve is used in applications above this pressure; the valve body is designed for a working pressure of 2000 psi at 300°C. The plug and seat are fabricated of tungsten carbide, an extremely hard material, for wear resistance.

Solution-Service Valve Trim[5]

Two Zircaloy-2 plugs were cycled with approximately 400 dumps each of uranyl sulfate in the valve test loop. The plugs were badly damaged. The first trim set is shown before and after testing in Figs. 81 and 82, respectively. Galling is quite evident in the seating line of the plug. There was no evidence of the ignition reaction that occurred with two titanium alloy plugs tested earlier.

The type 347 stainless steel plug flame-plated with tungsten carbide by Linde was examined metallographically,[6] and the plate was found to be intact in the seating area, as shown in Fig. 83. The plate thickness along the contour of the plug is shown in Fig. 84.

Stem-Sealing Bellows

Gold plating was tried in an attempt to increase the corrosion resistance of the stainless steel bellows used for control valve stem seals. No improvement was noted. The plates on two bellows cracked upon flexing

---

[5]D. S. Toomb et al., Instrumentation and Controls Ann. Prog. Rep. July 1, 1957, ORNL-2480, p 83.

[6]R. L. Fitzgerald, "Metallographic Examination of 347 Stainless Steel Valve Plug," memorandum to F. W. Cooke, Sept. 20, 1957.

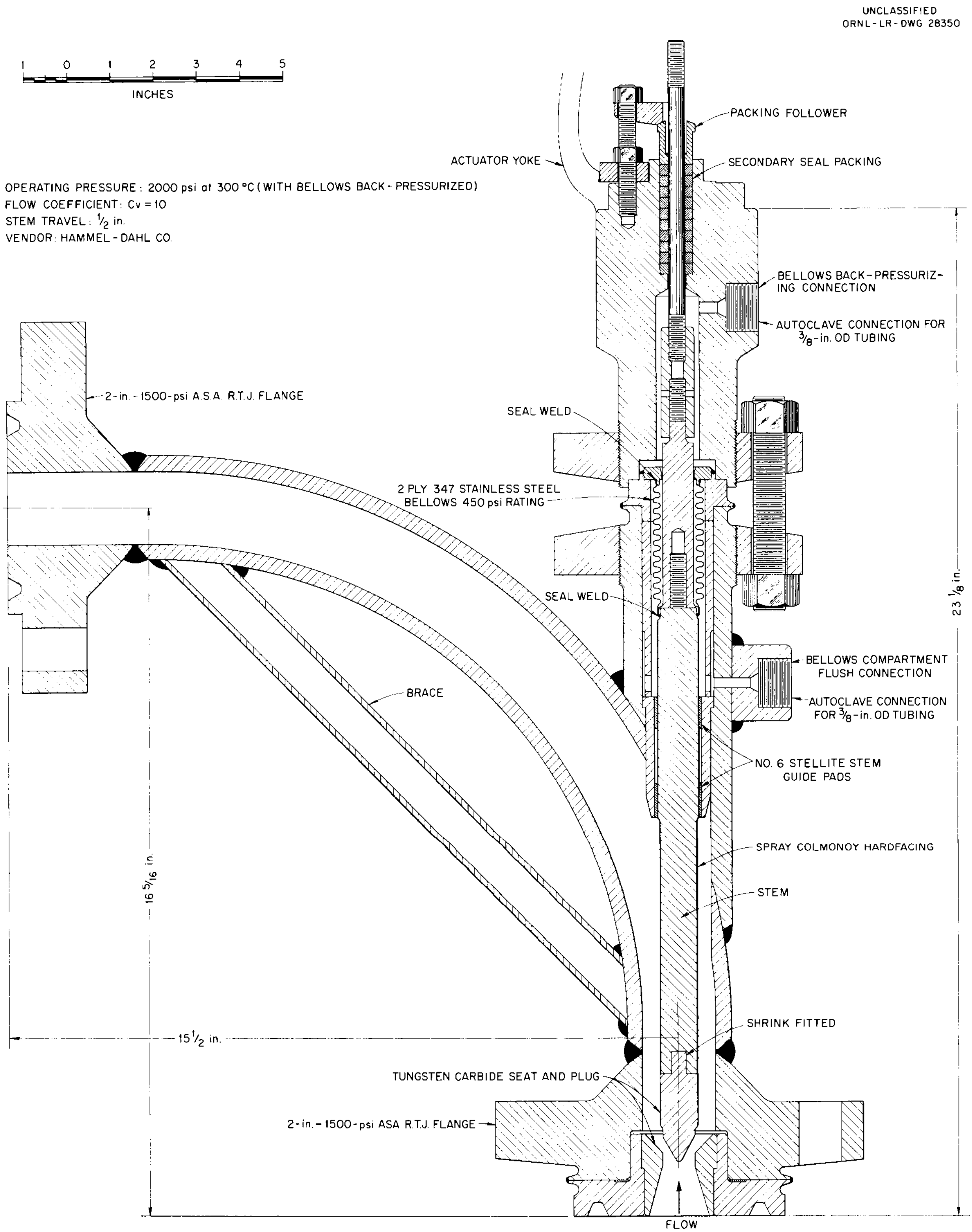

Fig. 80. Long-Sweep-Angle Slurry Valve.

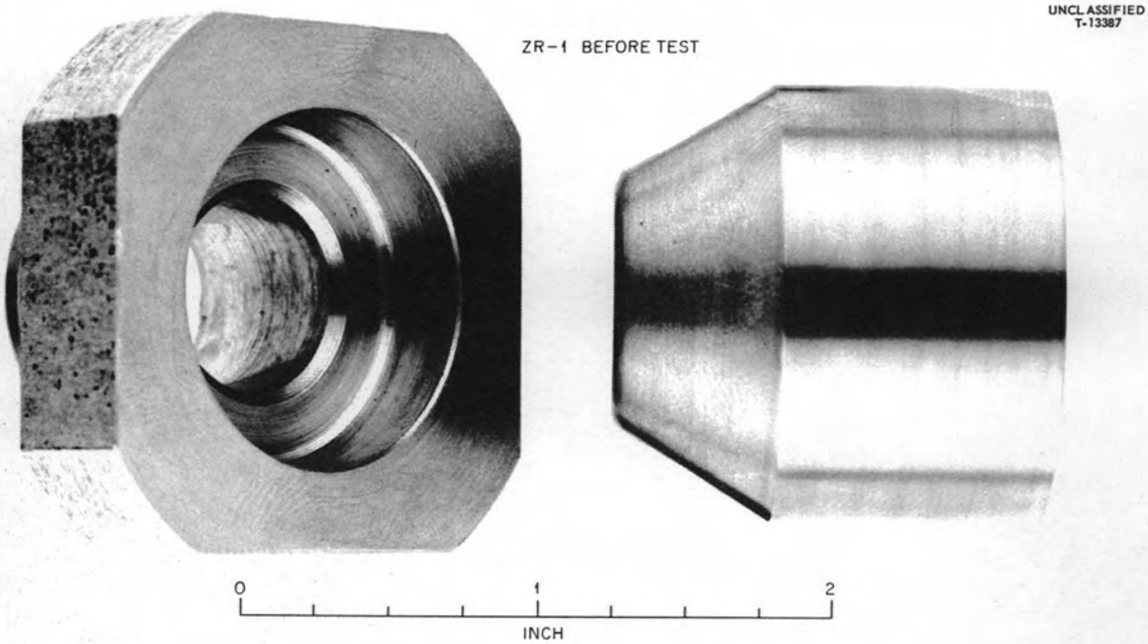

Fig. 81. Zircaloy-2 Trim Set Before Test.

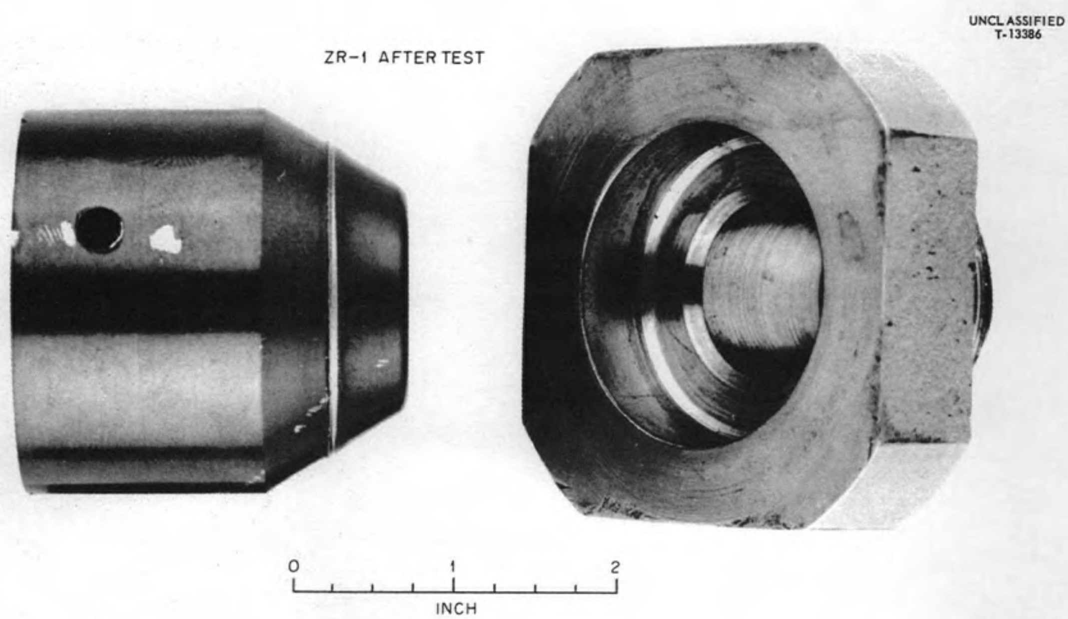

Fig. 82. Zircaloy-2 Trim Set After Test.

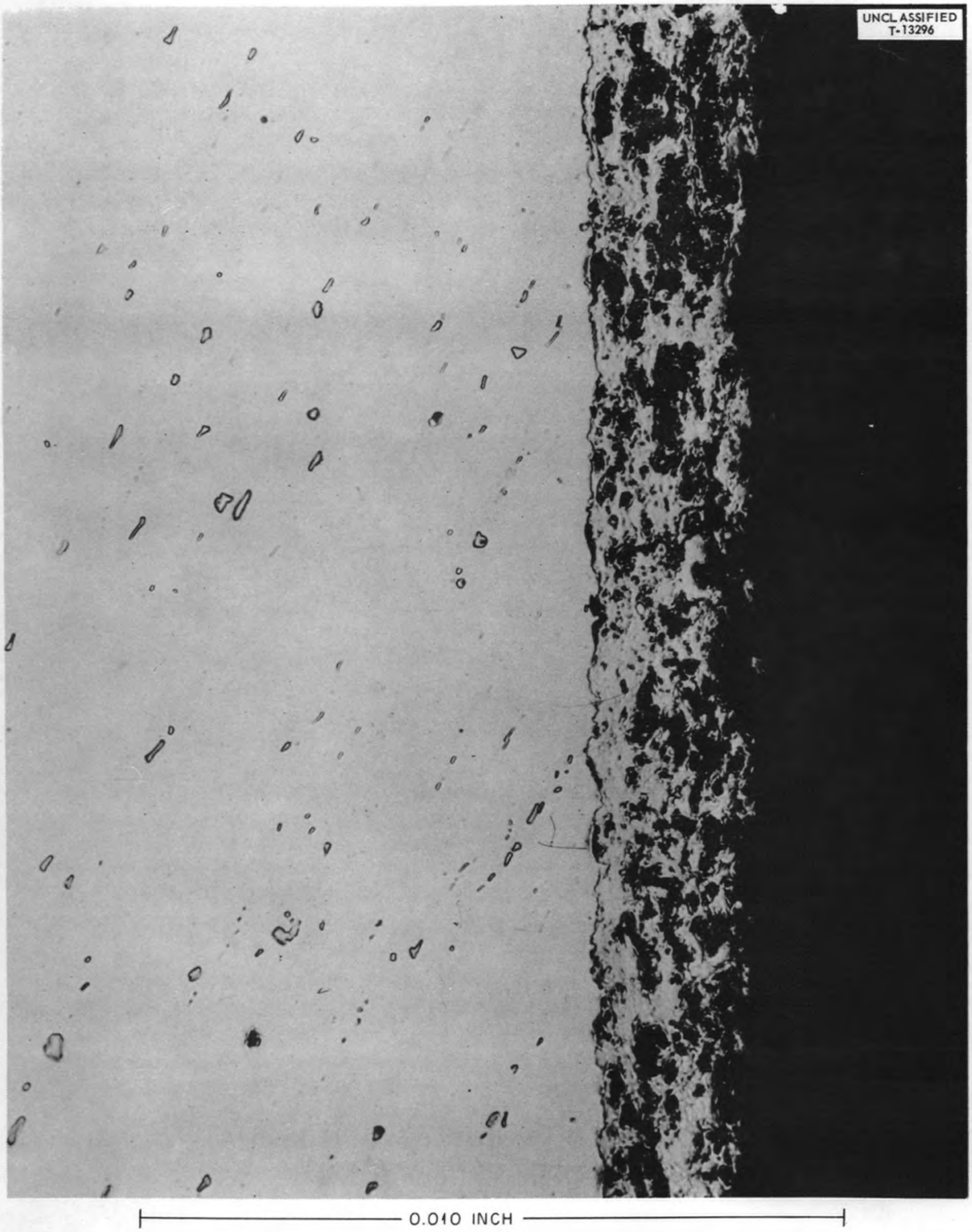

Fig. 83. Seat Area of Stainless Steel Valve Plug Flame-Plated with Tungsten Carbide.

and pitted when exposed to boiling 10 wt % hydrochloric acid.[7] Since three different plating techniques were unsatisfactory the project was discontinued.

Single- and three-ply titanium bellows were successfully formed by the Fulton Sylphon Division, Robertshaw-Fulton Controls Co., on an ORNL order. The specifications required the three-ply bellows formed of grade 55 titanium to withstand 2500-psi 300°C service. Dimensions of the three-ply test units were:

Thickness per ply	0.007 in.
Outside diameter	1 1/4 in.
Inside diameter	1 3/16 in.
Length	2 1/8 in.

Upon testing in uranyl sulfate at 2300 psi and 300°C with a stroke of 1/8 in., the first bellows failed at 78 cycles. A second unit was cycled at 1000 psi and 250°C with a stroke of 0.090 in. and failed at 5390 cycles.

On the basis of these tests and their own experimental findings, Fulton Sylphon increased the ply thickness of the bellows by 40% and doubled its length. Prototypes of the modified design are now being fabricated and will be available for testing in the near future.

A three-ply seamless type 347 stainless steel bellows was selected as the stem seal for all HRT valve applications where packing gland leakage might jeopardize reactor operation. The choice of this particular bellows (Fulton Sylphon Division, Robertshaw-Fulton Controls Co., drawing 10716-R3) was based on the HRE experience of no failures with similar units. That the choice was a good one was substantiated by the results of a recently completed life-testing program.[8]

Of four Fulton Sylphon 28-convolution light seal-welded bellows cycled at 2300 psi and 285°C in uranyl sulfate, the average number of 9/32-in.-stroke cycles before failure was 135,000. The minimum number was 59,000 and the maximum 185,000.

A 26-convolution version of the bellows described above is shown at the bottom of Fig. 85. The bellows shown at the top of the photograph is a three-ply type 316 stainless steel bellows with backup rings, rated at 10,000 psi by the manufacturer, The Foxboro Company. The construction of the backup rings is shown in Fig. 86. Two units were tested at 2000 psi and 250°C in water with a stroke of 0.076 in.; the numbers of cycles before failure were 26,450 and 30,783. The backup rings probably do not lend much support to the bellows at the 2000-psi test pressure.

---

[7] D. N. Hess, "Evaluation of Gold Plating on Type 347 Stainless Steel Bellows as Determined by Immersion in Boiling 10 wt % HCl," memorandum to A. M. Billings, Nov. 8, 1957.

[8] A. M. Billings, Life Test of Stem-Sealing Bellows for HRT Valves, ORNL CF-58-3-39 (March 17, 1958).

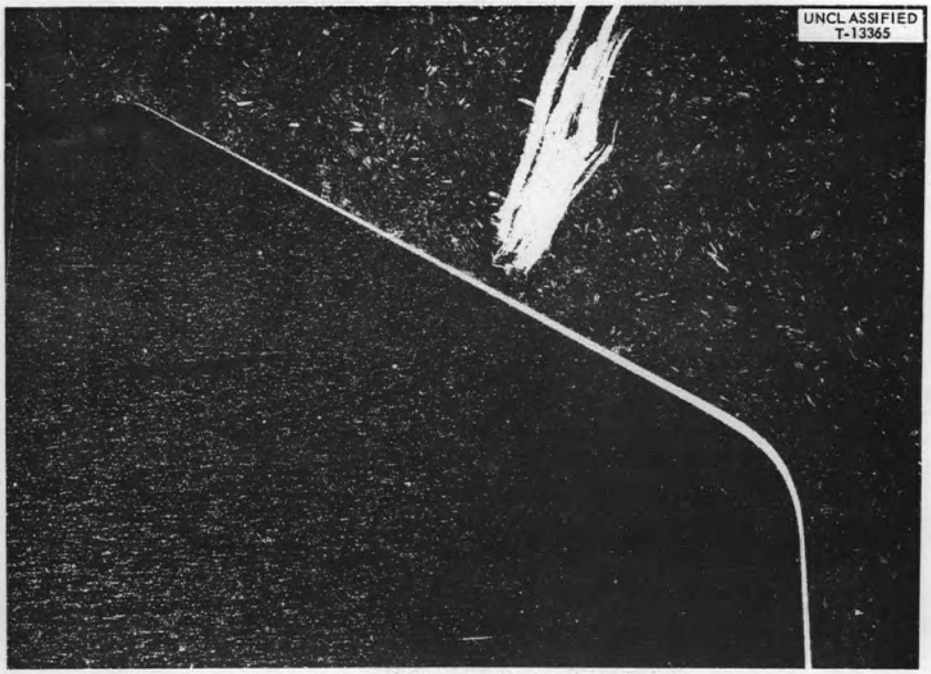

Fig. 84. Variation in Thickness of Tungsten Carbide Plate.

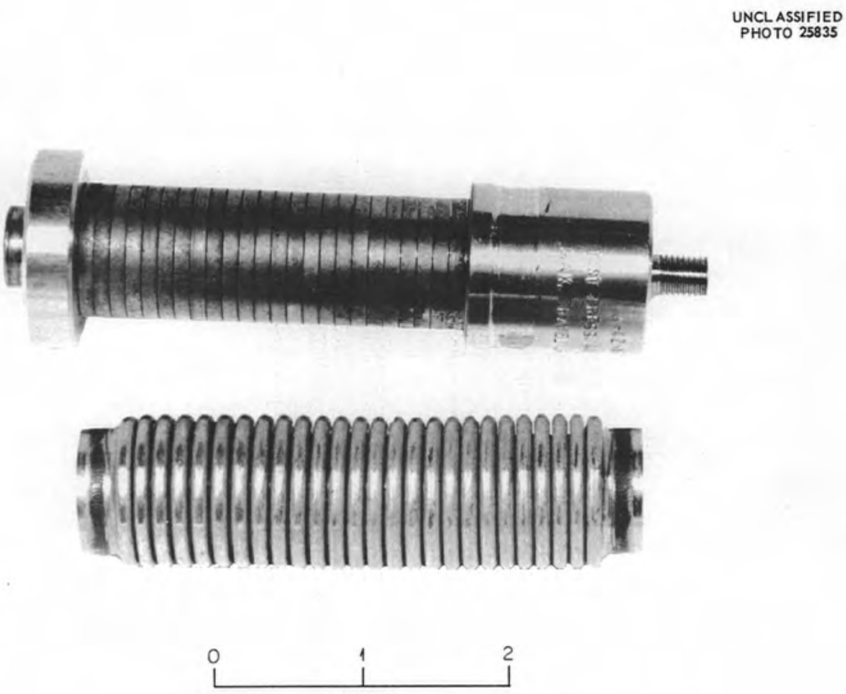

Fig. 85. Stainless Steel Valve-Stem Sealing Bellows.

UNCLASSIFIED
ORNL-LR-DWG 28847

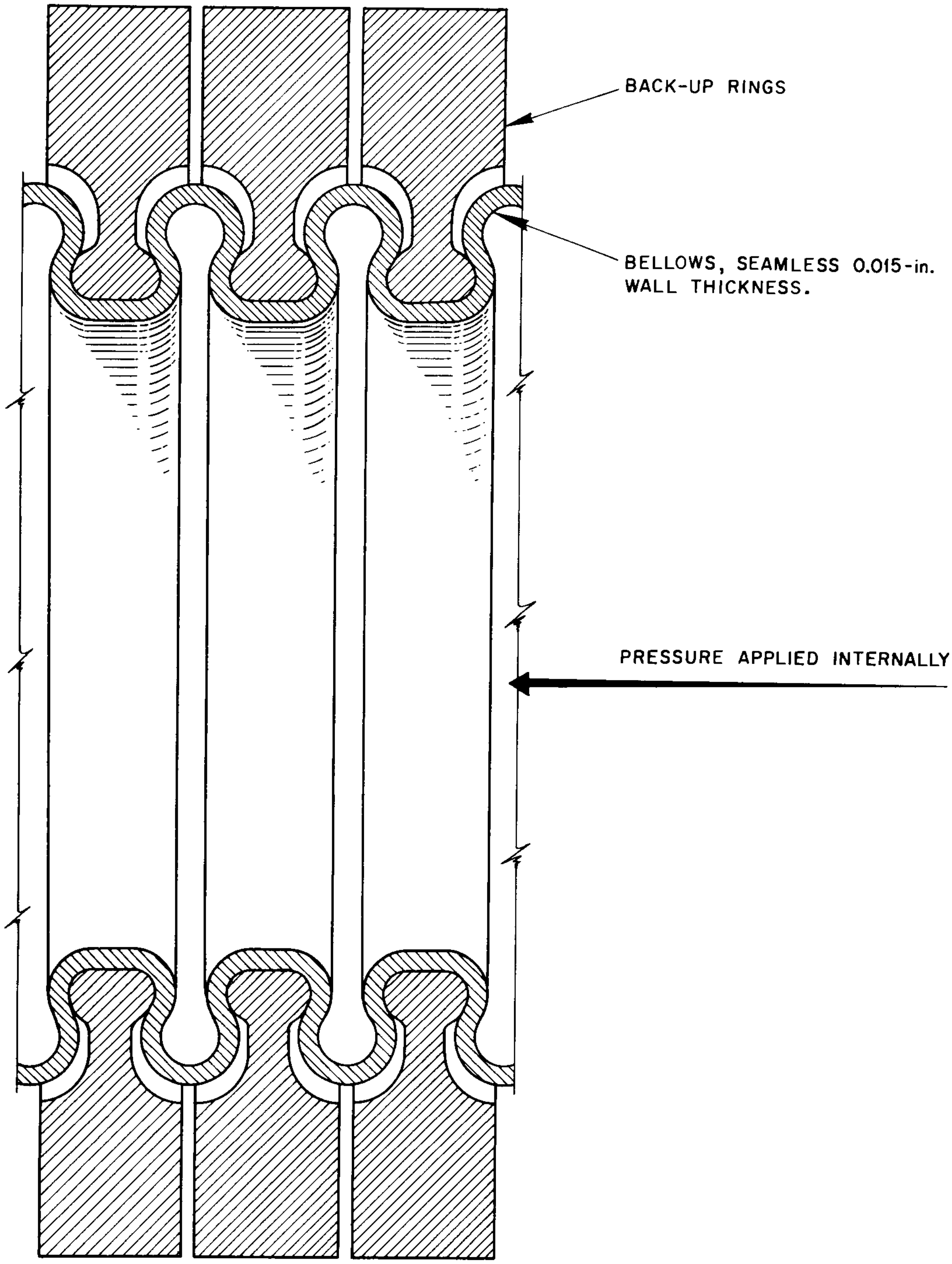

Fig. 86. Section Through Foxboro Super-Pressure Bellows.

Three-ply stainless steel bellows for stem sealing, 3 1/2 in. long and 1 1/8 in. in diameter, are also being life-cycled in thorium oxide slurry at 300°C and 2000 psi. The first bellows tested failed after 63,000 cycles of 1/8 in. Further testing will be done with longer strokes.

Valve Actuators

The 123-in.^{2} pneumatically powered bellows valve actuator described earlier[9] was cycled four times per minute at a stroke of 1/2 in. and a pressure of 80 psig for 265,000 cycles before it developed a small leak in the stem-sealing bellows. Testing was discontinued at this time although the small leak did not impair the operation of the actuator.

A developmental actuator for very large valves was then built utilizing two of the bellows described above (Fulton Sylphon 6745-R2). This unit, shown in Fig. 87, consists of the two (more may be used) metal bellows attached to a common shaft and connected in parallel to a source of air pressure. The prototype actuator is shown in Fig. 88 being cycled 1 in. against a maximum spring load of 5000 lb. During this test the first bellows failure occurred at 18,000 cycles. Minor difficulties were experienced during this cycling period. The lower Oilite bronze guide bushing slipped from the yoke into which it had been press-fitted.

A new all-metal reversible small-valve actuator supplied to ORNL specifications is shown in Fig. 89. The actuator, whose effective area is 40 in.^{2}, is considerably shorter than models used earlier. This reduction in length reduces side stem loading when the valve and associated actuator are mounted horizontally. Horizontal valve mounting has been used to facilitate remote maintenance. The more compact assembly is also desirable because of its space-saving feature. Other features include the internal stem-sealing bellows which eliminates actuating-air leakage, provision for fail-action spring loads adjustable from 50 to 3600 lb (by the use of different springs and spring tension adjustment), and provision for in-line stacked mounting. The new unit is now being life-tested with a valve load simulated by an opposing spring.

A control-valve actuating system using water at 500 psi as the working fluid is also being tested. Possible advantages of a water-operated system over air-operated and oil-operated systems for large valve actuators are, respectively, the size reduction of the cylinders and the relative immunity of water to radiation damage. Some difficulty was experienced with pump packing during the first 15,000 cycles, but cylinder operation remained satisfactory to approximately 35,000 cycles. At this point an appreciable leak developed, apparently due to worn piston rings. However, the system is still operable, and after a 30-min warmup period the leak disappears. Operation has proceeded to a total of 55,000 cycles with no further increase in leakage. When leakage becomes so great as to preclude operation, the Moyno pump and Askania cylinder will be dismantled and examined. The system is shown schematically in Fig. 90. The test stand, with the cantilevered 10-in. I-beams used as cylinder loading springs, is shown in Fig. 91.

---

[9]D. S. Toomb et al., Instrumentation and Controls Ann. Prog. Rep. July 1, 1957, ORNL-2480, p 82.

UNCLASSIFIED
PHOTO 30244

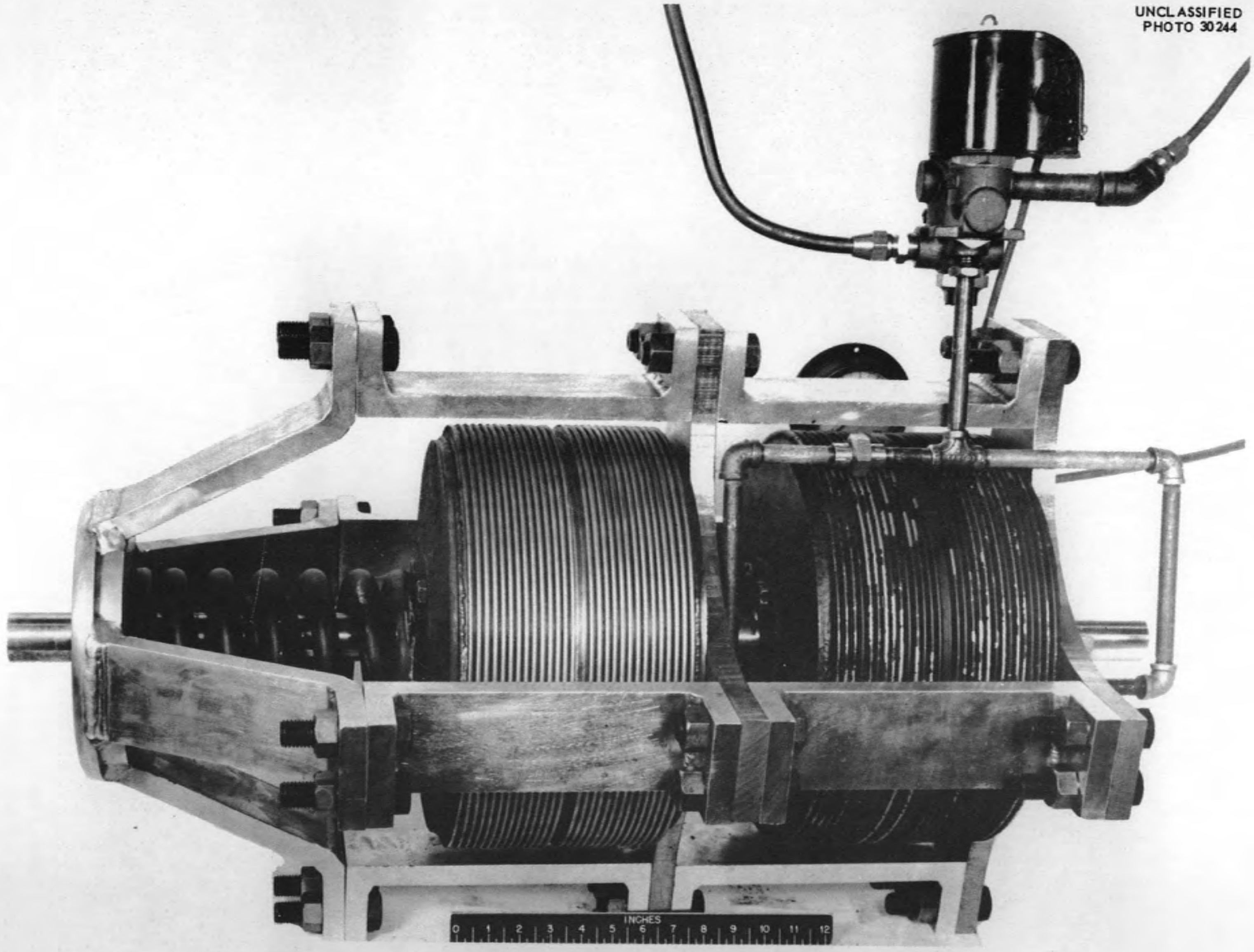

Fig. 87. Developmental Actuator for Large Valves.

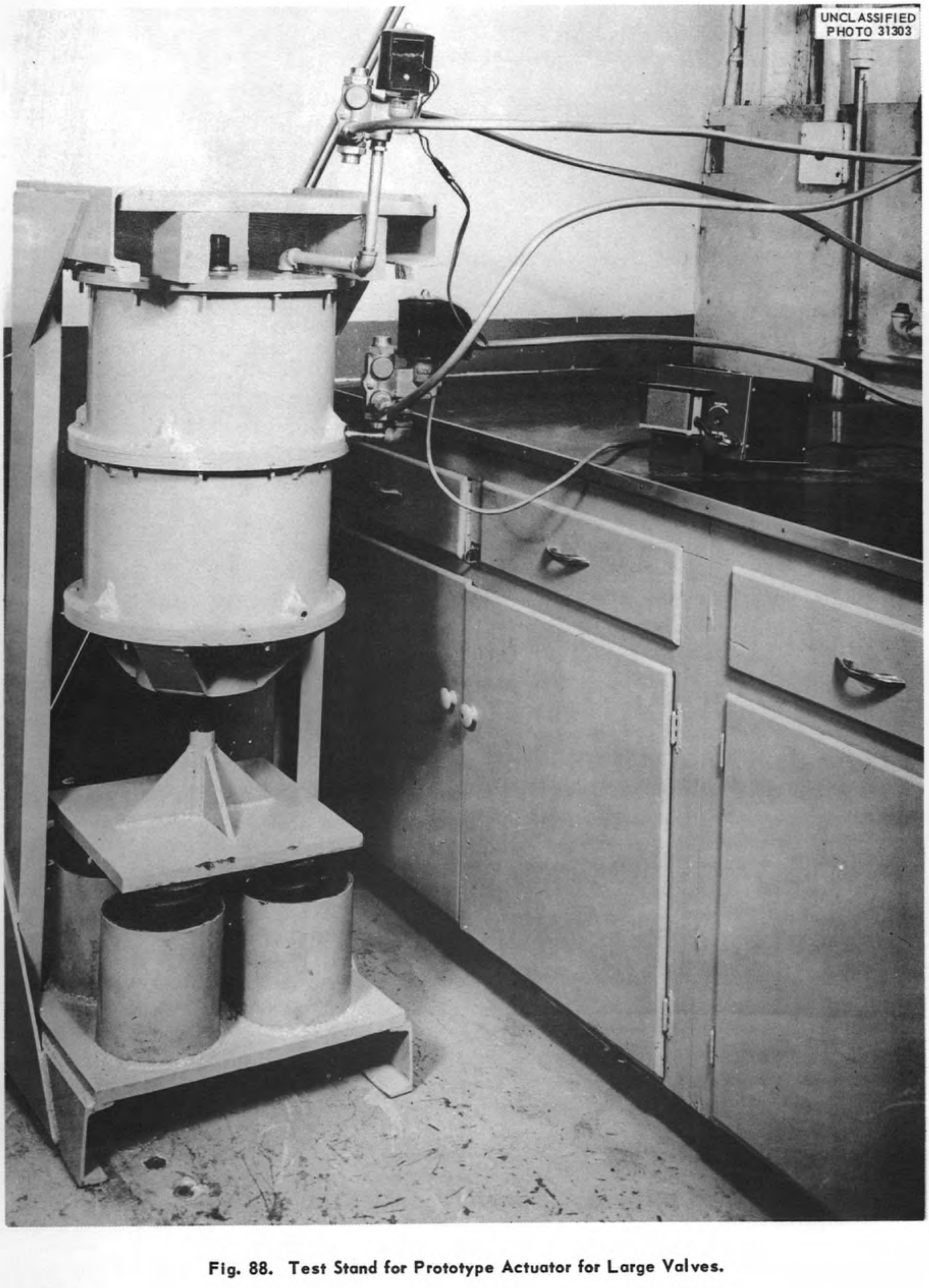

Fig. 88. Test Stand for Prototype Actuator for Large Valves.

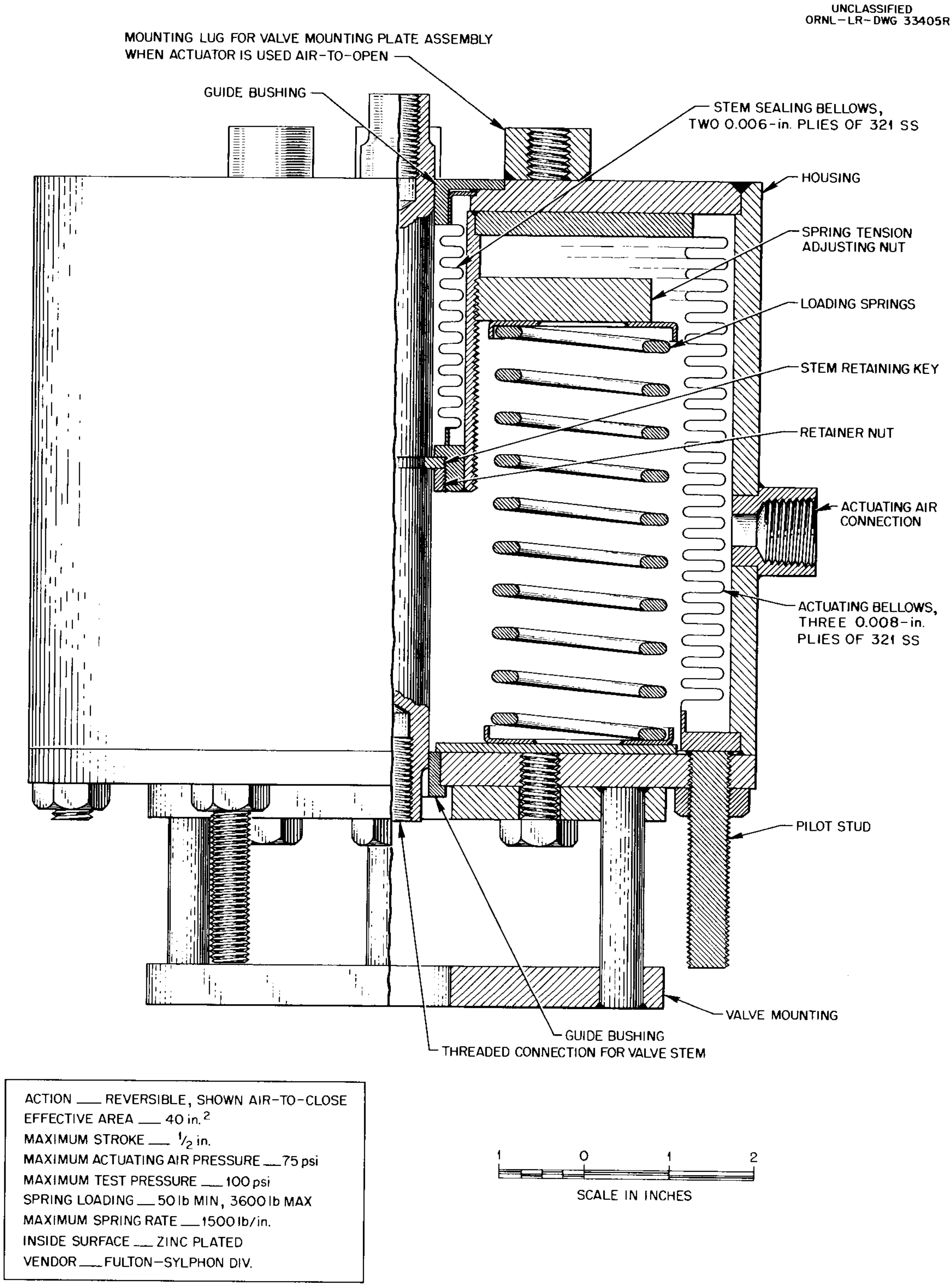

Fig. 89. Metal-Bellows-Type Control-Valve Actuator.

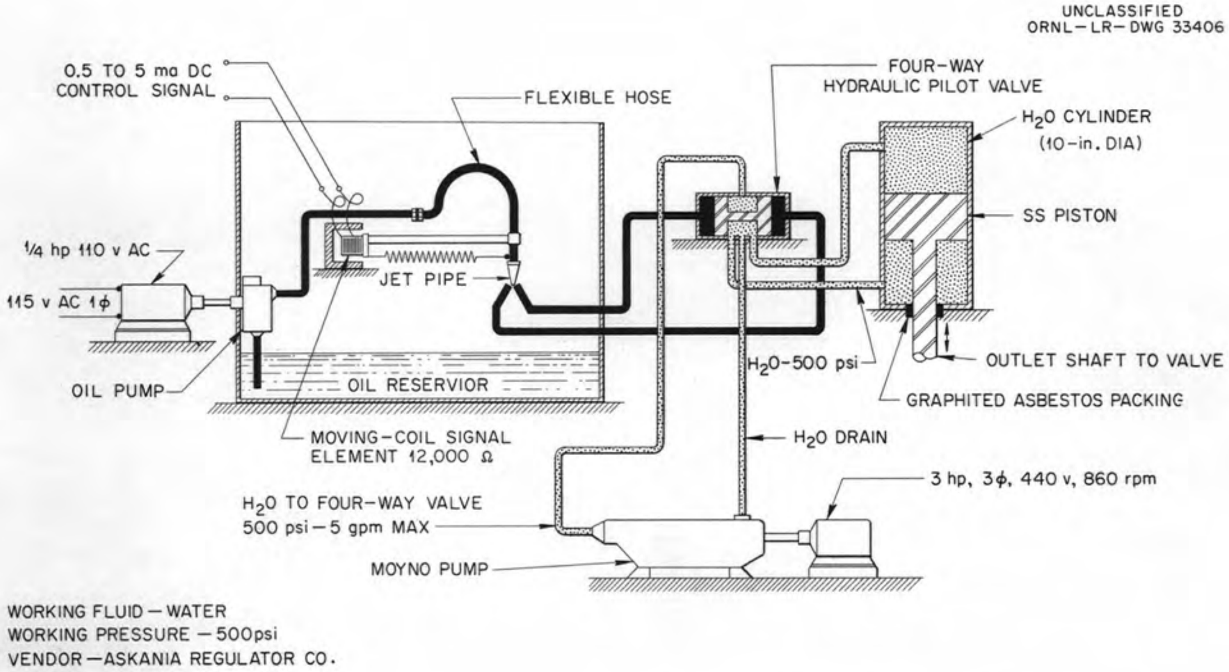

Fig. 90. Schematic Drawing of Hydraulic Control-Valve Actuating System.

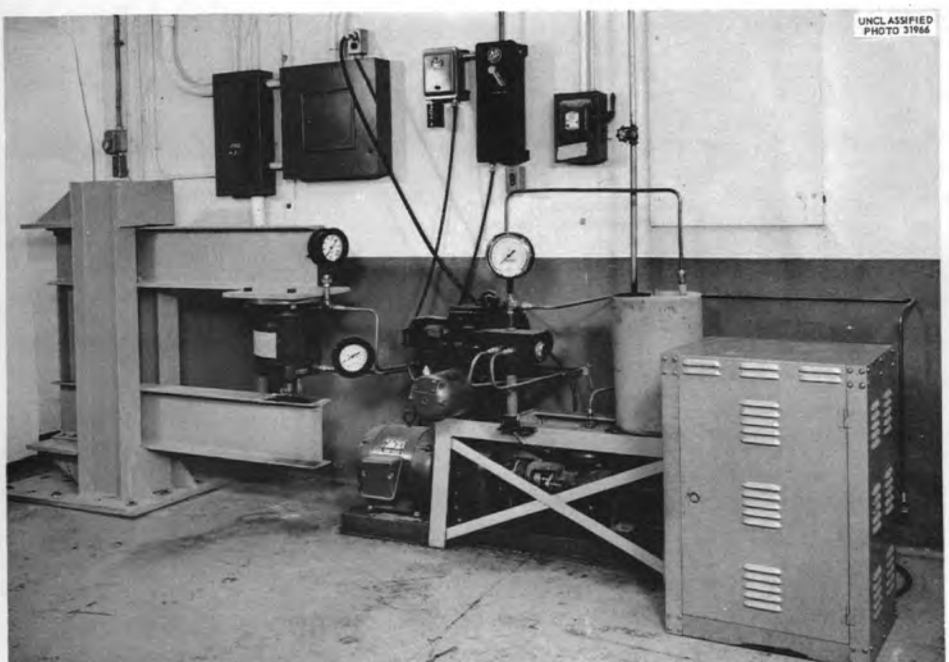

Fig. 91. Test Stand for Hydraulic Control-Valve Actuating System.

HRT INSTRUMENTATION AND CONTROLS SYSTEM COMPONENT DEVELOPMENT

Development work has continued to provide improvement for old instruments and components and to provide new instrumentation as required for changing operating conditions.

Oxygen Injection System

The differential-expansion metering valve[10] used to regulate the flow of oxygen gas from storage tanks to the reactor high-pressure system was replaced with a similar valve of improved design. The new valve, shown in Fig. 92, utilizes a plug of tantalum instead of zirconium to avoid any possibility of an ignition reaction between the oxygen and the metal. (At a flow of 2000 std cc/min with a 400-psi differential, the system can reach a temperature of 330°C.) The new design also incorporates all-welded construction, eliminating a threaded closure in the previous model. The heating elements and thermocouples are covered with a waterproof protective housing. The resistance heating element and thermocouple are duplicated to reduce the possibility of service interruption.

Remote Viewing Equipment

A 2-in.-dia television camera designed for resistance to radiation was received from the Dage Television Division, Thompson Products, Inc.

[10]D. S. Toomb et al., Instrumentation and Controls Ann. Prog. Rep. July 1, 1957, ORNL-2480, p 73.

UNCLASSIFIED
ORNL-LR-DWG 28826

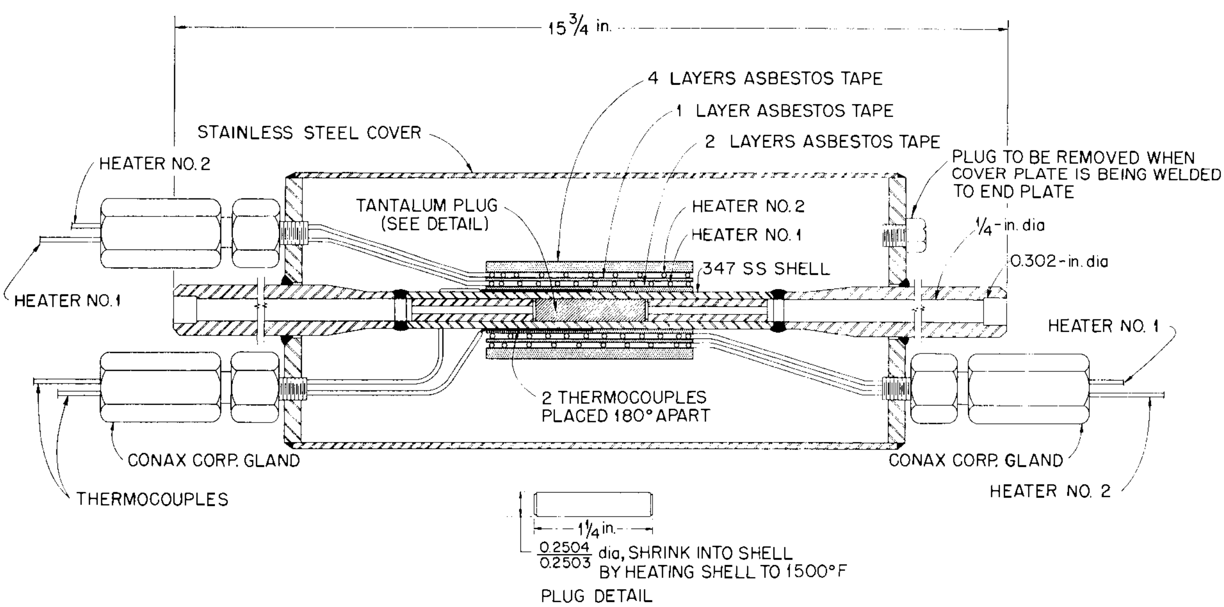

Fig. 92. Improved Differential-Expansion Gas Metering Valve.

The camera was installed in a remotely manipulated mechanism developed for viewing the HRT core vessel but has not yet been used in a radiation field. The camera head, including deflection coils, type 6198A Vidicon and lens, the polished Stellite right-angle mirror, and 50-cp G-E type 1183 spotlight bulb for illumination, is shown in Fig. 93. The preamplifier is at the end of a 10-ft cable to permit most of the electronic components to be located out of the high radiation field associated with the core vessel. By separating the preamplifier and camera head, a considerable reduction in the size of the assembly to be inserted in the core is achieved. One carbon resistor and one ceramic condenser remain in the camera head. The remainder of the electronic components are located in the preamplifier chassis, shown uncovered in Fig. 94.

Available information[11] indicates that the Vidicon sensitivity will decrease about 70% because of lens and Vidicon window browning for a gamma irradiation of 10^7 r. For the estimated 200,000 r/hr gamma flux in the HRT core, the expected useful viewing time is 50 hr. However, the effect on the camera of the beta activity present in the core is unknown, and the light-bulb glass is also expected to brown and thereby further reduce the viewing time.

To provide camera position indication to the operator of the manipulator, the angle of rotation of the three arm-positioning hydraulic cylinders is transmitted to the control console by miniature linear slidewires manufactured by Bourns Laboratories, Inc.

High-Temperature Radiation-Resistant Differential Transformers

The development of radiation-resistant linear variable differential transformers suitable for sensing instrument primary element motions in

---

[11]E. R. Pfaff and R. B. Shelton, Effects of Nuclear Radiation on Electronic Components, WADC-TR-57-361, vol II (Aug. 1958).

UNCLASSIFIED
PHOTO 31870

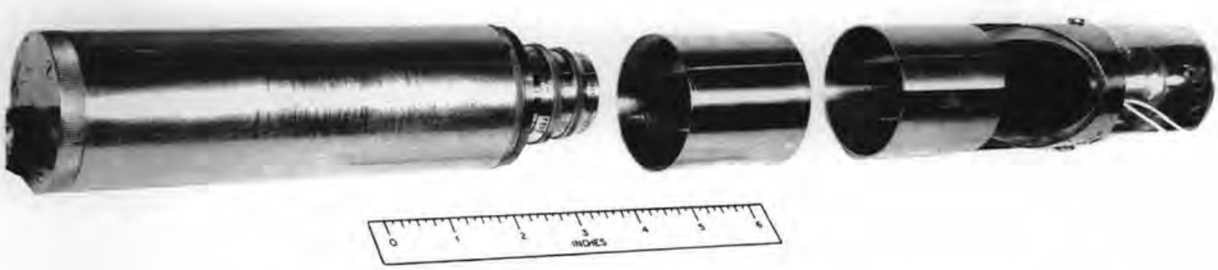

Fig. 93. Miniature Television Camera Head, Mirror, and Light Source.

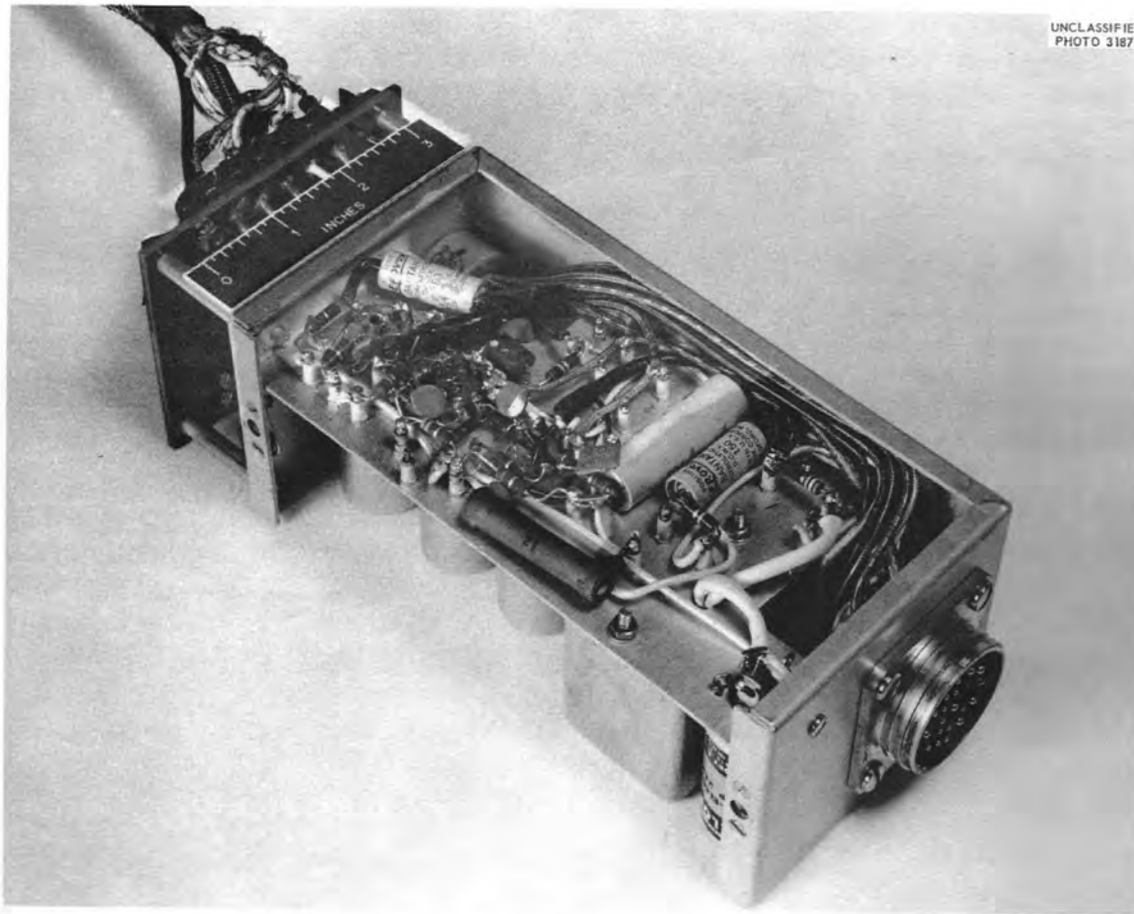

Fig. 94. Preamplifier Chassis for Miniature Television Camera.

a homogeneous reactor environment is continuing. A unit similar in design to the ORNL-developed transformer mentioned in an earlier report,[12] but wound with 30-gage anodized aluminum wire supplied by the Sigmund Cohn Corp., has withstood temperatures to 300°C without insulation failure. The only electrical insulation on the wire is that afforded by the oxide film on the aluminum. This film can be expected to be highly temperature and radiation resistant. Tests of the coil indicated that impregnation of the winding is necessary to avoid zero and null shifts with temperature. These shifts are believed to be due to mechanical displacement of the windings and reduction of the resistivity of the anodized coating with temperature. As failures have occurred because of oxidation of solder at the terminals, pressure-crimped joints and aluminum-clad mineral-insulated connecting cable are now being evaluated.

---

[12]D. S. Toomb et al., Instrumentation and Controls Ann. Prog. Rep. July 1, 1957, ORNL-2480, p 64.

Reactor Power System Rewiring

The design, procurement, and installation of a new power-wiring system inside the HRT reactor containment tank were completed in March. This system supplies electrical power to the pressurizer heaters, circulating pumps, and space coolers.

The first wiring system consisted of stranded copper wire insulated with a double layer of Fiberglas woven sleeving lightly impregnated with an oleoresinous varnish. The wiring was routed to the equipment location in sealed conduits. Inside the containment tank the conduits were terminated in sealed boxes containing glass-to-metal seals to which ceramic-beaded wires from the remote-disconnect boards were connected. At the control-room end, the conduits and wires were sealed in a box filled with asphalt.

Much difficulty was experienced with moisture, which is thought to have entered the conduit at an electrical junction box screwed connection, causing the Fiberglas insulation to break down at the operating voltage of 460 v ac. The dry insulation breakdown point in the conduits as measured at 7.2 psia was 1500 v dc.

The new wiring system consists of swaged magnesium oxide—insulated wires in copper tube sheaths (General Cable Corporation "MI"). The cable ends are terminated inside the containment tank by special hermetic ceramic-to-metal seals and on the control-room side of the shield wall by standard General Cable plastic insulating compound sealed terminals. The new cables are terminated at the various remote-disconnect boards by the compression fitting shown in Fig. 95, which also shows the ceramic-to-metal cable end seal.

The Fiberglas-insulated wire in sealed conduits is still being used in the containment cell of the chemical plant, and no electrical trouble has been experienced to date. However, mineral-insulated cables were installed near the electrical equipment in this cell and may be connected later, if necessary. An experimental waterproof disconnect designed to be broken remotely was constructed, as shown in Fig. 96, to permit the removal of reactor electrical equipment connected with mineral-insulated cable. The electrical connectors are terminated inside the disconnect with a multiple header ceramic-to-metal seal, the voids being filled with magnesium oxide powder. The outside guides are tapered to simplify remote makeup. Long insulators are used on the connecting terminals to minimize leakage currents after submersion.

HRT Valves

The fuel letdown valve,[13] which is throttled to maintain a constant pressurizer liquid level, was removed after the initial reactor power operation because of excessive leakage. The leakage was caused by erosion in the seating cone of the type 17-4 PH stainless steel plug. The valve had been sized originally for a mixture of liquid (1 gpm) and gas (15 cfm)

---

[13] <u>Ibid</u>., p 77.

UNCLASSIFIED
ORNL-LR-DWG 27522R2

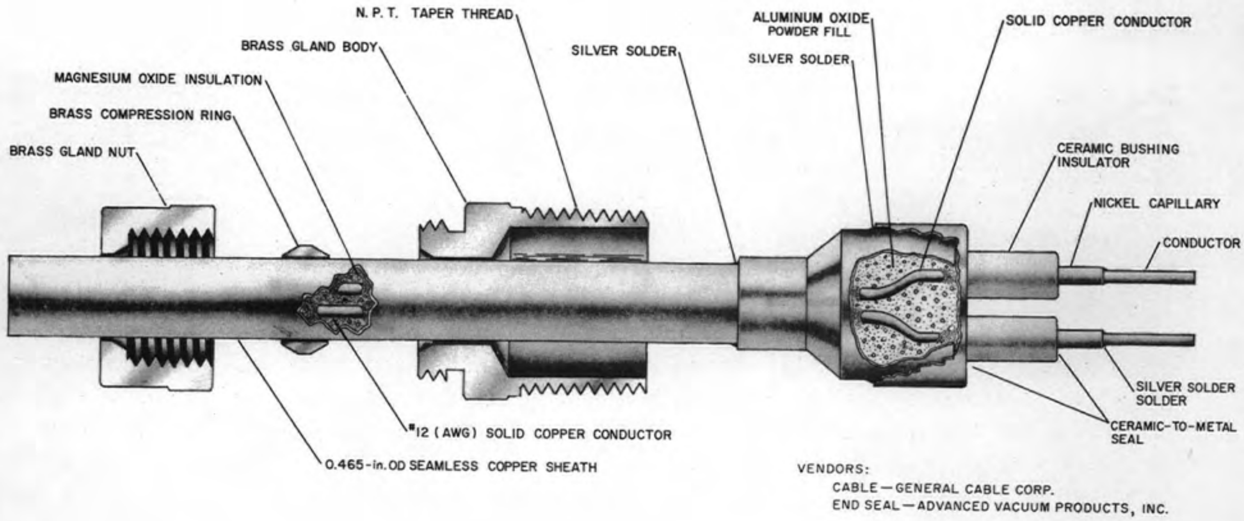

Fig. 95. Mineral-Insulated Cable and Associated Compression Fitting and Hermetic End Seal.

UNCLASSIFIED
PHOTO 30605

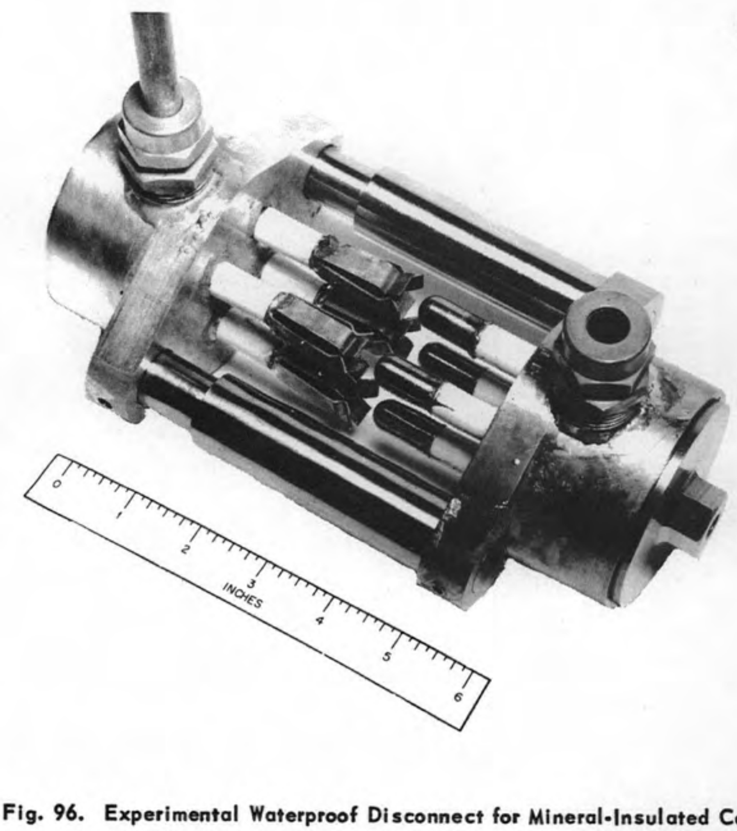

Fig. 96. Experimental Waterproof Disconnect for Mineral-Insulated Cable.

and thus was oversized for the revised operating condition of no gas letdown. The valve position indicator showed that the valve operated in a nearly closed position, and the wear in the seating cone of the plug resulted. This conical surface mates with the seat in the valve body to effect tight shutoff; wear in a properly sized valve occurs well out on the plug, permitting a reasonable life before erosion occurs in the seating area.

An experimental letdown valve was designed which incorporates a 1/8-in.-dia body port instead of the presently used 1/4-in. port. This design, shown in Fig. 97, will permit an increase in the close plug-to-seat clearance which is necessary to adequately throttle the letdown flow. The new design also utilizes a lower stem guide to provide better plug-to-seat alignment. The guide is ported to avoid fuel-solution stagnation in the stem-sealing-bellows compartment. This valve (which has now undergone 1500 hr of testing in the HRT mockup loop), because of the increased annular clearance which is possible with the smaller port diameter, should also reduce the possibility of solid particles wedging the plug in the seat.

UNCLASSIFIED
ORNL-LR-DWG 33203

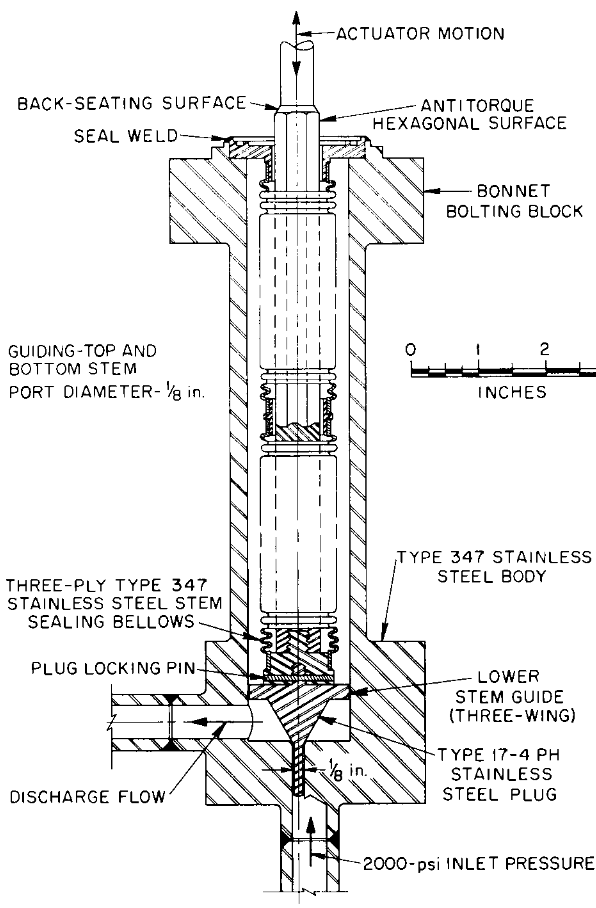

Fig. 97. Modified HRT Letdown Valve.

The blanket system dump valve[14] was also replaced after reactor power operation because of excessive leakage caused by misalignment of the valve plug in the seat. The misalignment was attributed to galling of the stem at the juncture of the tandem stem-sealing-bellows assembly.

Instrumentation and Controls System Modifications

To facilitate reactor operation as a single-region machine and to provide for the consequent increased heat generation in the blanket system, revisions were made to the instrumentation and controls system.

Several changes in size of the steam system valves were necessary to provide for the increased blanket system heat-exchanger steam generation and to permit the tying together of the two steam generating systems. The sizes of the heat exchanger blowdown valves were decreased to minimize the pressure upset occurring during this operation.

Control circuit changes include:

1. automatic dilution of the fuel solution if the blanket vessel outlet temperature exceeds 310°C,
2. elimination of automatic control action for venting the blanket system pressurizer,
3. automatic closing of steam removal valves if either the fuel or blanket system circulating pumps are stopped,
4. automatic stopping of both fuel and blanket system circulating pumps if the steam system pressure drops at a rate exceeding 20 psi/sec,
5. addition of circuitry to prevent the pumping of fuel solution into the high-pressure system from the blanket system dump tanks.

To help in the determination of the cause of the periodic power surges experienced with single-region reactor operation, minor revisions to the instrumentation were made to permit the connection of a high-speed recording system to the neutron level, period, pressure, and pressurizer level measurement channels. The equipment used for these measurements was the Sanborn Company "150" direct-writing oscillographic recording system and associated amplifiers.

---

[14]*Ibid.*, p 80.

POOL CRITICAL ASSEMBLY

A. E. G. Bates

The Pool Critical Assembly (PCA), completed and placed in service near the end of fiscal year 1958, is located in the northwest corner of the same pool of water that serves the Bulk Shielding Reactor (BSR), which it resembles in many respects (see Fig. 98). The purpose for the construction of the PCA was to relieve the ORR and BSR programs of a variety of tasks which do not use the full capabilities of these large installations. Typical work in this category includes criticality experiments with various fuel loadings, flux distribution experiments, and assays of spent fuel elements. Secondary functions include running various void experiments, serving as a test facility for the Reactor Controls Department, and training ORSORT students.

All these requirements can be met by a facility which, among other things, is stationary (rather than movable, as is the BSR) and which, though mainly intended for operation at essentially zero power, is authorized to run at levels up to 10 kw. An installation such as this requires relatively uncomplicated support structures, and by taking advantage of the coaxial control rod drives recently developed and installed in the BSR, it was possible to effect further simplification. Not only are these drives interchangeable with those of the BSR, but their use makes it possible to support all the fuel elements, reflector pieces, and rod and fission chamber drives directly on the grid plate and independently of the operating platform.

The control system[1] employed is identical with that used with the BSR (except for minor refinements). This system permits automatic startups and may be operated unattended for extended periods of time. The physical arrangement of the controls and their associated relays is modular. Such construction is assuming increasing importance with experimental reactors because of the flexibility afforded.

Since both BSR- and ORR-type fuel elements will be installed in the present grid plate of the PCA, this plate was designed to handle fuel elements and reflector pieces having either round or square end boxes. In addition, the present grid plate is easily replaced if desired.

Much of the credit for this program is due to J. S. Lewin, who is responsible for the grid plate, to C. W. Angel and P. E. Oliver, who engineered the operating platform, and to G. C. Guerrant for his invaluable assistance.

---

[1]A. E. G. Bates, Description of ORNL Pool Type Critical Facility, ORNL CF-57-7-51 (July 16, 1957).

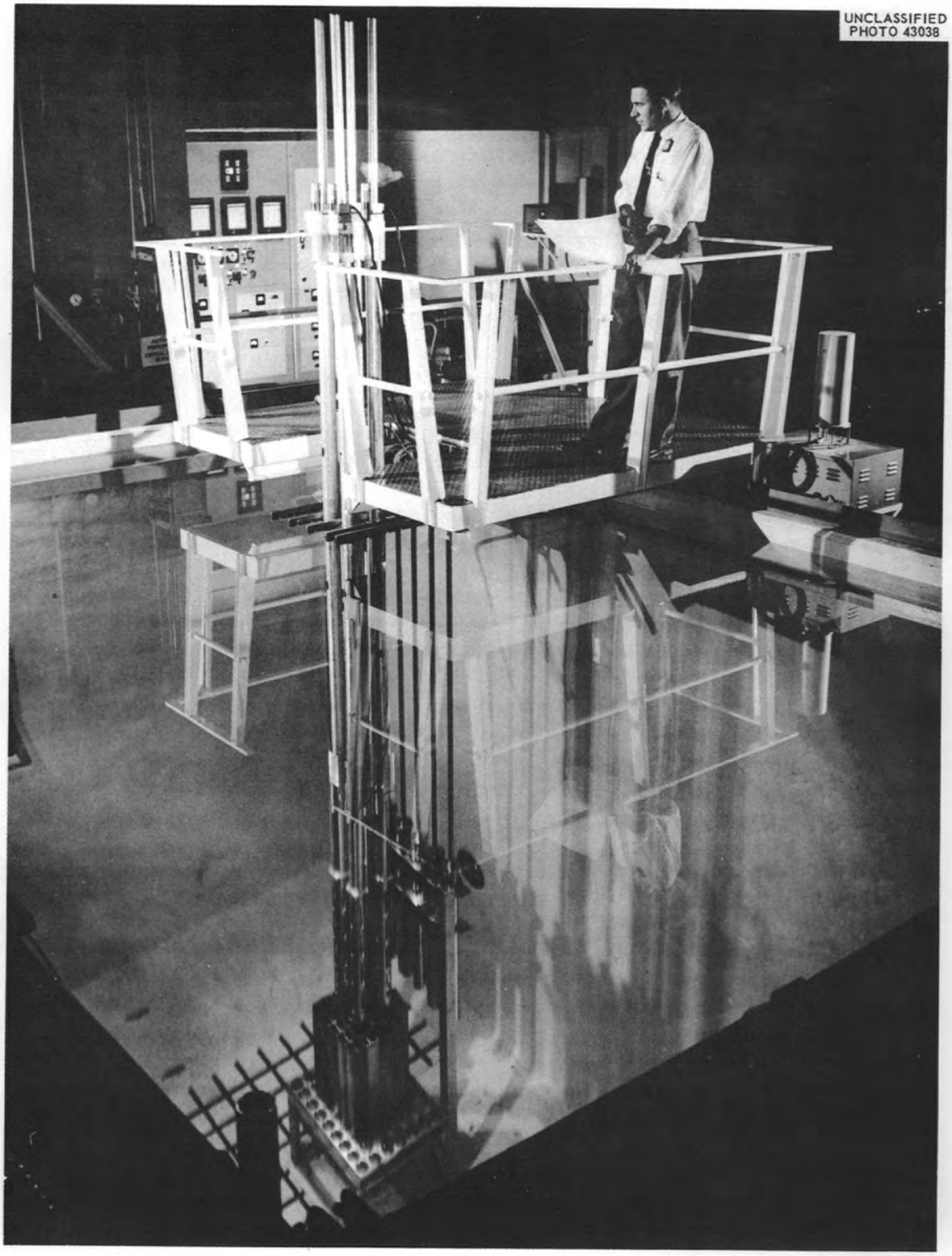

Fig. 98. Pool Critical Assembly.

SAFETY DEVELOPMENT PROGRAM

E. P. Epler   J. R. Tallackson   L. C. Oakes

Work during prior years resulted in the development of the coaxial rod drive and improved magnets.[1,2] Current work on slotted ferronickel magnets, described by Michelson in this report, has further improved the force and time response characteristics. To determine the lower limits in time response consistent with satisfactory reactor operation, full sets of improved magnets were installed in the PCA, BSR, and ORR.

In cooperation with the Neutron Physics Division a stainless steel core and a control system are being readied for a series of transient tests at the SPERT facility, after which the core will be placed in operation as BSR-II.[3] These tests will be a cooperative effort by ORNL and SPERT-I. The geometry and calculated nuclear characteristics of the BSR-II will provide data in an area yet to be covered by the general, continuing SPERT program. Test results will be of general interest to all who are concerned with reactor safety and reactor transient behavior. The core will be subjected to transients which increase in severity to the point of incipient damage to the fuel plates. This point is expected to occur at a period of approximately 5 msec. The program will establish the ability of the core to withstand severe transients and at the same time will verify the operability of the safety system during violent expulsions of the moderator which accompany the transients.

For the purposes of this program a rod drive mechanism featuring fast-response electromagnets and high initial acceleration was designed and tested.

In connection with the TSR-II program it became necessary to construct a hydraulic facility capable of testing reactor components and control rod drives at rated water flow and pressure. A photograph of the installation is shown in Fig. 99. The successful completion of another testing project using this facility provided the design data for improving the performance of the Graphite Reactor drives.

New Facilities. – Several new facilities have recently been added:

1. The hydraulic facility, described above, was constructed.

2. The completion of the PCA has made accessible a small reactor with a flexible operating schedule which will be of considerable value in establishing the serviceability of newly developed components. Several individuals of the Reactor Controls Department are being qualified as operators in order that the facility may be fully exploited.

---

[1] C. Michelson, Design and Experimental Evaluation of Electromagnets for Research Reactors, ORNL CF-57-9-48 (Sept. 6, 1957).

[2] F. P. Green, Reactor Safety System Response, ORNL-2318 (Feb. 14, 1958).

[3] E. G. Silver and J. Lewin, Safeguard Report for a Stainless Steel Research Reactor for the BSF (BSR-II), ORNL-2470 (July 16, 1958).

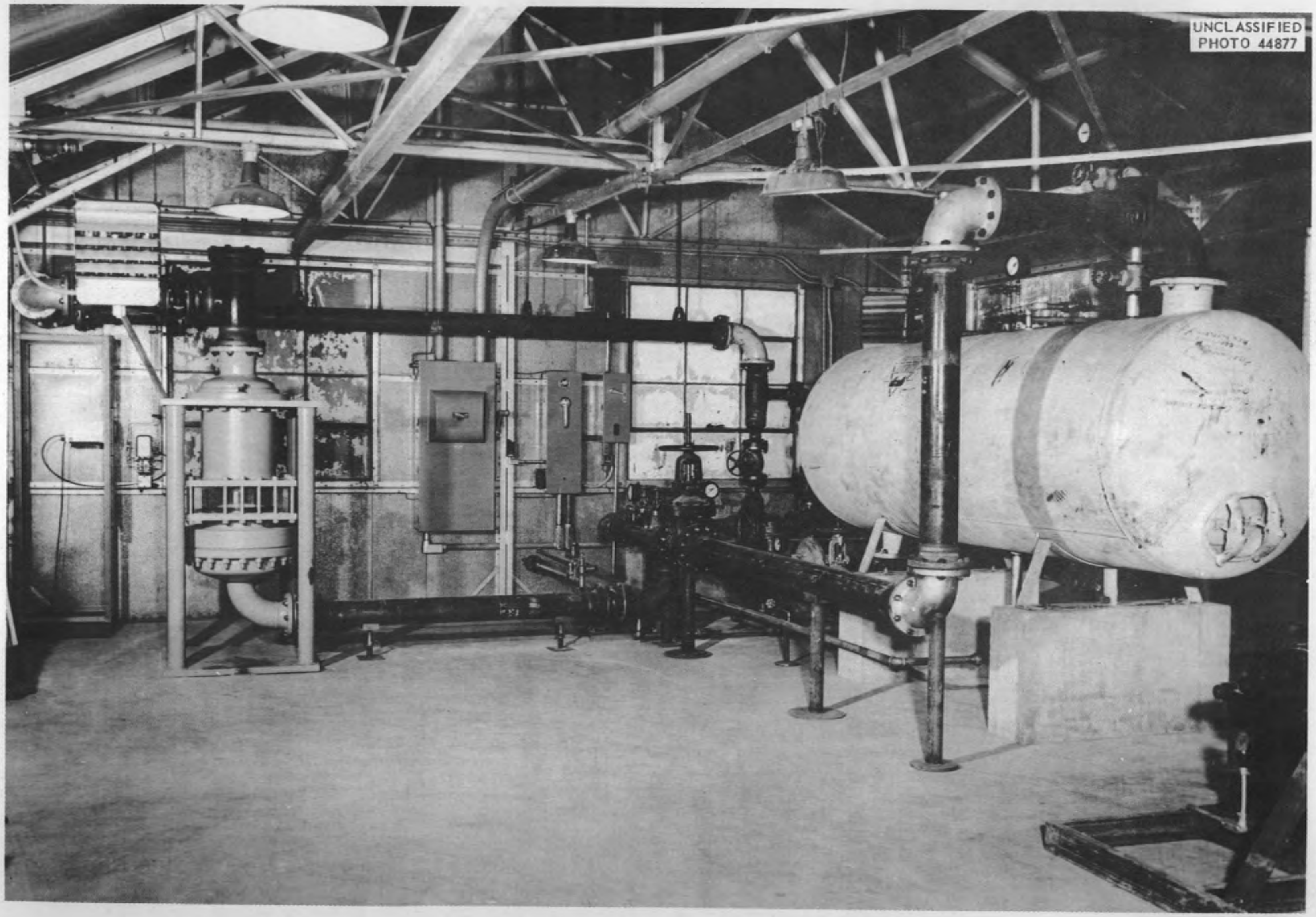

Fig. 99. Hydraulic Testing Facility.

3. A new section has been added to the Analog Computer, consisting of a patch panel and 20 additional amplifiers. This facility is now capable of effective analysis of large reactor systems in the Maritime and Gas Reactor programs.

A FAST-RELEASE ELECTROMAGNET FOR POOL-TYPE REACTORS

C. Michelson

In the pool-type research reactor an electromagnet is the link between the instruments which sense a nuclear excursion and the safety rod which stops it. The first requirement of this magnet from a safeguards point of view is that it release the safety rod within a specified time after initiation of a scram signal, regardless of the magnet current. From an operational point of view it is desirable that this magnet not release as a result of nonnuclear incidents, such as mechanical shock or vibration, or become inoperative due to dirty or misaligned contact surfaces.

A study was made of the parameters affecting magnet performance, the results of which were used to design a fast-acting magnet operable over a wide loading range.[1] Delays in release are mainly due to eddy currents in the ferromagnetic core which are induced when the magnetic field changes. These currents, in turn, establish a magnetic field which opposes the change. The eddy current power density (P_{de}) which results from a flux density B_0 decaying uniformly as a function of time f(t) in a right circular cylinder of radius r_1 and resistivity ρ is

$$P_{de} = \frac{B_0^2 r_1^2}{8\rho} \left[\frac{d\ f(t)}{dt}\right]^2 .$$

From this equation it can be seen that a reduction in eddy current power density can be attained by increasing the resistivity of the pole material or by decreasing the pole radius.

The effect of core resistivity was determined by using two magnet cores of identical physical dimensions but made from magnet materials with different resistivities. The first core was fabricated from Armco ingot iron billet, the second from an Allegheny Ludlum ferronickel bar. Both were heat-treated after fabrication.

The effect of core slotting was determined for the same ferronickel and ingot iron cores. The maximum practical number of slots through the core assembly was found to be 4. The design of the core assembly allowed the slots to extend from the magnet face to beyond the pole tops, thus

[1]C. Michelson, Development of a Fast-Release Electromagnet for Pool-Type Research Reactors, ORNL CF-58-2-3 (Feb. 14, 1958).

separating the assembly into eight individual magnets having a common exciting coil.

Figure 100 shows the effect of slotting a solid ingot iron core assembly with a 0.020-in. air gap on the center pole. Similar data for a solid ferronickel core with a 0.005-in. uniform air gap are given in Fig. 101.

A very small permanent air gap between the magnet and its armature is required to overcome the effects of residual magnetism. The coercive intensity of ingot iron is over ten times that of ferronickel, and a somewhat larger built-in air gap is required to overcome this coercive force. Even with the larger air gap, the release time of ingot iron is much more sensitive to changes in gap dimensions than that of ferronickel.

Since most magnet design specifications call for a combination of small physical size and a large holding force, a very small air gap is necessary. When the mating surfaces between the magnet and the armature are separated in water, a void forms. The resulting decelerating force on the armature is sufficient to measurably retard armature movement. Delays of several hundred milliseconds have been observed in the laboratory for matched surfaces. Delays may be reduced by providing openings from the water to an annular groove in one of the mating surfaces. The groove speeds pressure equalization by providing shorter paths between potential void points and the surrounding water.

At the instant of magnet current interruption, a high-voltage spike appears between the magnet leads and from magnet coil to ground. High-voltage insulation must be used on all leadins and coil wiring. The spike can be reduced in amplitude by shunting the coil with General Electric

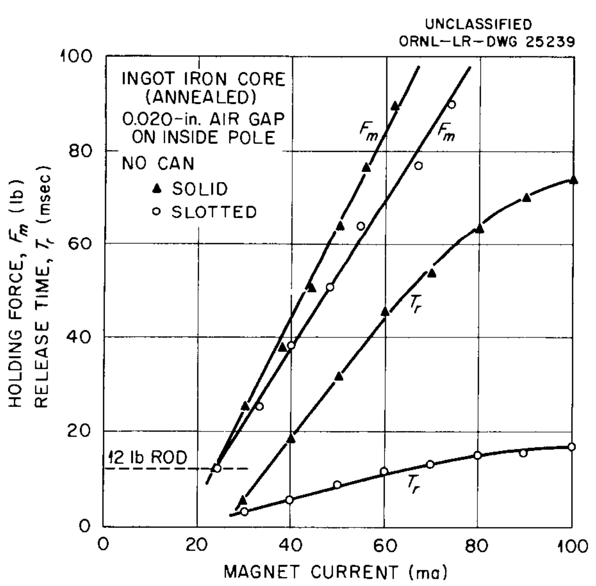

Fig. 100. Holding Force and Release Time for Solid and Slotted Ingot Iron Cores.

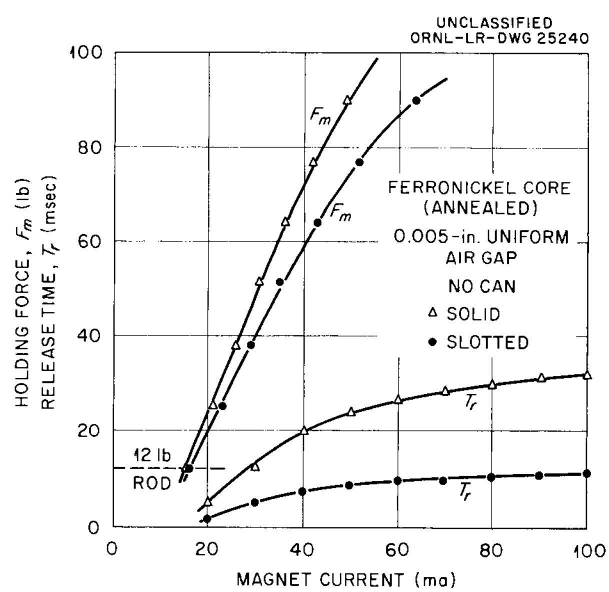

Fig. 101. Holding Force and Release Time for Solid and Slotted Ferronickel Cores.

Thyrite resistors, but since the release time is increased by this technique, its use is limited.

Using the design criteria developed in this study, a lifting magnet was designed and built of slotted ferronickel (Fig. 102). The objective was to obtain a rod magnet operable at loads of from 12 to 77 lb. Performance characteristics for this rod are summarized below.

	12-lb Rod Weight	77-lb Rod Weight
Air gap to match this load, in.	0.015	None
Magnet current at zero (reactor) power, ma	58	54
Excess holding force at zero power, lb	63	53
Release time at zero power, msec	10.5	4.5

The release time of this magnet increases 20% when operated under water with a 12-lb safety rod. As additional accelerating force is added, the underwater response rapidly approaches the dry release characteristics.

If a reduction of excess holding force is permissible, a considerable improvement in release time for the 12-lb rod can be obtained (see Fig. 103). For instance, a dry release time of about 5 msec is possible if the excess holding force is reduced to 30 lb. Many pool-type research reactors now operate with this excess holding force but have an order of magnitude longer release time.

UNCLASSIFIED
PHOTO 41901

Fig. 102. Magnet Assembly.

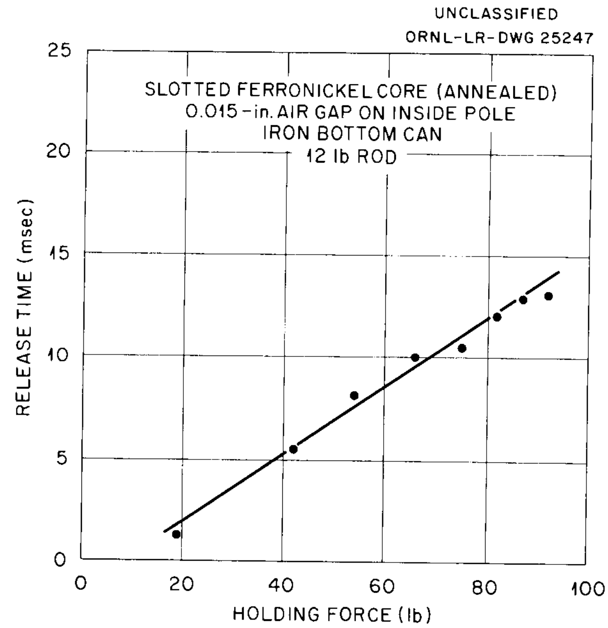

Fig. 103. Release Time vs Holding Force for Free Fall.

It should be emphasized that the optimum performance cannot be obtained for all holding forces within the range originally specified. Considerable improvement in performance can be obtained if the magnet is designed specifically for a 12-lb accelerating force.

Magnets of this design have been built and installed in the PCA and the BSR.

TSR-II INSTRUMENTATION

L. C. Oakes C. F. Holloway J. E. Marks

The Tower Shielding Reactor II is being designed to replace the existing TSR. The reactor consists of a spherical shell of fuel which provides a source of neutrons having the spherical symmetry needed for shielding tests. The center of the fuel sphere (the control region) is a 17 1/2-in. water-filled space which houses all the rods for controlling the reactor. This control region is accessible through a 2 3/4-in. hole through which all rod motion must be controlled. The bidirectional control movement of the rods is obtained from a motor located outside the control region. The fast unidirectional scram motion is provided by springs located in the central spherical section, and only the pilot valves which instigate the scram are located outside. The reactor may be operated at any altitude between ground level and 200 ft. During operation the reactor must be supplied with 1000 gpm of cooling water through 6-in. flexible hoses. The small core volume and the increased probability of losing coolant flow for such reasons as hose breakage and pressurizer failure emphasize the need for reliable water flow instrumentation.

During the past year the design of the reactor controls continued, with the major effort centered in three areas: the development and testing of those components of the safety system to be mounted near the reactor, the design of a cubicle to house the control system, and the development of a process water system flow diagram.

The mechanical safety system has been designed, and a prototype is under construction. The coupling of these mechanical controls to the electrical system is described elsewhere in this report ("TSR-II Electrohydraulic Transducer").

The control system will be housed in a single cubicle designed for unattended operation of the reactor. The cubicle will house all electronic instruments, recorders, control relays, power distribution panels, etc. The control panel will be located in the front of the cubicle beside a graphic panel from which the water system may be operated.

The water system process flowsheet shown in Fig. 104 was designed to couple the reactor to the water cooling system.

Many features of the TSR-I, such as the grounds warning system and the interconnection between the reactor and control room, were modernized and carried over into the TSR-II design.

A five-decade count-rate meter designed by the Reactor Controls Department development group, and described elsewhere in this report ["Counting-Rate Meter (RC-9-11-5)"], was incorporated in the TSR-II. An improved fission chamber preamplifier and a new log N amplifier ["Log N Amplifier (RC-9-11-4)", this report] are under development by that group and will be used in the TSR-II when available.

TSR-II CONTROL MECHANISM TEST

L. C. Oakes   C. F. Holloway   J. E. Marks

The Reactor Controls Department cooperated with the Engineering and Mechanical Division in their development of a drive system for the control elements of the TSR-II.

The geometry of the TSR-II fuel is that of a hollow sphere with six boron carbide control elements contained within the sphere. Each of these elements is shaped as a section of a spherical shell. When all elements are at their positions of closest proximity to the fuel, their surfaces are coincident with the surface of a common sphere, the diameter of which is approximately 1% less than the inner diameter of the fuel. Each element can be moved through a 2 1/2-in. stroke, permitting the poison to assume the shape of a spheroidal shell of varying diameter.

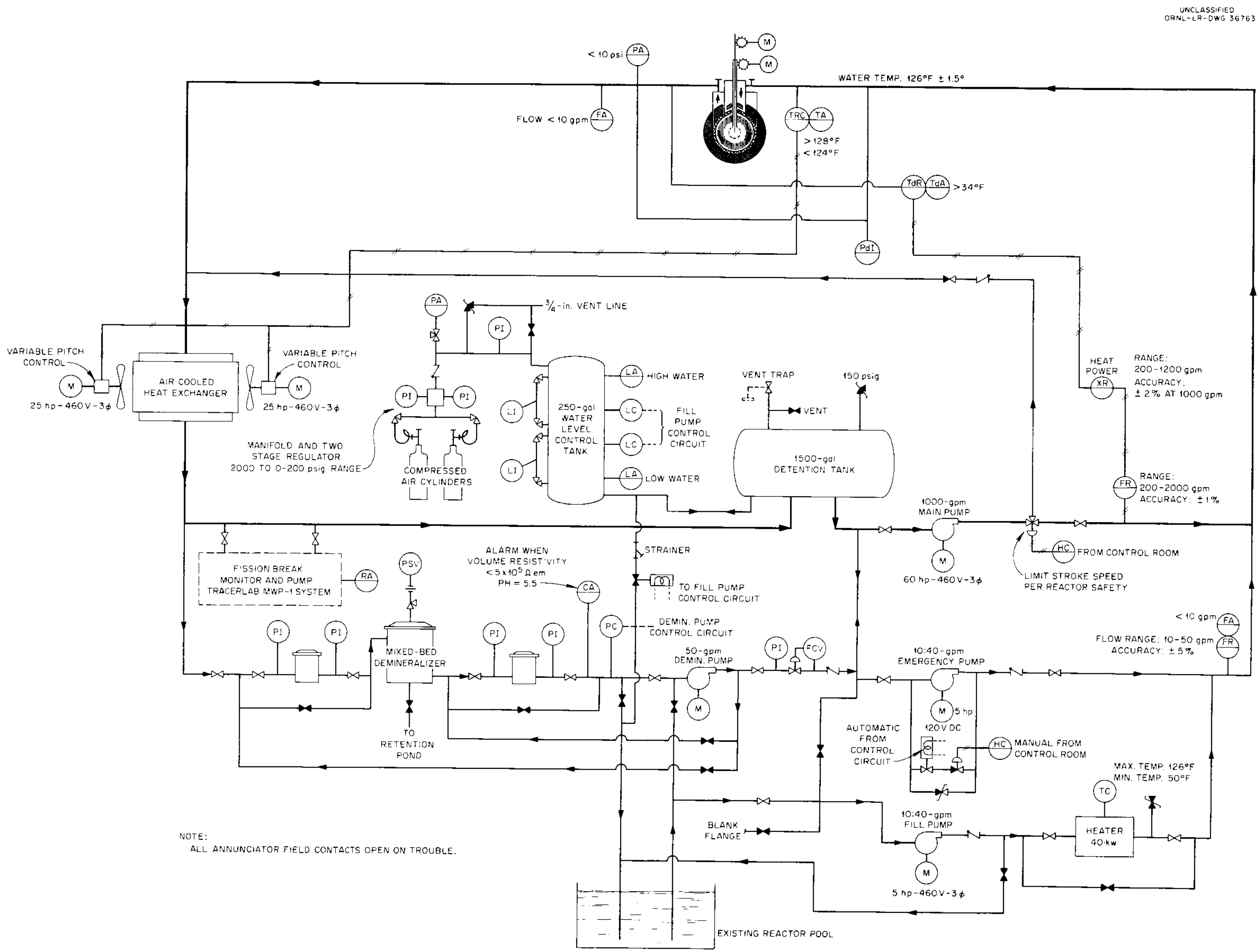

Fig. 104. Cooling Water Process Flowsheet for TSR-II.

In the system developed, five of the six control elements are simultaneously positioned through individual lead screws which are geared to a common shaft. To permit emergency shutdown, the poison-bearing elements were made separable from their lead screws; the separation which is effected when pressure is lost from a hydraulic cylinder permits spring loading to act. The device used to actuate this cylinder is described in another section of this report ("TSR-II Electrohydraulic Transducer").

Since the control mechanism is covered by water in the reactor installation, a test rig was assembled which allowed underwater operation of the mechanism and provided a means of driving the positioning mechanism, a water supply with a scram signal source, and a control circuit for manual and automatic operation of the mechanism both for short experimental runs and for life tests.

As the design progressed, tests were made to determine wear on moving parts and reliability of operation. Three techniques were used to measure travel time of the control element over various strokes. Measurements were also made of such characteristics as the torque to drive the positioning mechanism, orifice coefficients, and operating pressures and flows.

Tests on life expectancy are to continue, as there will be no opportunity for maintenance work on these devices once installed. Long-time, trouble-free operation is mandatory. So far, the unit has operated continuously for 5000 cycles of a pickup-withdraw-scram sequence.

TSR-II ELECTROHYDRAULIC TRANSDUCER

L. C. Oakes   C. F. Holloway   J. E. Marks

The electrohydraulic transducer was intended to couple the standard safety system circuitry to the nonstandard control elements of the TSR-II. The input to the transducer was a signal from a magnet amplifier, and the output was a water pressure related to the input current and self-regulated about the control point. Because this component had to transmit the fast scram signal it was necessary that it have a short response time. In the final assembly there were to be five transducers, one associated with each control mechanism in the reactor.

The first modification of the first design was tested for three months and gave satisfactory service throughout 5000 cycles of a pickup-withdraw-scram sequence of a control mechanism with which it was associated in a test assembly. Response data and reactor simulations indicated that the speed of the system was sufficient to turn back power excursions with periods as short as 8 msec before physical damage to the reactor could occur. The transducer provided 3% pressure regulation over the required flow range and had a 3-msec response time to a step input scram signal as measured at the inlet port. (The regulator operated in a bypass capacity, and the controlled pressure appeared at the inlet.)

However, because of a 70-cps resonant frequency and transmission line mismatches, the effective response time was much less. For these reasons and to improve some of the mechanical features, it was decided to develop a new transducer in an effort to make the operating characteristics less marginal with respect to the safety requirements.

INSTALLATION OF THE AIRCRAFT SHIELDING TEST REACTOR

L. C. Oakes   C. F. Holloway   J. E. Marks

During the first part of 1958, operation of the TSR-I was discontinued and installation of the Aircraft Shielding Test Reactor (ASTR) was started at the Tower Shielding Facility. The ASTR was formerly operated as an in-flight shielding test by Convair and was brought to this site for further tests in order to correlate the data taken in flight with similar data taken from a ground installation. The reactor came equipped with a control cubicle, which was installed in the underground control room beside the existing TSR-I control cubicle. The control cubicle was interconnected with the existing control system so as to utilize such devices as the radiation hazard electrometer and monitron monitors, the area scram switches, the hoist and door interlocks, and the startup hazard delay circuits. It was also connected to the outgoing control and coaxial cables so that full use could be made of the existing aerial cables to the reactor proper.

This reactor was still in operation at the end of the fiscal year.

COUNTING-RATE METER (RC-9-11-5)

J. L. Anderson   R. E. Wintenberg

A wide-range counting-rate meter is needed in reactor instrumentation to close the gap between the maximum neutron level indicated by the pulse ion chambers and the minimum neutron level indicated by compensated current ion chambers. An instrument (Fig. 105) was designed for this purpose and makes full use of the range of the pulse amplifiers within the limits of their resolving power. A block diagram is shown in Fig. 106. The range is 1 count/sec to 10^5 counts/sec. The maximum error is less than 10% of reading from 1 to 10^4 counts/sec and increases to approximately 20% at 10^5 counts/sec (because of coincidence loss). The double pulse resolution is less than 1 μsec, which is less than that of the amplifiers currently available. Drive is low because of the use of chopper-stabilized d-c amplifiers and Zener diode regulation of the logarithmic diode heater supply. A circuit is included which computes the derivative of the logarithm of the counting rate and displays this signal as reactor period. The time constants were chosen to provide an optimum compromise between speed of response and statistical smoothing of the derivative signal. The instrument has exhibited satisfactory performance during extended test periods in the PCA and will soon be installed in the TSR-II.

UNCLASSIFIED
PHOTO 46062

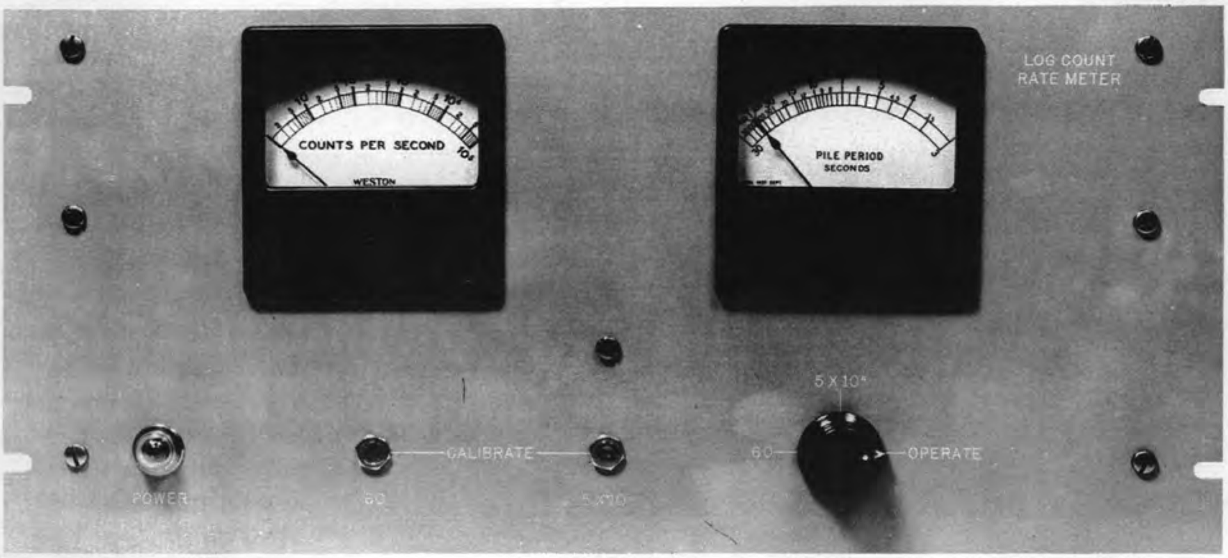

Fig. 105. Logarithmic Count-Rate Meter RC-9-11-5.

UNCLASSIFIED
ORNL-LR-DWG 36764

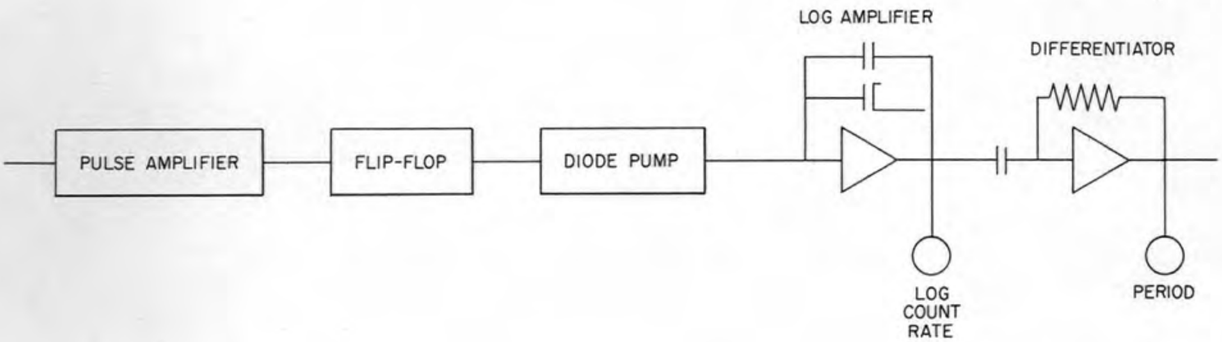

Fig. 106. Block Diagram of Logarithmic Count-Rate Meter.

LOG N AMPLIFIER (RC-9-11-4)

J. L. Anderson R. E. Wintenberg

Design was begun on an improved log N amplifier. By using an input amplifier with 100% feedback through a logarithmic diode, the effect of the input cable capacitance can be degenerated to a substantial degree. This could make the response time independent of input cable length and thus make the instrument non-installation-sensitive. This scheme was tried at the TSR-I using modified laboratory instruments. The tests indicated that the scheme is effective in maintaining reasonable response times with upwards of 1000 ft of cable between ion chamber and amplifier, but showed that special attention will be required to reduce electrical noise and microphonics induced on the cable itself. The design is considered feasible, and an experimental unit is under construction to be used for more extensive field testing. Figure 107 is a block diagram of the unit, which consists of a logarithmic amplifier, an operational-amplifier differentiator, and two self-contained regulated power supplies for the ion chamber. There is a possibility that the system will have eight decades of logarithmic response. The self-contained differentiator will produce a reactor period signal of sufficient amplitude to drive the safety system without the need for an external period amplifier.

UNCLASSIFIED
ORNL-LR-DWG 36765

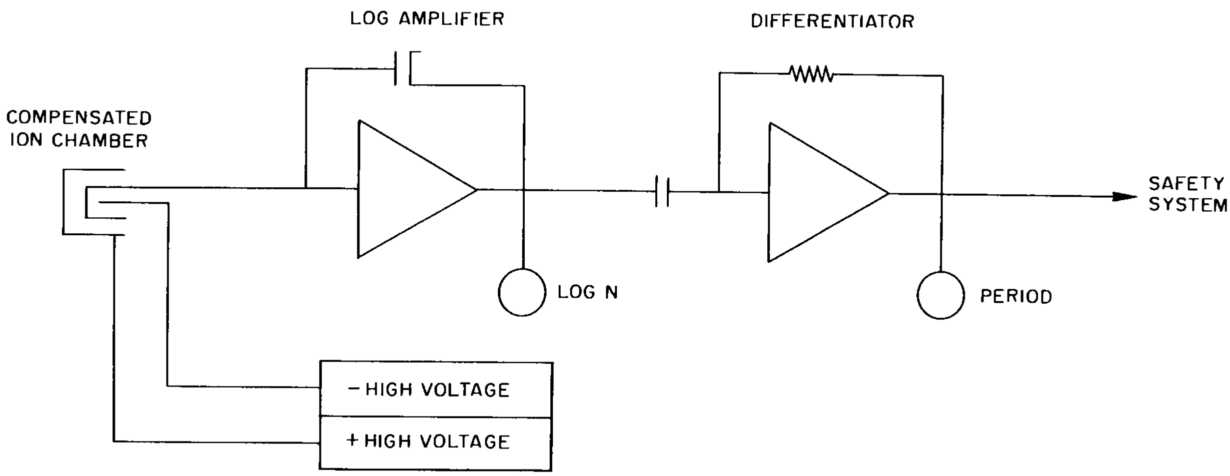

Fig. 107. Block Diagram of Log N Amplifier System.

THE ORNL ANALOG COMPUTER FACILITY

E. R. Mann F. P. Green

Numerous problems have been investigated by means of the ORNL Analog Computer Facility (Fig. 108). These problems can be divided into two distinct categories. One category involves the solutions of sets of equations suitable for such a computing device; the other involves reactor systems analyses.

The problems in the first category, which were usually unrelated to reactor controls projects, are listed here by title only:

1. Pulsafeeder pump diaphragm development,
2. gas recombination system development,
3. theory of particulate fallout and diffusion evaluation,
4. theory of uranium dissemination in human organs evaluation,
5. diffusion column isotope separation development,
6. spectrograph design evaluation,

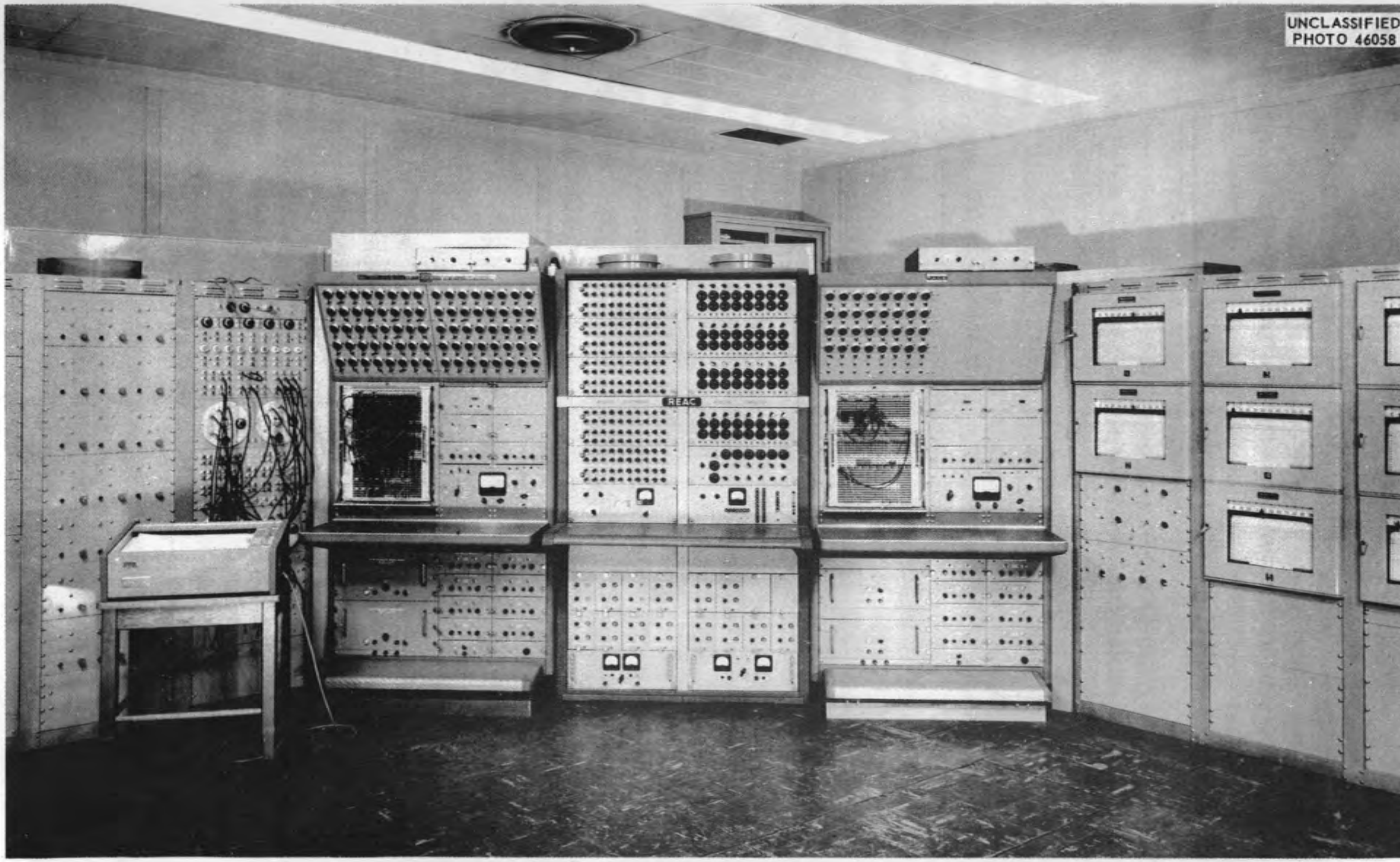

Fig. 108. Reactor Control Analog Facility As Expanded.

7. shock absorber development,

8. theory of thermonuclear reactions evaluations,

9. planimeter computation, dual integration of recorded strip-chart data,

10. thermal study of radioisotope storage in salt domes and well holes.

Some if not all of these investigations have been at least partially described, either in topical reports or in project reports in the fields of activity where the problems originated.

The scope of the problems in the second category (reactor systems analysis) is greater than that usually attempted elsewhere. Whereas the work at other sites is usually limited to studies of the suitability of previously selected equipment to a particular reactor system, the work done here is mainly devoted to the detailed study of complete systems; the type of controls required and the response characteristics of the controls are deduced from the system dynamics.

Major analyses of the nature described above have been reported in refs 1 and 2; partial reports giving results of such work are included in refs 3–5. Certain simulation techniques developed to assist in reactor systems analyses are reported in refs 6 and 7.

The proposed gas-cooled in-pile loop system[1] consisted of blowers, fuel elements, heaters, heat exchangers, an economizer, and long sections of insulated piping. Examination of this loop required use of practically all the computing elements of the analog facility. Even so it was necessary to make some rather coarse approximations in evaluating the heat transfer taking place at various places in the system in order to reduce the number of equations to match the equipment available.

Additional computing elements were purchased near the end of the year for analyses of larger and more complex systems than had previously been possible.

---

[1]F. P. Green *et al.*, *Analog Computer Study of the Operation of the Gas-Cooled Loop on the Oak Ridge Research Reactor*, ORNL CF-58-7-48 (July 7, 1958).

[2]E. R. Mann, *Evaluation of GCRE Reactor and Heat Transfer System by Means of the ORNL Analog Computer Facility*, ORNL CF-58-7-2 (July 2, 1958).

[3]*Molten Salt Reactor Program Status Report*, ORNL CF-58-5-3 (May 1, 1958).

[4]*The ORNL Gas-Cooled Reactor*, ORNL-2500 (Part 3) (April 1, 1958).

[5]J. A. Swartout, *Convair ASTR Experiment at the Tower Shielding Facility*, ORNL CF-57-11-99 (Nov. 14, 1957).

[6]F. P. Green, *ORNL Reactor Controls Analog Facility*, ORNL-2405 (Aug. 4, 1958).

[7]F. P. Green (ed.), *Reactor Safety System Response*, ORNL-2318 (Jan. 31, 1958).

ORNL-2647
Instruments
TID-4500 (14th ed.)

INTERNAL DISTRIBUTION

1. C. E. Center
2. Biology Library
3. Health Physics Library
4-6. Central Research Library
7. Reactor Experimental Engineering Library
8-27. Laboratory Records Department
28. Laboratory Records, ORNL R.C.
29. A. M. Weinberg
30. L. B. Emlet (K-25)
31. J. P. Murray (Y-12)
32. J. A. Swartout
33. E. H. Taylor
34. E. D. Shipley
35. C. S. Harrill
36. M. L. Nelson
37. W. H. Jordan
38. S. C. Lind
39. F. L. Culler
40. A. H. Snell
41. A. Hollaender
42. M. T. Kelley
43. K. Z. Morgan
44. T. A. Lincoln
45. A. S. Householder
46. C. E. Winters
47. H. E. Seagren
48. D. Phillips
49. C. J. Borkowski
50. P. R. Bell
51. J. L. Lovvorn
52. G. S. Hurst
53. R. S. Livingston
54. E. E. Fairstein
55. C. W. Sheppard
56. W. G. Stone
57. C. P. Keim
58. C. D. Susano
59. P. M. Reyling
60. G. C. Williams
61. M. J. Skinner
62. J. V. Francis
63. R. W. Johnson
64. D. J. Fisher
65. E. G. Struxness
66. J. R. McNally, Jr.
67. J. L. Gabbard
68. R. A. Charpie
69. T. V. Blosser
70. E. L. Olson
71. J. A. Auxier
72. R. K. Abele
73. J. R. Tallackson
74. H. E. Banta
75. E. W. Burdette
76. R. R. Dickison
77. C. A. Mossman
78. D. S. Toomb
79. R. G. Affel
80. H. J. Stripling
81. E. P. Epler
82. F. W. Manning
83. ORNL-Y-12 Technical Library, Document Reference Section

EXTERNAL DISTRIBUTION

84-85. Ohio State University (Professor of Naval Science)
86. R. Hofstadter, Stanford University
87. J. C. Nance, Consolidated-Vultee Aircraft Corporation
88. E. A. Rollor, ANP Project Office, Fort Worth
89. R. N. Keller, University of Colorado
90. Division of Research and Development, AEC, ORO
91-713. Given distribution as shown in TID-4500 (14th ed.) under Instruments category (100 copies, OTS)